Ternary intermetallics in aluminium–refractory metal–X systems (X = V, Cr, Mn, Fe, Co, Ni, Cu, Zn)

K. S. Kumar

The phase equilibria of aluminium containing ternary systems are reviewed with particular emphasis on the structure, composition, and stability of the intermetallic compounds present in these systems. The ternary systems are of the type Al–refractory metal (Ti, Zr, Hf, V, Nb, Ta, Mo)–X (X = V, Cr, Mn, Fe, Co, Ni, Cu, Zn), with the majority of the information originating from Soviet and German literature. Inconsistencies between the results of various investigations are highlighted when such comparison is at all possible, although frequently only a single source is available. Potential ternary intermetallics of interest are discussed based on their density, crystal structure, melting point, and compositional range of existence. A trend is noted in the crystal structure of Al_3X-type compounds as a function of the location of the constituent elements in the periodic table. In the last section of this review, current theoretical approaches for predicting crystal structure stability and phase diagrams are outlined with illustrative examples. IMR/214

 The author is with Martin Marietta Laboratories, Baltimore, MD, USA.

Introduction

Ordered intermetallics are a class of materials that form long range ordered crystal structures below a critical ordering temperature T_c, or melting point T_m. Hence, these materials offer potential advantages over conventional disordered alloys for structural applications at elevated temperatures.[1] Among these benefits are high modulus, especially at elevated temperatures, high melting point, and high strain hardening rate, as well as low self-diffusion rate, which confers excellent creep resistance and a high recrystallisation temperature. In addition, intermetallics, such as some aluminides, are also oxidation and corrosion resistant as a result of the protective aluminium oxide film that forms on their surfaces.

Despite these advantages, the development of ordered intermetallics for structural applications has heretofore met with limited success, primarily because of their low ductility and tendency for brittle failure.[2] The reasons for the low ductility can be quite varied depending on the alloy system. For example, in the case of polycrystalline Ni_3Al, it results from poor grain boundary cohesion;[2] single crystal Ni_3Al is highly ductile. Other factors that contribute to poor ductility in ordered intermetallics include an insufficient number of slip systems (primarily in non-cubic alloys, e.g. tetragonal TiAl), limited cross slip, and impurity locking of dislocations. Remedies for these problems include both microalloying[2] and macroalloying,[3,4] removal of impurities[5] and second phase particles, alloying to transform a non-cubic to a cubic structure,[6] grain refinement,[7] thermomechanical processing,[8] and rapid solidification.[9,10]

Currently, there is a tremendous interest in new structural materials with high specific strength for elevated temperature applications and an evergrowing demand for such materials in the aerospace arena. Hence, there is a significant amount of research interest in ordered intermetallics. Current approaches to the design and development of new alloys are, of necessity, largely empirical in nature, with scientific principles applied mostly for interpretation rather than prediction. Interactions among the materials scientist, chemist, and solid state physicist, however, have started to reverse this trend. Further, recent rapid advances in computing capabilities, as well as in instrumentation for structural and chemical characterisation, have allowed more rigorous application of scientific principles to the characterisation, design, and development of new alloys. For example, the growing capability for performing quantum mechanical calculations on equilibrium properties of ordered alloys is beginning to have an enormous impact on the development of additional alloys. Such calculations would provide predictive capabilities to complement the usual methods of alloy development.

In 1984, the National Materials Advisory Board (NMAB) reviewed the potential of ordered intermetallics for structural applications, identified the need for further scientific investigations in several areas, and concluded that results from such investigations would form the basis for the development of ordered alloys of practical interest in the future. Areas that required further research included additional phase diagrams, the deformation behaviour of ternary and higher order systems, the effect of point defects on processing and properties, and the behaviour of grain boundaries under thermal and mechanical stresses.[1]

Of the different types of ordered intermetallics investigated, the cubic $L1_2$ type (Cu_3Au) has by far received the most attention.[1–3,5,8–15] These investigations show that several of the $L1_2$ intermetallics exhibit two desirable features: (a) some show an increase in yield strength with increasing temperature that makes them suitable for elevated

temperature applications and (b) a few of them show ambient ductility. The drawback, however, is the high density of the nickel, cobalt, or platinum based binary $L1_2$ intermetallics. Ordered intermetallics at the aluminium rich end could help alleviate the density problem, but binary aluminides rich in aluminium do not generally occur in the $L1_2$ cubic structure. Of the few rare earth elements that form equilibrium $L1_2$ trialuminides, $ScAl_3$, with a density of 3·02 g cm^{-3} and a melting point of 1320°C, is the only one with a density <4·5 g cm^{-3}. However, the exorbitant cost of scandium precludes extensive experimentation as well as widespread applications. Further, these rare earth trialuminides invariably are line compounds that are in equilibrium with aluminium (m.p. = 660°C), and therefore do not offer much processing flexibility. So, to find low density $L1_2$ compounds, one must examine ternary and higher order systems. An example of such a situation is seen in the Al–Ti system, where a line compound, Al_3Ti (density 3·3 g cm^{-3}) with a $D0_{22}$ structure exists in equilibrium with aluminium at the Al-rich end of the binary phase diagram. The addition of Cu to Al_3Ti yields an $L1_2$ compound of the formula Al_5CuTi_2, which is not in equilibrium with aluminium, exists over a range of stoichiometry, and has a density of 4·0 g cm^{-3}.

This review centres around a detailed literature survey, primarily of German and Soviet origin, of the phase equilibria of ternary Al–X–Y systems where Y = Ti, Zr, Hf, V, Nb, Ta, and Mo and X = Cr, Mn, Fe, Co, Ni, Cu, and Zn, and reveals (a) the presence of several unique ternary phases and (b) solubility limits of ternary elements in binary intermetallics. One of the major problems that was realised from this survey is the significant inconsistencies between investigations; frequently, however, only a single source was identified – for example, in the case of the Al–Ti–Co, Al–Zr–Cu, Al–Mo–Co, Al–Mo–Cu, and Al–Hf–Cu systems, to name a few, only one isotherm was available, making comparison impossible. The task of reviewing the investigations is made doubly difficult as most investigations are reported in Russian or German. In addition, the Soviet investigations, in particular, were reported in journals that are not readily accessible. In several of these investigations, the goal was not to construct accurate phase diagrams; rather, the intention was to identify the phases formed and if possible, identify the solidification sequences. Where, for a particular ternary system, more than one reference source was available, the isotherms were at different temperatures making it difficult to explain contradictions present between two studies. For example, observed differences between two isotherms for a particular system at different temperatures can arise from temperature differences influencing the stability of a phase, as well as its solubility for the constituents, from experimental inadequacy, from impurity effects, or from a combination of these factors. In spite of all these drawbacks, one must start somewhere to try to bring together this knowledge base scattered in literature and that is the intent of this report. Information on these ternary intermetallics would permit verification, extension, and generalisation of fundamental principles that have to date been formulated based on binary structures. The last section of the review includes a concise overview of the various theoretical approaches that have been used over the past two decades to interpret and, even at times, predict crystal structure stability and binary phase diagrams.

Phase equilibria in Al–Y (Y = Ti, Zr, Hf, V, Nb, Ta and Mo)–X(X = V, Cr, Mn, Fe, Co, Ni, Cu, and Zn) systems

Geometrically close packed (GCP) structures

The bulk of the crystal structures appearing in alloy phase diagrams can be conveniently grouped into three broad classifications according to differences in chemical bonding, and mechanical and physical properties. First, there are the geometrically close packed (GCP) structures, such as the fcc, the hcp, the $L1_2$, $L1_0$, $D0_{19}$, $D0_{22}$, $D0_{23}$, $D0_{24}$, and their variations. Second, there are the bcc structures and their derivatives such as the $B2$, $L2_1$, $D0_3$, and the $B32$ structures. Typically, the $A1$, $A2$, and $A3$ structures exhibit ambient ductility, whereas the ordered compounds belonging to these classifications are generally brittle at room temperature. However, isolated examples can be found where some ambient ductility is realised in a few of these intermetallics. Third, there are the topologically close packed (TCP) structures, such as the $A15$, $C15$, $C14$, and $C36$ structures, which tend to be quite brittle. These TCP phases are all characterised by exclusively tetrahedral interstices and coordination numbers of 12, 14, 15, and 16, Several have high melting points.

Of the various GCP phases, the $A1$ and $L1_2$ structure are cubic, $D0_{22}$ and $D0_{23}$ are tetragonal, and $A3$, $D0_{19}$, and $D0_{24}$ are hexagonal. The relationship between some of these phases is shown schematically in terms of defect energies in Fig. 1. Of relevance to this review are the $L1_2$, $D0_{22}$, and $D0_{23}$ crystal structures, which are shown as hard sphere models in Fig. 2. The symbols 'T' and 'R' in Fig. 1 indicate triangular and rectangular ordering of the atomic layers on the close packed planes, as seen in the $L1_2$ and $D0_{22}$ structures, respectively, and the symbols 'c' and 'h' denote cubic and hexagonal stacking sequences. The $D0_{22}$ resembles the $L1_2$ or Cu_3Au structure in that both consist of half –A (atom) half –B (atom) square lattice layers normal to the tetragonal axis, alternating with all –B layers. In the Cu_3Au structure, all of the mixed layers are in register, while in the $D0_{22}$ structure, successive mixed layers are displaced by (½,½,0). The $D0_{23}$ or Al_3Zr structure is a combination of the Cu_3Au and the Al_3Ti structures.

The stacking fault (SF) and antiphase boundary (APB) energies on {111} planes are important factors in determining the slip mode and strength of an $L1_2$ compound, since they affect the phase stability of the compound with respect to the ordered hcp phase ($D0_{19}$) and the disordered fcc phase (Al). The value of the APB energy of {100}

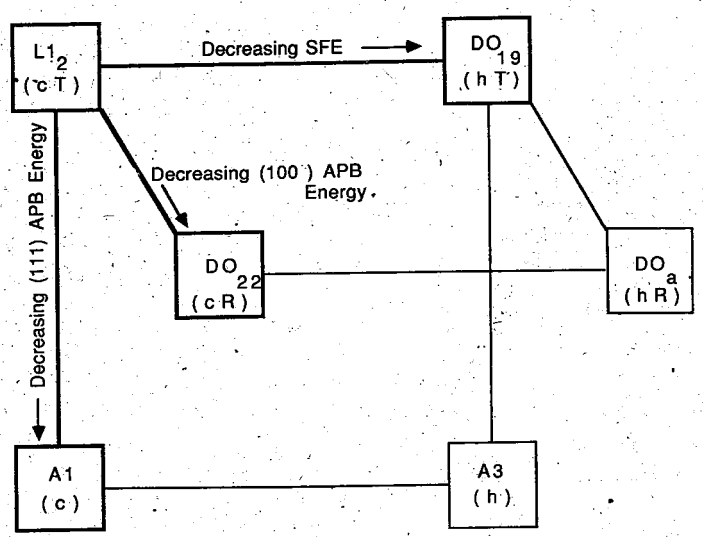

1 Role of defect energies in influencing stability of $L1_2$ crystal structure with respect to other GCP phases

planes is important for thermally activated cross slip in $L1_2$ compounds and is closely related to the phase stability of the $L1_2$ phase with respect to the $D0_{22}$, $D0_{23}$, or long period superlattice phases (Fig. 1). These phases may therefore be viewed as consisting of unit cells of the $L1_2$ structure with regularly spaced APBs on {100} planes at definite multiples of the unit cell length. Thus, the mechanical properties of the $L1_2$ intermetallic can be viewed as being influenced by the phase stability of the $L1_2$ structure relative to other GCP phases.

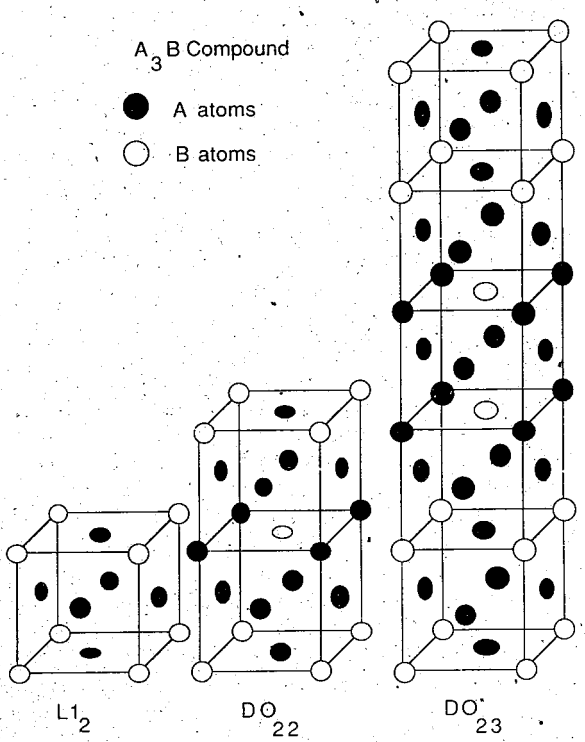

2 Cubic $L1_2$ and related tetragonal $D0_{22}$ and $D0_{23}$ unit cells for binary A_3B compound

Al-Group IVA–X systems

Al–Ti–X systems

In the binary Al–Ti systems, at least three intermetallics are known to exist, with compositions Ti_3Al, TiAl, and Al_3Ti. In addition, long period superstructures of the type Al_2Ti, Ti_5Al_{11}, and Ti_9Al_{23} have all been reported, but their existence is still in question. The Al_3Ti compound with a $D0_{22}$ structure is brittle; however, its relatively high melting point, good oxidation resistance, and low density make it attractive for aerospace applications. Recently, Yamaguchi *et al.*[16] examined single and polycrystalline Al_3Ti in compression and identified twinning as the major deformation mode at ambient temperatures. In another investigation,[17] they evaluated the effect of alloying additions on the ambient compressive ductility of Al_3Ti, without changing the $D0_{22}$ crystal structure. A 1373 K isotherm for the Al–Ti–V system[18] showed that Al_3Ti and Al_3V exhibited unlimited mutual solid solubility at this temperature, while TiAl and Ti_3Al dissolved significant amounts of vanadium. No uniquely ternary compounds were identified. Umakoshi *et al.*[19] studied the deformation characteristics of Al_3V and $(V_{0.95}Ti_{0.05})Al_3$ and found improvements in ductility in the ternary compound over the binary Al_3V, which they attributed to a substantial increase in twinning activity in the ternary composition.

Recently, there has been a great deal of interest in the Al–Ti–Cu, Al–Ti–Ni, and Al–Ti–Fe systems[20–27] because of the presence of a low density $L1_2$ compound at the Al-rich end of each of these ternary systems. Markiv *et al.*[28] examined these ternary systems in detail and generated the isotherms for the respective systems at 1073 K. In the Al–Ti–Fe system (Fig. 3*a*), they identified three ternary phases that they refer to as A, X, and T. The A phase was identified as $L1_2$ with a composition corresponding to 25Ti–9Fe–66Al (at.-%), and a lattice parameter of 0·3981 nm. The X phase had a composition of 6Ti–25Fe–69Al (at.-%), while

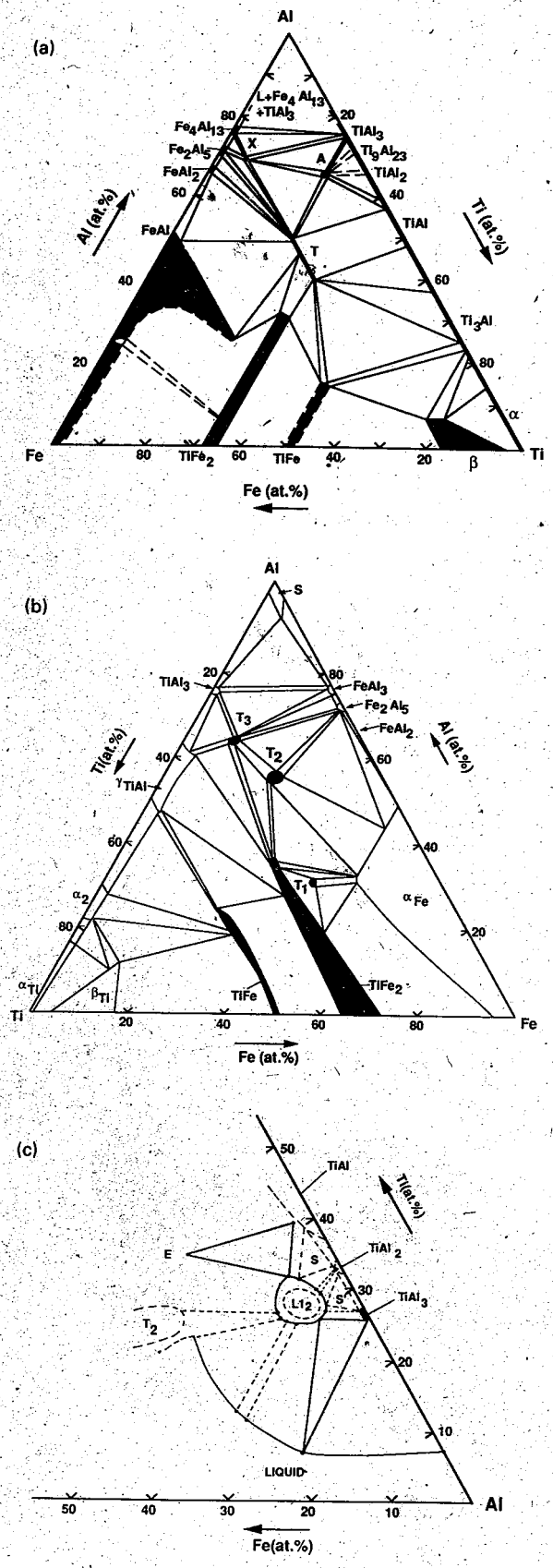

3 Isotherms in Al–Ti–Fe system *a* at 1073 K (Ref. 28) and *b* at 1073 K (Ref. 29); *c* extent of Al-rich $L1_2$ phase field at 1473 K (solid lines) and 1073 K (broken lines), (Ref. 26)

the T phase existed over a range of compositions from 24 at.-% Fe, 40 at.-% Al to 24 at.-% Fe, 50 at.-% Al. The binary phase $TiFe_2$ showed a significant solubility for aluminium (~35 at.-%), while the equiatomic TiFe phase dissolved up to ~15 at.-% Al. Lattice parameter variation for $TiFe_2$ as a function of aluminium content was measured.

Subsequently, Seibold[29] examined the Al–Ti–Fe system in detail, generating an isotherm at 1073 K (Fig. 3*b*), the liquidus projection, and the entire reaction summary in the respective binary systems, as well as in the ternary system. She identified three ternary compounds with stoichiometries corresponding to $TiFe_2Al$ (T_1), $TiFeAl_2$ (T_2), and $Ti_8Al_{22}Fe_3$ (T_3) and claimed they formed from the liquid rather than by a solid state decomposition. The T_3 phase was found to be $L1_2$, in agreement with the earlier work of Markiv *et al.*,[28] although the lattice parameter from Seibold's study[29] was 0·393 nm. The melting point of this compound was 1603 K, which is in agreement with the later work of Kumar and Pickens.[24] The crystal structure of the T_2 phase, which is the equivalent of the T phase in the investigation of Markiv *et al.*,[28] was fcc ($Mg_6Cu_{16}Si_7$), with a lattice parameter of 1·182 nm. However, the compositional range of existence of this T_2 phase was very different from that shown by Markiv *et al.*[28] even though the isotherms generated in the two investigations were at the same temperature (Fig. 3*a* and *b*).

Recently, Mazdiyasni *et al.*[26] re-examined the Al-rich portion of the Al–Ti–Fe, Al–Ti–Ni, and Al–Ti–Cu systems to identify the exact location and size of the single phase field corresponding to the $L1_2$ compound in each system. After examining the phase field for the Al–Ti–Fe system at 1473 and 1073 K, they found that the shrinkage of the single phase field at 1073 K was not concentric with respect to 1473 K, but skewed (Fig. 3*c*). They claimed that the centre of this single phase field had a composition of 64Al–28Ti–8Fe (at.-%). They also identified the binary $TiAl_2$ compound in equilibrium with the $L1_2$ phase, an observation which conflicts with the work of Seibold[29] but agrees with the isotherm presented by Markiv *et al.*[28] In this context, Seibold,[29] indicated that she knowingly omitted the Ti_5Al_{11} and Ti_9Al_{23} phases in her analysis. Markiv *et al.*[28] claimed that the $L1_2$ phase was in equilibrium with a binary Ti_9Al_{23} phase. However, a comparison of their isotherm with that due to Siebold (Fig. 3*a* and *b*) shows a major difference in the composition of the third ternary compound. While Markiv *et al.*[28] claimed the existence of a Ti-poor X phase, Seibold[29] pointed to a T_1 phase which was cubic and had the formula, $TiFe_2Al$; such a compound is absent from the isotherm due to Markiv *et al.*[28] In addition, Seibold[29] cast a composition corresponding to the X phase ($Ti_2Al_{23}Fe_8$) and found it to be a two phase mixture of primary Fe_2Al_5 in a eutectic mixture of Fe_2Al_5 and T_3. Similarly, the X phase observed by Markiv *et al.*[28] to be in equilibrium with the $L1_2$ phase was not observed by Mazdiyasni *et al.*[26] Thus, while the existence of an $L1_2$ compound in

this system is certain, the exact solidification sequence, and, consequently, the resulting microstructures, in the rest of the ternary system requires further consideration.

Such differences in phase equilibria as illustrated above typically arise because of insufficient accuracy in experimentation and inadequate purity of starting materials. Frequently, compositions of alloys are assumed to be starting nominal compositions and losses during processing (for example, Al loss during melting) and interstitial pick up are not accounted for. Further, experimental techniques used in quantifying microstructures vary in accuracy depending on the technique used and this in turn influences the shape and extent of a phase field. Mazdiyasni *et al.*[26] in their study used 50–100 g ingots obtained by vacuum arc melting elemental constituents. Subsequently, the resulting product was chemically analysed to obtain exact compositions. Their heat treatments were done in argon and they used a variety of techniques to characterise the microstructure including metallography, electron microprobe analysis, and X-ray diffraction. In addition, they controlled the level of interstitials to low values. Seibold's samples[29] were typically 10 g in size and, obtained from elemental constituents by electron beam melting in an argon atmosphere. The resulting compositions, however, were not measured but assumed to be the same as the intended composition. Primary techniques to characterise the microstructure involved optical metallography and X-ray diffraction. However, since Seibold's study[29] is in good agreement with the later work of Mazdiyasni *et al.*,[26] it can be assumed that her observations are reasonably accurate. The exact experimental procedure adopted by Markiv *et al.*[28] is not clear, although X-ray diffraction and optical metallography were primarily used to characterise the microstructure.

Raman and Schubert[30] provided an isotherm for the Al–Ti–Ni system (Fig. 4*a*) at 1073 K which can be directly compared with the isotherm due to Markiv *et al.*[28] (Fig. 4*b*). Kaufman and Nesor[31] calculated several isotherms in this ternary system, but they disregarded the existence of the $L1_2$ phase in their study. The $L1_2$ phase field was investigated by Mazdiyasni *et al.*[26] at 1473 K; this section of the isotherm is shown in Fig. 4*c*. From Fig. 4*c*, it is apparent that the $L1_2$ phase is stable at least up to 1473 K, which contradicts the observations of Nash *et al.*[32] that this phase is stable only below 1273 K and forms via a solid state reaction. The composition of the geometric centre of the $L1_2$ single phase field in Fig. 4*c* corresponds to 66Al–27Ti–7Ni (at.-%), which is in fairly good agreement with the results of Raman and Schubert[30] (Fig. 4*a*) and Huang *et al.*[33] The size of the single phase field, however, is much larger at 1473 than at 1073 K (cf Fig. 4*a* and *c*). The 1073 K isotherm due to Markiv *et al.*[28] is in good agreement with that of Raman and Schubert[30] (Fig. 4*a* and *b*) with respect to the location and size of the Al-rich $L1_2$ compound $Al_{67}Ni_8Ti_{25}$, as well as the number of ternary compounds present in this ternary system.

In addition to the $L1_2$ compound, Markiv *et al.*[28]

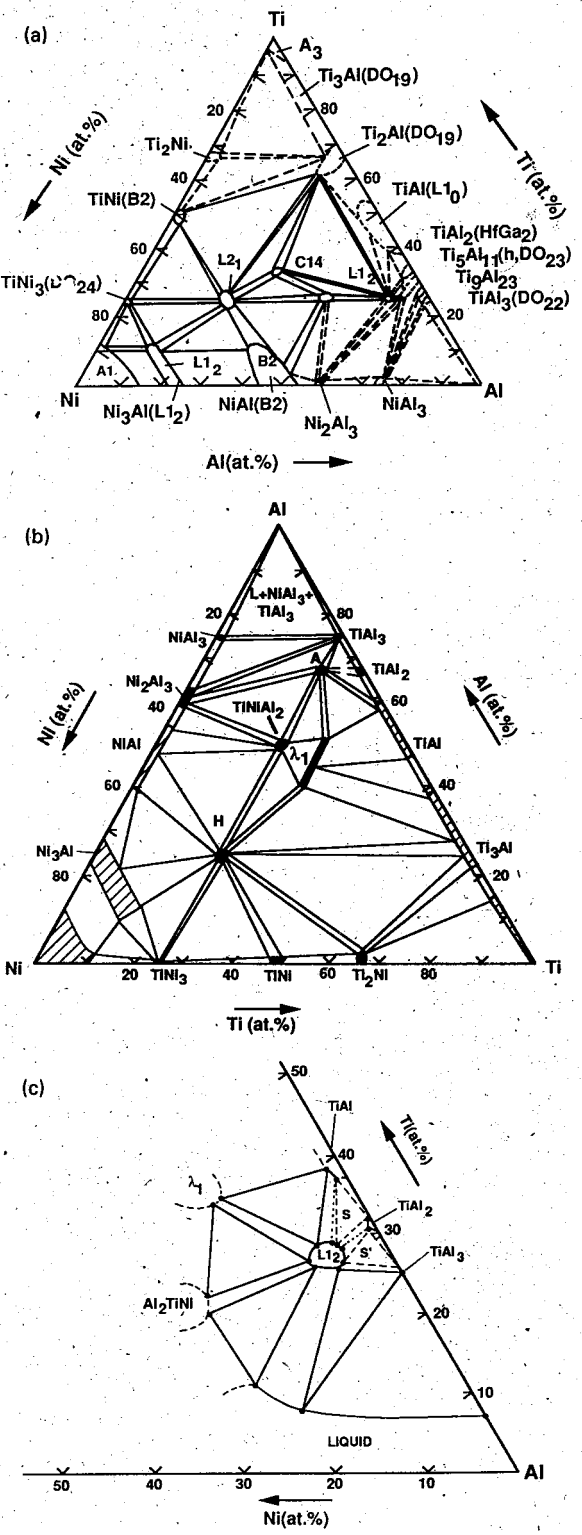

4 Isotherms in Al–Ti–Ni system *a* at 1073 K (Ref. 30) and *b* at 1073 K (Ref. 28); *c* extent of Al-rich $L1_2$ phase field at 1473 K (Ref. 26)

claimed that three other ternary compounds existed in the Al–Ti–Ni system: $TiNiAl_2$ with a cubic structure of the type $Mg_6Cu_{16}Si_7$ and a lattice parameter of 1·190 nm (similar to the T_2 phase[29] or the T phase,[28] $TiFeAl_2$, in the Al–Ti–Fe system); a

Heusler's phase ($L2_1$) of the type $TiNi_2Al$ with a lattice parameter 0·586 nm (labelled H in Fig. 4*b*); and a *C*14 ($MgZn_2$) phase, TiNiAl, with lattice parameters $a = 0{\cdot}4999$ nm and $c = 0{\cdot}8049$ nm.[28] While Markiv *et al.*[28] indicated the presence of a ternary compound λ, which corresponds to the TiNiAl (*C*14) composition of Raman and Schubert[30] (Fig. 4*a* and *b*), the range of compositions over which this compound was supposed to exist was very different in the two studies. Markiv *et al.*[28] associated a composition range of 33·3 at.-% Ti and 41–51 at.-% Al with λ, whereas Raman and Schubert[30] indicated a very small composition range centred on 33·3Ti–33·3Al–33·3Ni (at.-%). Finally, the binary compounds Ni_3Al ($L1_2$) and NiAl (*B*2) both showed a significant solubility for Ti (greater than 10 at.-%) according to Raman and Schubert,[30] whereas Markiv *et al.*[28] claimed this to be true only for Ni_3Al. A comparison of the phase equilibria in the Al–Ti–Ni system based on the isotherm due to Raman and Schubert[30] with that due to Markiv *et al.*[28] reveals several differences. For example, a three phase region of AlNiTi + $Al_{67}Ni_8Ti_{25}$ + TiAl is found in the isotherm due to Markiv *et al.*[28] (Fig. 4*b*), whereas a three phase field of AlNiTi + $Al_{67}Ni_8Ti_{25}$ + Ti_3Al is shown by Raman and Schubert[30] (Fig. 4*a*). Such differences imply different solidification sequences and therefore other differences in phase equilibria. Both these studies used similar characterisation techniques, namely optical metallography and X-ray diffraction, to develop the isotherms for the same temperature. Raman and Schubert,[30] however, used only a limited number of samples, whereas Markiv *et al.*[28] used a large number of alloys; Nash *et al.*[32] believe that in spite of using large numbers of specimens, Markiv and co-workers[28] were limited in their accuracy of phase boundary determination by a combination of the complexity of the phase equilibria and the experimental techniques used, although they prefer the 1023 K section due to Markiv *et al.*[28] to that due to Raman and Schubert.[30]

Finally, a comparison of the Al–Ti–Fe and Al–Ti–Ni systems shows that the ternary $L1_2$ compounds exhibited similar stoichiometries in both cases and also a similar sized single phase field for a particular temperature. In addition, in both cases, the size of the phase field decreased when temperature was decreased from 1473 to 1073 K.

Figure 5 shows isotherms for the Al–Ti–Cu system at 1073 and 773 K due to Markiv *et al.*,[28] at 1073 K due to Raman and Schubert,[30] at 813 K from the investigations of Virdis and Zwicker,[34] and at 1473 K for the $L1_2$ phase field.[26] These investigations all agree on the presence of three ternary compounds in this system, with compositions and structures as follows: (a) a Heusler alloy, Cu_2TiAl (T_1), with an $L2_1$ structure, a lattice parameter of 0·601 nm, and a melting point of 1398 K (in other studies,[35,36] Cu_2TiAl is claimed to have a CsCl structure with $a = 0{\cdot}394$ nm); (b) CuTiAl (T_2), with a *C*14 ($MgZn_2$) structure, parameters of $a = 0{\cdot}500$ nm and $c = 0{\cdot}810$ nm, and a melting point of 1423 K; and (c) $CuTi_2Al_5$ (T3), with an $L1_2$ structure, $a = 0{\cdot}3927$ nm, and a melting point of 1623 K, in agreement with later work.[24] These phases are labelled H, λ, and A in the isotherms due to Markiv *et al.*[28] Of the various binary phases, only $CuTi_2$ and TiAl have any appreciable solubility for the ternary element. All three ternary compounds show a significant compositional range of existence at 813 K according to Virdis and Zwicker[34] (Fig. 5*d*), whereas Raman and Schubert[30] show this to be true only for the *C*14 compound, CuTiAl. In fact, the $L1_2$ phase field is much smaller at 1073 K (Fig. 5*c*) than at 813 K (Fig. 5*d*). Markiv *et al.*[28] show the shape of the $L1_2$ single phase field as a line, implying an almost fixed titanium content for a range of aluminium and copper levels (Fig. 5*a* and *b*). At 1473 K, the $L1_2$ phase field, according to Mazdiyasni *et al.*,[26] is fairly large in comparison with that reported by Raman and Schubert[30] at 1073 K, and is more in line with the compositional range indicated by Virdis and Zwicker.[34] The isotherm due to Raman and Schubert,[30] however, was developed based on a limited number of samples and is therefore not a reliable indicator of the shape and extent of the single phase $L1_2$ compound. The phase field described by Mazdiyasni *et al.*[26] is believed to be accurate and is preferred over the other isotherms.

Virdis and Zwicker[34] examined the Al–Ti–Cu system in detail, generating the liquidus projection as well as the reaction summary for the three binary and the ternary systems. In their study, however, they did not consider the presence of long period superstructures in the Al–Ti system; thus, the $L1_2$ phase was shown to be in equilibrium with TiAl and Al_3Ti only, and not Al_2Ti as observed by Mazdiyasni *et al.*[26] and Markiv *et al.*[28] In fact, Markiv *et al.*[28] showed that the $L1_2$ compound was not in equilibrium with Al_3Ti. Such differences in results in the binary system influence the determination of solidification sequences and compositional stability as a function of temperature for alloys of interest (in this case, the $L1_2$ compound Ti_2CuAl_5) and must be resolved.

Although Co is located on the periodic table between Fe and Ni, the Al–Ti–Co system has received much less attention than the Al–Ti–Fe, Al–Ti–Ni, and Al–Ti–Cu systems. In terms of electronic configuration, Co has a structure given by $[Ar]3d^74s^2$, which lies between the $[Ar]3d^64s^2$ and $[Ar]3d^84s^2$ of Fe and Ni. Cobalt, however, has a hexagonal structure at room temperature, similar to zinc, whereas Fe, Ni, and Cu are all cubic. At temperatures above 673 K, Co goes from a hexagonal to a cubic structure. It would appear logical that if an Al-rich $L1_2$ compound is present in the Al–Ti–Fe, Al–Ti–Ni, Al–Ti–Cu, and Al–Ti–Zn systems, it could also be expected to be present in the Al–Ti–Co system.

Markiv[37] examined the Al–Ti–Co system using more than 100 alloy compositions, and generated a complete isotherm at 1073 K with the aid of X-ray, microstructural, and dilatometric analysis. For this purpose, alloys were annealed in evacuated quartz ampoules containing titanium chips at 1073 K for a

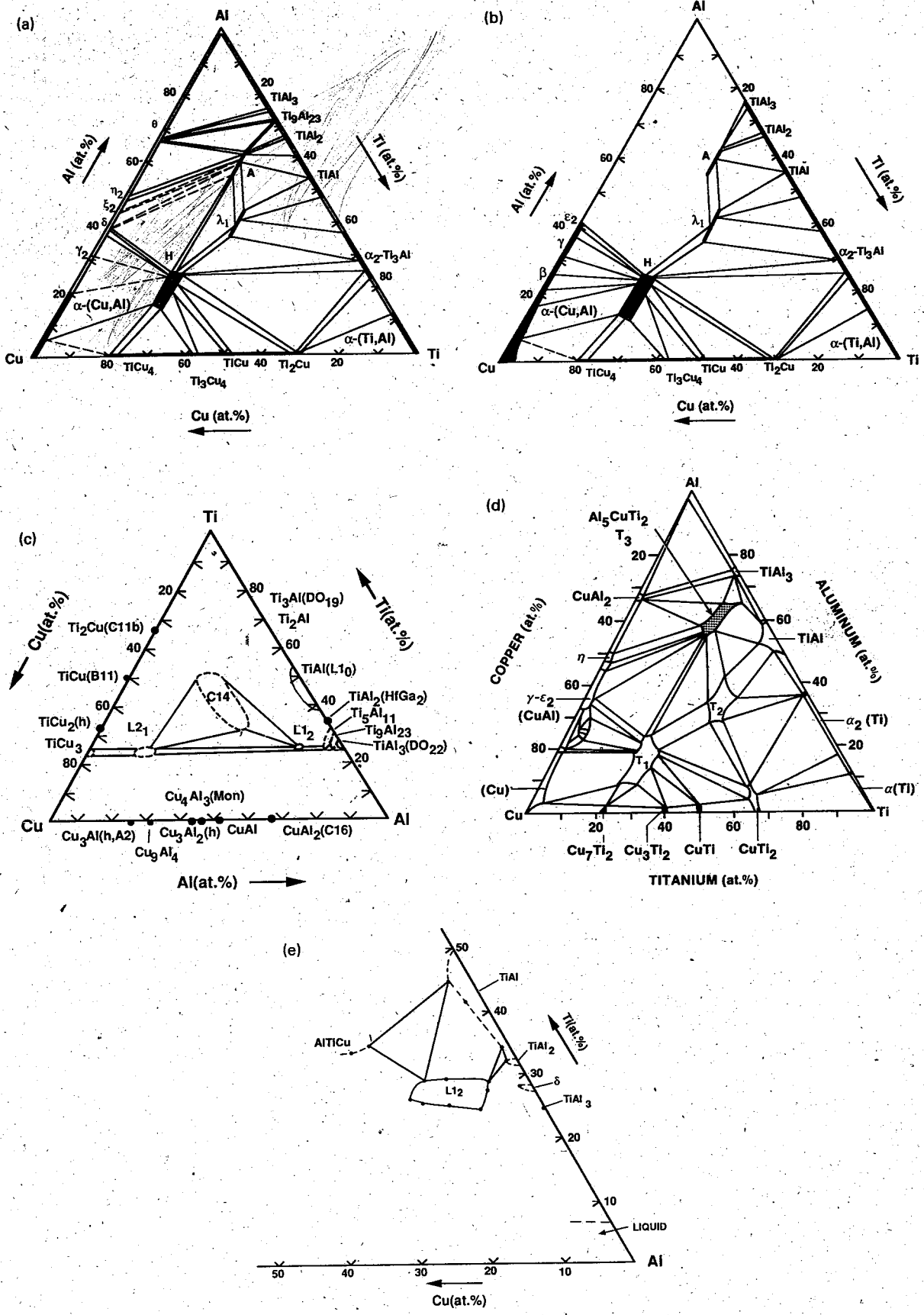

5 Isotherms in Al–Ti–Cu system *a* at 1073 K (Ref. 28), *b* at 773 K (Ref. 28), *c* at 1073 K (Ref. 30), *d* at 813 K (Ref. 34); *e* extent of Al-rich $L1_2$ phase field at 1473 K (Ref. 26)

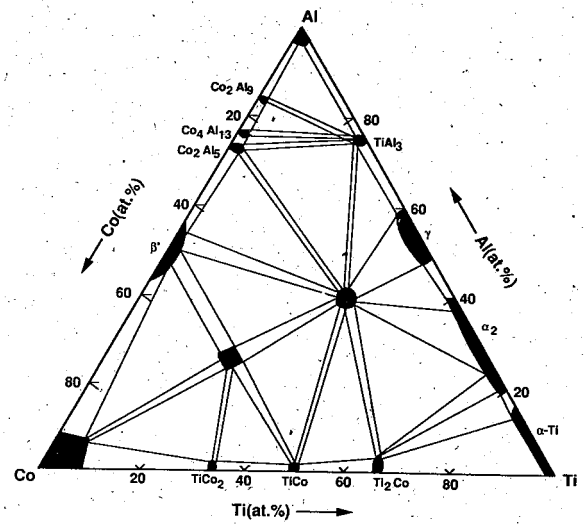

6 1073 K isothermal section of Al–Ti–Co system (Ref. 37)

period of one month and then water quenched. The resulting isotherm is shown in Fig. 6. The first interesting feature is that Al_3Ti is in equilibrium with Co_2Al_9, Co_4Al_{13}, Co_2Al_5, a ternary compound Ti_2CoAl_2, and TiAl. No ternary Al-rich $L1_2$ compound was identified in this system at 1073 K. The crystal structure of Ti_2CoAl_2 was not determined. Another ternary compound, $TiCo_2Al$, with the $L2_1$ structure (Heusler alloy) and a lattice parameter of 0·5847 nm, was in equilibrium with Ti_2CoAl_2, Co-based solid solution, Ti–Co, $TiCo_2$, and CoAl. At this temperature, the Co solid solution had a cubic structure. Thus, the exact requirements for the formation of an Al-rich $L1_2$ compound in the Al–Ti–X systems are not clear, as there appears to be no systematic pattern in the alloying additions required for 'converting' Al_3Ti ($D0_{22}$) to an $L1_2$ structure'. The uncertainties involved are compounded by insufficient experimental data in terms of isotherms at various temperatures, especially near ambient. For example, it is possible that an $L1_2$ compound exists in the Al–Ti–Co system, but is not stable at 1073 K and is therefore not seen on a 1073 K isotherm.

Raman and Schubert[38] studied the Zn_3Ti–Al_3Ti section of the Al–Ti–Zn system. Binary Al_3Ti has a $D0_{22}$ structure, while Zn_3Ti crystallises in the $L1_2$ structure. A ternary $L1_2$ compound of the composition $Ti_{25}Zn_9Al_{66}$, with $a = 0{\cdot}392$ nm, was reported. In addition, a ternary $D0_{23}$ compound, Ti_4ZnAl_{11}, was reported, possibly in equilibrium with the $L1_2$ compound. Based on an extensive study, Raman and Schubert[38] concluded that as the outer electronic concentration was increased, the crystal structure stability increased in the order $L1_2$ to $D0_{23}$ to $D0_{22}$. Until recently, phase equilibria information could not be found in the Al-rich portion of the Al–Ti–Cr and Al–Ti–Mn systems, except for the existence of an equiatomic Al–Ti–Mn phase with the $MgZn_2$ structure, $a = 0{\cdot}4978$ nm, $c/a = 1/64$ (Ref. 39). Recently, however, Mabuchi *et al.*[40] have found an Al-rich $L1_2$ compound in the Al–Ti–Mn system with a composition corresponding to $Al_{66}Mn_9Ti_{25}$. This compound was shown to have significant compressive ductility at room temperature. In addition, Zhang *et al.*,[25] have confirmed the existence of an Al-rich $L1_2$ compound in the Al–Ti–Mn system and also claim the presence of a similar compound in the Al–Ti–Cr system. Of significant relevance is the observation of some ambient bend ductility in these two $L1_2$ compounds, although failure was primarily by transgranular cleavage. This is the first instance where plastic deformation has been observed in a tensile deformation mode in these $L1_2$ compounds.

Al–Zr–X systems

The binary Al–Zr system has received less attention than the binary Al–Ti system, but is known to contain at least nine intermetallics, with compositions corresponding to Zr_3Al, Zr_2Al, Zr_5Al_3, Zr_3Al_2, Zr_4Al_3, ZrAl, $ZrAl_2$, and $ZrAl_3$. Of the various compounds studied in the Al–Zr system, Zr_3Al with an $L1_2$ structure has received the most attention.[41,42] The trialuminide Al_3Zr, with a melting point of 1850 K, a density of 4·1 g cm^{-3}, an elastic modulus of 196 GN m^{-2} (Ref. 43), and a $D0_{23}$ crystal structure, however, has been the centre of interest in this binary system recently. Although Al_3Zr has a $D0_{23}$ crystal structure, it is interesting to note that under certain conditions, in a supersaturated aluminium alloy matrix, it can be made to precipitate from the solid state with a metastable $L1_2$ structure,[44,45] which after prolonged high temperature exposure, transforms to the equilibrium $D0_{23}$ structure. Gayle and Vandersande[46] showed that the metastable $L1_2$ Al_3Zr had a significant solubility for Li.

Schneibel and Porter[47] studied the compression behaviour of Al_3Zr at 1373 K and found significant cracking even at this temperature under a compressive load. The possibility of transforming the $D0_{23}$ Al_3Zr to a more symmetric $L1_2$ structure via alloying, thereby improving its ductility, is intriguing and indeed this approach was recently attempted using theory[48] and experiments.[47] It must be pointed out, however, that even though the ternary $L1_2$ compounds appear to have improved ductility over their $D0_{22}$ binary counterparts, they appear to be brittle in tension at room temperature, except for the observation of ambient bend ductility of ~0·5% in the Al–Ti–Mn and Al–Ti–Cr systems,[25] and even then, failure occurred by transgranular cleavage. George *et al.*[27] have used selected area electron channelling patterns to identify the cleavage planes in an $L1_2$, Al–Ti–Fe–V alloy. They found two cleavage planes in this alloy – the {110} type and the {111} type planes. They speculate that the presence of several such low cleavage strength planes may explain the brittle behaviour of these compounds. It is interesting to note that the alloy investigated in this study,[27] was directionally solidified with the ⟨100⟩ growth direction and bend tests were made on samples lying along the growth direction. This would make the {100} planes lie normal to the tensile axis and yet no {100} cleavage was observed, suggesting high cleavage strength for {100} planes.

Freeman and co-workers[48,49] used band energy calculations to identify potential alloying additions for transforming $D0_{23}$ Al_3Zr to a ternary $L1_2$ compound. The results of his calculations pointed to Mg and Li as potential candidates to yield compounds of the type Al_5MgZr_2 and Al_5LiZr_2, although no experimental evidence is as yet available to confirm the theoretical predictions. Drits *et al.*[50] studied the Al-rich region of the Al–Mg–Zr system and tentatively identified a ternary $Al_xMg_yZr_z$ (T) phase which was in equilibrium with aluminium solid solution at 673 K. They did not, however, provide any details on the composition, crystal structure, or melting point of this T phase. Whether this phase corresponds to the $L1_2$ phase predicted by Freeman[49] remains to be verified.

Raman[18] provides an isotherm for the Al–Zr–V system at 1373 K (Fig. 7*a*). A ternary $L1_2$ compound in equilibrium with Al_3Zr, Al_2Zr, and the $A2$ vanadium solid solution was identified and claimed to have a composition $Zr_{22}V_9Al_{69}$, with vanadium atoms substituting in both the aluminium and titanium sites. The lattice parameter of this $L1_2$ phase was identified as 0·407 nm. The $C14$ $ZrAl_2$ phase shows extensive solubility for vanadium (~60 at.-% V) and is in equilibrium with the $C15$ phase ZrV_2, which exhibits about 10 at.-% solubility for aluminium. $D0_{23}$ $ZrAl_3$ dissolves ~5 at.-% V, forming a two phase region with $D0_{22}$ Al_3V, which exhibits ~5 at.-% solubility for zirconium. No other ternary phases were identified in this system.

Studies on the Al–Zr–Cr system by Zarechnyuk *et al.*[51] were restricted to the regions confined by Al, $CrAl_7$, and $ZrAl_3$. Based on this study, they concluded that there was no ternary phase in equilibrium with aluminium solid solution and that the two binary compounds $CrAl_7$ and $ZrAl_3$ were in equilibrium with each other. Subsequently, Markiv and Burnashova[52] investigated the entire Al–Zr–Cr system using arc melted samples, characterising them in the as cast and heat treated conditions. Samples weighed 10 g and spot chemical analysis and weight determinations established that aluminium or chromium loss did not exceed 0·05–0·03 g. Thus, an excess of aluminium and chromium were incorporated in the starting charge to compensate for losses. In each case, the final alloy composition was assumed to correspond to the calculated charge composition. Alloy specimens were annealed in evacuated quartz capsules at 1073 and 773 K for periods of 1000 and 2200 h, respectively, and then cold water quenched. Microstructural characterisation included X-ray diffraction using unfiltered Cr radiation and optical metallography. The results of their study are shown in the form of an isotherm at 1073 K in Fig. 7*b*. The first observation is that no ternary compounds formed in this system. $ZrAl_2$ exhibits significant solubility for chromium (up to ~55 at.-% Cr) and is in equilibrium with $ZrCr_2$, which dissolves up to ~7·5 at.-% Al at 1073 K. $ZrAl_3$ exhibits a two phase equilibrium with each of the Al–Cr binary compounds Cr_2Al_{11}, $CrAl_4$, $CrAl_3$, Cr_4Al_9, and Cr_5Al_8. While this might initially appear to contradict the earlier work of Zarechnyuk *et al.*,[51] where $ZrAl_3$ was shown to be

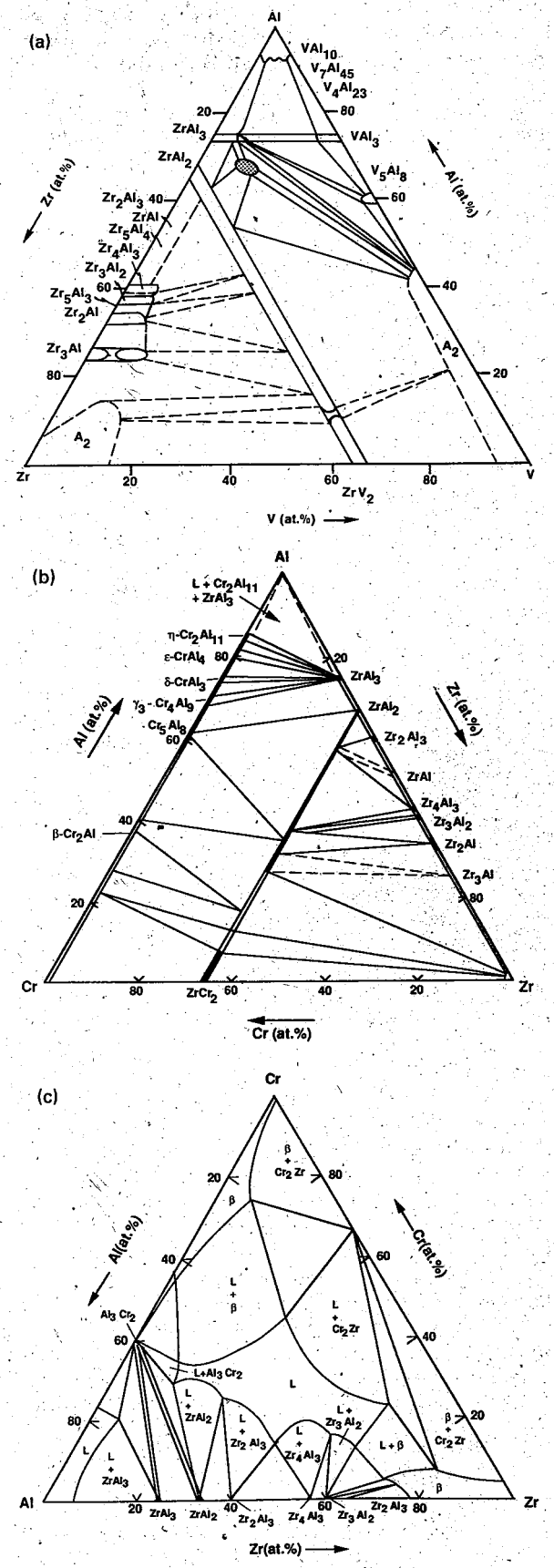

7 Isothermal sections in *a* Al–Zr–V system at 1373 K (Ref. 18); *b* Al–Zr–Cr system at 1073 K (Ref. 52); *c* 1523 K isotherm in Al–Zr–Cr system (Ref. 53)

in equilibrium with $CrAl_7$, it must be pointed out that $CrAl_7$ forms peritectically at ~1000 K, while the isotherm due to Markiv and Burnashova[52] (Fig. 7*b*) is at 1073 K.

Chart[53] calculated the Al–Zr–Cr phase diagram using thermodynamic data available for the respective binary systems and minimising the Gibb's free energy of formation of the various phases to generate phase boundaries. However, in these computations, Chart assumed the absence of ternary compounds, at least down to 1523 K, and the mutual insolubility of the *C*14 Laves phase $ZrAl_2$ and the cubic *C*15 Cr_2Zr phase. A 1523 K isotherm resulting from these calculations is shown in Fig. 7*c*. At 1523 K, $ZrAl_3$ is in equilibrium with Al_3Cr_2, which is also in equilibrium with Al_2Zr. Markiv and Burnashova[52] do not show an Al_3Cr_2 phase, but rather Cr_5Al_8 in equilibrium with Al_2Zr and Al_3Zr (cf Fig. 7*b* and *c*). Also, Chart's computations allowed no aluminium solubility in Cr_2Zr and no chromium solubility in Al_2Zr, even at 1523 K; in contrast, Markiv and Burnashova showed experimentally significant solubilities for the third element in these binary compounds at 1073 K (cf Fig. 7*b* and *c*).

Recently, Schneibel and Porter[47] claimed the presence of an Al-rich $L1_2$ compound in the Al–Zr–Cr system with a composition corresponding to 25Zr–6Cr–69Al (at.-%). However, in their earlier work, Markiv and Burnashova[52] contended that no ternary compounds were present in the Al–Cr–Zr system. It is conceivable that the $L1_2$ compound reported by Schneibel and Porter[47] was stable at lower temperatures (<1073 K), although no further information on its stability was provided. Thus, more work is needed in this ternary system to clarify the differences observed in the various investigations.

No information is available on the Al–Zr–Mn system, except for the identification of two ternary phases: $ZrMn_6Al_6$ with a $ThMn_{12}$ structure (a = 0·867 nm and c = 0·501 nm) (Ref. 54) and an equiatomic ZrMnAl with the hexagonal $MgZn_2$ structure (a = 0·525 nm and c/a = 1·63).[39] ZrMnAl was claimed to be a solid solution of $ZrMn_2$ and $ZrAl_2$, both of which are $MgZn_2$-type phases; thus it is not a true ternary phase.

Figure 8 shows isotherms at 1173 K for the Al–Zr–Fe and Al–Zr–Co systems, and at 1073 K for the Al–Zr–Ni and Al–Zr–Cu systems, respectively. These four systems are very similar in the types of ternary phases present; gradual differences can be seen in the progression Al–Zr–Fe to Al–Zr–Co to Al–Zr–Ni to Al–Zr–Cu.

In the Al–Zr–Fe system,[55,58] four ternary intermetallic phases are seen at 1173 K: Zr_6FeAl_2 with a hexagonal structure (a = 0·794 nm, c = 0·332 nm), $ZrFe_{7\cdot4}Al_{5\cdot8}$ with the $ThMn_{12}$ structure, λ_1 with a composition $ZrFe_{1\cdot25-0\cdot5}Al_{0\cdot75-1\cdot50}$ and the $MgZn_2$ structure, and λ_2 with a composition $ZrFe_{0\cdot35-0\cdot30}Al_{1\cdot65-1\cdot70}$ and the $MgCu_2$ structure. The binary $ZrFe_2$ phase extends ~15 at.-% Al into the ternary isotherm at 1173 K, whereas $ZrAl_2$ does not show any significant solubility for iron. No ternary Al-rich $L1_2$ phase is seen at 1173 K in this system, unlike the Al–Ti–Fe system discussed above. However, recently Schneibel and Porter[47] claimed the existence of a ternary $L1_2$ Al–Zr–Fe phase with the composition Al–5·5Fe–25Zr (at.-%) and actually claimed to have tested this $L1_2$ phase in compression at 1373 K. Why this phase is not present in the 1173 K isotherm of Burnashova and Markiv[55] is not clear. It is possible that the reported Al–Zr–Fe $L1_2$ phase was not stable at 1173 K and that Schneibel and Porter[47] were not really testing the $L1_2$ phase at 1373 K. These differences still remain unresolved and require further careful attention.

The $Zr–ZrAl_2–ZrCo_2$ section of the Al–Zr–Co system is remarkably similar to the $Zr–ZrAl_2–ZrFe_2$ section of the Al–Zr–Fe system (cf Fig. 8*a* and *b*), in that both contain λ_1 and λ_2, and a ternary phase of the type Zr_6CoAl_2 (Zr_6FeAl_2), where λ_1 and λ_2 in both cases exhibit similar compositional ranges of stability. Further, like $ZrFe_2$, $ZrCo_2$ exhibits significant (~10 at.-%) solubility for aluminium, and $ZrAl_2$ shows negligible solubility for iron, as well as cobalt. The section of the Al–Zr–Co isotherm bounded by $Al–Co–ZrCo_2–ZrAl_2$ is different from the corresponding region in the Al–Fe–Zr system, in that three ternary compounds are present, with compositions corresponding to $ZrCoAl_4$, $Zr_6Co_7Al_{16}$, and $ZrCo_2Al$. $ZrCoAl_4$ is hexagonal with a = 0·726 nm and c = 0·909 nm, while $Zr_6Co_7Al_{16}$ is cubic with the Th_6Mn_{23} structure and a lattice parameter of 1·217 nm. $ZrCo_2Al$ is a Heusler phase ($L2_1$) with a = 0·6081 nm.[36] Once again, no Al-rich $L1_2$ phase was identified in the Al–Zr–Co system. In both the Al–Zr–Fe and the Al–Zr–Co systems,[55,56] the crystal structures and phase equilibria were studied using X-ray diffraction and metallography. Over 100 samples were prepared in each system by electric arc melting of the appropriate amounts of the pure constituent elements in an argon atmosphere. The resulting alloys, assumed to have the calculated compositions, were annealed in evacuated quartz capsules at 1173 K for 2100 h and then cold water quenched and characterised.

The Al–Zr–Ni system has been investigated to a greater extent than the Al–Zr–Fe or Al–Zr–Co systems. The isotherm in Fig. 8*c* was taken from the work of Burnashova and Markiv[57] and a comparison with the Al–Zr–Co system (Fig. 8*b*) reveals several similarities and differences. At least seven ternary phases are present in the Al–Zr–Ni system, and the phase Zr_6NiAl_2 is isostructural with Zr_6CoAl_2 and Zr_6FeAl_2.[59] Further, the λ_2 phase with the $MgCu_2$ structure, which is in equilibrium with $ZrAl_2$ in the Al–Zr–Co and Al–Zr–Fe systems, is also present in the Al–Zr–Ni system, with a compositional range of stability defined by $ZrNi_{0\cdot5-0\cdot2}Al_{1\cdot5-1\cdot8}$. The Heusler phase, $ZrNi_2Al$ (H; a = 0·6123 nm), in the Al–Zr–Ni system is the analogue of the $ZrCo_2Al$ in the Al–Zr–Co system. In an earlier study by Heine and Zwicker,[35] the $ZrNi_2Al$ compound was assigned a CsCl structure, which contradicts the study of Burnashova and Markiv,[57] as well as an earlier study by Markiv *et al.*[36] In addition, there are four ternary phases with

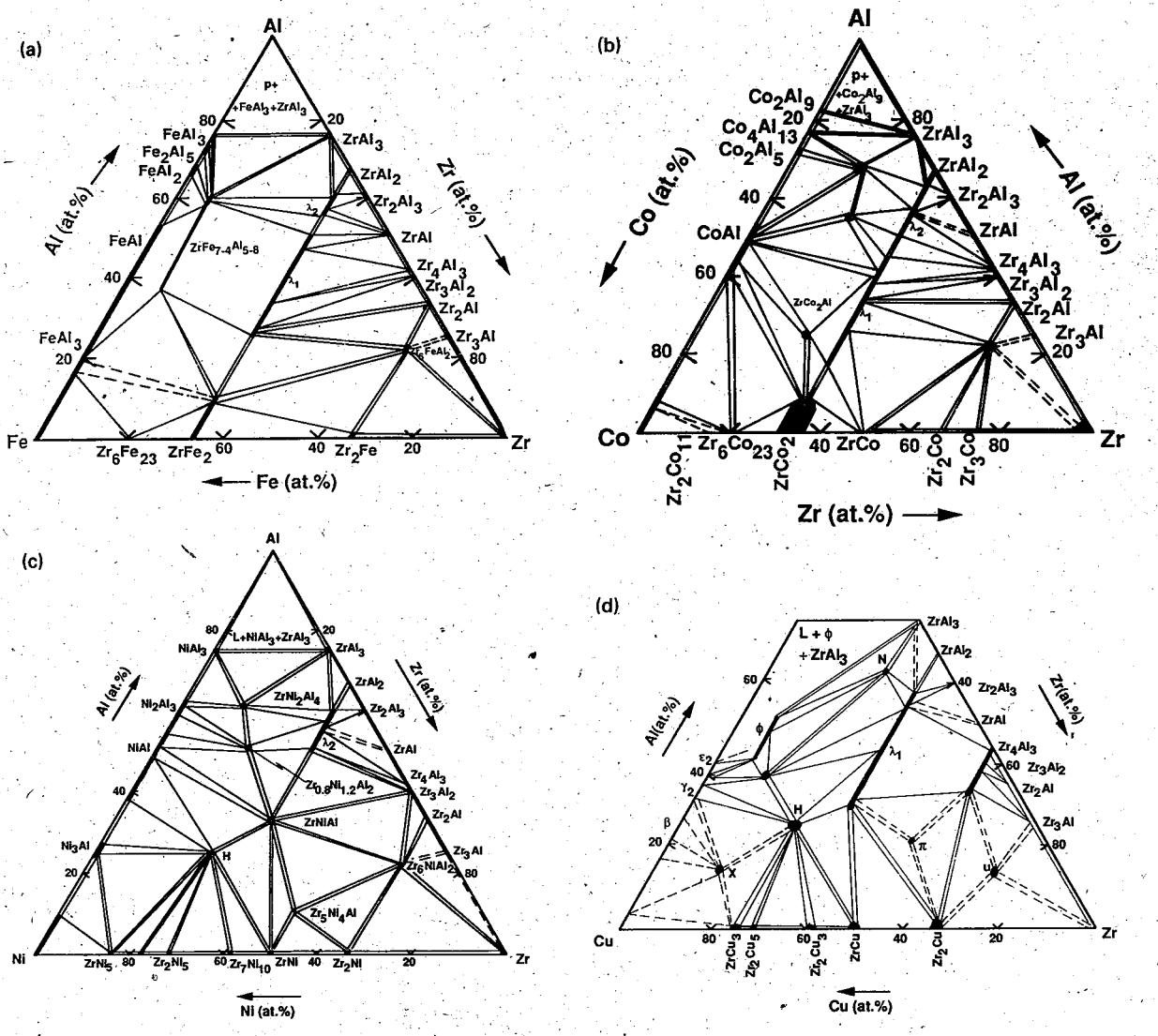

8 Isotherms in *a* Al–Zr–Fe system at 1173 K (Ref. 55); *b* Al–Zr–Co system at 1173 K (Ref. 56); *c* Al–Zr–Ni system at 1073 K (Ref. 57); *d* Al–Zr–Cu system at 1073 K (Ref. 52)

compositions corresponding to Zr_5Ni_4Al; the equiatomic ZrNiAl with the hexagonal iron phosphide structure (Fe_2P); $Zr_{0.8}Ni_{1.2}Al_2$ with $a = 1{\cdot}208$ nm; and $Zr_3Ni_6Al_{16}$ with a tetragonal structure, lattice parameters of $a = 0{\cdot}401$ nm and $c = 1{\cdot}441$ nm, and a unit cell containing 14 atoms. Subsequently,[60] the composition of the last compound ($Zr_3Ni_6Al_{16}$) was changed to Al_5Ni_2Zr and assigned a new structure belonging to the symmetry class of *I*4/*mmm* with 16 atoms per unit cell.

In contrast, Raman and Schubert,[30] from their investigation of the Al–Zr–Ni system, claimed that the equiatomic phase, ZrNiAl, had the cubic *C*15 structure with a lattice parameter of $a = 0{\cdot}734$ nm. In addition, they also reported the presence of a ternary Al-rich $L1_2$ compound, Zr_2NiAl_5, with a lattice parameter of 0·406 nm. Such a single phase field was not found in the Soviet investigations. In fact, Markiv *et al.*[61] specifically referred to the work of Raman and Schubert[30] and emphasised the disagreement between their two investigations, including the absence of the $L1_2$ phase Zr_2NiAl_5. These differences in observations need to be clarified.

In this context, Raman and Schubert[30,38,62] have provided only brief details of the experimental procedure adopted in their phase equilibria efforts and the purities of the starting materials are not provided. It appears that their samples were arc melted in an argon atmosphere and then subsequently vacuum heat treated at 1073 or 1223 K for extended periods of time. The sample size is not specified. No mention is made of agreement between intended and final alloy compositions or if the compositions were even measured. On the other hand, Markiv *et al.*[61] provide complete details of their experimental procedure. They examined 99 alloy compositions and prepared the alloys by melting a charge of zirconium iodide (99·96% Zr), 99·99% Ni, and 99·9% Al in an electric arc furnace using an unconsumable tungsten electrode on a water cooled copper plate. Excess aluminium

(50–150 mg/10 g of sample) was added to compensate for losses during melting. However, the alloy composition was never measured, but assumed to be that intended. The cast alloys were heat treated in evacuated quartz ampoules at 1173 K for 700 h and then cold water quenched. The microstructure was analysed using X-ray diffraction and metallography. What is extremely puzzling is the fact that Raman and Schubert[30] claimed the presence of the $L1_2$ compound Zr_2NiAl_5 with very few samples and yet Markiv *et al.*,[61] who examined several samples around the above composition did not find the $L1_2$ phase. Unfortunately, none of the investigators specifies the impurity levels in their alloys and it is well known that minor impurity levels can significantly influence the stability of these $L1_2$ phases.[63,64]

The presence of an $L1_2$ compound in the Al–Cu–Zr system with a composition Zr_2CuAl_5 and a lattice parameter of 0·404 nm was confirmed by Raman and Schubert,[30] Markiv and Burnashova,[52] and Zarechnyuk *et al.*[51] Figure 8*d* shows an isotherm at 1073 K from the work of Markiv and Burnashova.[52] In addition to the $L1_2$ compound, Raman and Schubert reported the existence of two other ternary compounds, $ZrCu_2Al$ with the $L2_1$ structure and ZrCuAl with a $C15$ structure. They claimed that the $L1_2$ compound, Zr_2CuAl_5, was in equilibrium with the binary compounds $ZrAl_3$, $ZrAl_2$, and $CuAl_2$, but not with aluminium,[51] although the isotherm at 1073 K (Fig. 8*d*), due to Markiv and Burnashova,[52] shows the $L1_2$ compound (N) to be in equilibrium with $ZrAl_3$, ψ ($ZrCu_6Al_6$), Z, λ_2, and $ZrAl_3$. Zarechnyuk *et al.*[51] investigated only the Al-rich corner of this ternary system, and it is likely that their investigation was not complete enough to identify the other ternary phases reported by Markiv and Burnashova.[52] The ψ phase was assigned the $ThMn_{12}$ structure (tetragonal), with $a = 0{\cdot}490$–$0{\cdot}512$ nm and $c = 0{\cdot}856$–$0{\cdot}850$ nm. The H phase ($ZrCu_2Al$) was found to be $L2_1$, with a lattice parameter of $a = 0{\cdot}6215$ nm, in agreement with Raman and Schubert[30] but in contradiction to the earlier claim of Heine and Zwicker[35] that $ZrCu_2Al$ had the CsCl structure. The isotherm at 1073 K (Fig. 8*d*) does not show the equiatomic phase ZrCuAl, reported by Raman and Schubert[30] to have a $C15$ structure, but does show the λ_2 phase with a composition range 33Zr–37-10Cu–30-57Al (at.-%) and the $MgCu_2$ structure.

Once again, the reasons for these observed differences are not clear, but further work is required to clarify the situation. All the other ternary compounds in the Al–Zr–Cu system (K, U, π, and Z) exhibited a very small compositional range of existence and their crystal structures have not been identified. In addition, a lower temperature isotherm at 773 K (figure not shown)[52] suggests the presence of an additional ternary compound, E, whose composition corresponds to 12Zr–24Cu–64Al (at.-%). This phase is in equilibrium with $CuAl_2$, ψ (which has a more restricted compositional range of stability at 773 K than at 1073 K), and $ZrAl_3$. Its crystal structure was not determined. Of the various binary compounds, Zr_4Al_3 was the only one that exhibited appreciable solubility (~10 at.-%) for the third element (Cu in this case) at 1073 K.

At 1073 K, the pseudobinary system $ZrZn_3$–$ZrAl_3$ exhibited an $L1_2$ compound, $ZrZnAl_2$,[38] with a lattice parameter $a = 0{\cdot}403$ nm, which was probably in equilibrium with $ZrZn_3$, $ZrAl_3$, $ZrAl_2$, and $ZrZn_2$. Subsequently, Drasner and Blazina[65] examined the pseudobinary $ZrZn_2$–$ZrAl_2$ section and found that, depending on the composition and/or thermal treatment, they obtained alloys with the $L1_2$ structure. $ZrZn_2$ exhibits the MgCu-type $C15$ structure, while $ZrAl_2$ is of the $C14$ $MgZn_2$ type. Two new ternary phases were identified, $ZrZn_{0{\cdot}5}Al_{1{\cdot}5}$ with the $C15$ structure type and $ZrZn_{1{\cdot}5}Al_{0{\cdot}5}$ with the $L1_2$ structure. The observation of an $L1_2$ structure along the $ZrZn_2$–$ZrAl_2$ tie line was attributed to the widely extended homogeneity region of the $L1_2$ phase field in the region $ZrZn_2Al$–$ZrZn_{0{\cdot}8}Al_{2{\cdot}2}$ on the $ZrZn_3$–$ZrAl_3$ tie line. Correlation of measured and calculated X-ray intensities of the $L1_2$ phase revealed a best fit described by the formula $Zr(Zr, Zn, Al)_3$, implying that the Zr atoms occupied corner and face centred sites. The authors argued[65] that this is not unusual because in binary Zr_3Al ($L1_2$) and Al_3Zr, zirconium atoms occupy the face centred and corner sites, respectively.

While the focus of this review is largely ternary additions leading to the formation of $L1_2$ phases from binary $D0_{22}$ (or $D0_{23}$) structures, it is interesting to consider cases where the $D0_{22}$ structure is stabilised with ternary additions in preference to the binary $D0_{23}$, or even $L1_2$ structures. A case in point is the addition of Cu to Al_3U, which transforms the binary $L1_2$ compound to a ternary $D0_{22}$ structure.[66] Similarly, the addition of Si to Al_3Ti extends the $D0_{22}$ composition significantly. Al_3Ti exhibits as much as 15 at.-% solubility for Si at 973 K.[62] In fact, the addition of Si to Al_3Zr ($D0_{23}$) actually promotes the formation of a ternary $D0_{22}$ phase at 973 K (Ref. 62) which has a stoichiometry corresponding to Zr_2Al_5Si and is in equilibrium with $ZrAl_3$ (Fig. 9). The composition of this phase in terms of the ratio of the three constituents is similar to that of the ternary $L1_2$ intermetallics Al_5CuTi_2 or $Al_{67}Fe_8Ti_{25}$. Other features that are noteworthy in the Al–Zr–Si system include the extensive solubility of Al in the binary phases Zr_5Si_3, Zr_5Si_4, ZrSi, and $ZrSi_2$, and the presence of a ternary tetragonal phase $Zr_3Al_4Si_5$ with $a = 0{\cdot}371$ nm and $c = 2{\cdot}935$ nm.

Al–Hf–X systems

The binary Hf–Al phase diagram is not very well established in terms of the liquidus temperatures. At least seven binary intermetallics are known to exist in the system,[67] including Hf_2Al ($C16$), Hf_3Al_2, Hf_4Al_3, HfAl, Hf_2Al_3, $HfAl_2$ ($C14$), and $HfAl_3$. $HfAl_3$ is $D0_{23}$ at low temperature and $D0_{22}$ at high temperatures. It is claimed to melt congruently with a melting point of ~1863 K. In the binary system, HfAl is believed to be the highest melting intermetallic (~2073 K).

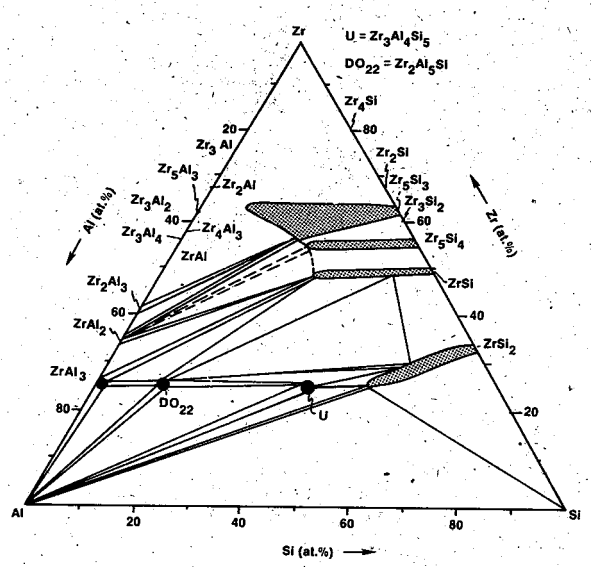

9 Isothermal section in Al–Zr–Si system at 973 K (Ref. 52)

The grain refining effect of Hf in aluminium alloys, together with its ability to inhibit recrystallisation, was examined in Al–Hf alloys prepared by rapid solidification techniques with a wide range of Hf content.[68] In another investigation,[69] the precipitation characteristics of Al_3Hf in aluminium were examined for Al–Hf alloys containing up to 10 wt-% Hf. The role of small Si additions in influencing precipitation kinetics was delineated,[70] and a new metastable intermediate H phase was found to be present when Al_3Hf transitioned from the $L1_2$ to the $D0_{23}$ phase. Subsequently, a mechanism for this transition was proposed,[71] which involved a shear of $\frac{1}{2}[110](110)L1_2$ on every second plane to produce the *Pmmm* H phase, and then a $\frac{1}{2}[010](101)_H$ shear on every second plane to produce the $D0_{22}$ phase. It is not clear, at present, whether the equilibrium form of Al_3Hf in an aluminium matrix is $D0_{22}$ or $D0_{23}$ – although these investigations[68–71] refer to equilibrium Al_3Hf as $D0_{22}$, it is known that the single phase compound Al_3Hf adopts the $D0_{23}$ structure at low temperatures. However, it was clearly shown[71] that the intermediate structure, H, is neither $D0_{23}$ nor $D0_{22}$.

While investigations on the binary Al–Hf system are scant, even less is known about the ternary Al–Hf–X systems (X = Cr, Mn, Fe, Co, Ni, Cu, and Zn). Ternary isotherms or portions thereof are shown in Fig. 10 for the Al–Hf–Fe, Al–Hf–Co, Al–Hf–Ni, and Al–Hf–Cu systems. Each of these isotherms is discussed below and compared with the corresponding ternary isotherms of the Al–Zr–X systems where pertinent.

Figure 10*a* shows the Al–Fe–$HfFe_2$ (λ_1)–$HfAl_2$ (λ_1) portion of the ternary Al–Hf–Fe isotherm at 1073 K.[72] $HfAl_2$ and $HfFe_2$ both exhibit the *C*14 $MgZn_2$ structure and continuous mutual solubility along the tie line $HfAl_2$–$HfFe_2$. In addition, there are two ternary phases, ψ and χ. The ψ phase has a homogeneity range extending along 7·7 at.-% Hf and from ~37 to 61 at.-% Al. It was reported to have the tetragonal $ThMn_{12}$ structure, with a lattice parameter a_0 varying from 0·850 nm (at 37 at.-% Al) to 0·865 nm (at 61 at.-% Al) and $c_0 \approx$ 0·492 nm. The χ phase has a limited homogeneity range, with a composition given by 14Hf–20Fe–66Al (at.-%), but its crystal structure was not determined. A comparison of the Al–Fe–$HfFe_2$–$HfAl_2$ portion of the Al–Hf–Fe isotherm with the corresponding section of the Al–Zr–Fe system (Fig. 8*a*) reveals that the ψ phase ($ZrFe_{7-4}Al_{5-8}$ in the Al–Zr–Fe system) exists over a similar stoichiometric range in both systems. Unlike the Al–Zr–Fe system, where λ_1 and λ_2 are present, $HfFe_2$ (λ_1) and $HfAl_2$ (λ_1) exhibit continuous unlimited mutual solid solubility.

The Al–Co–$HfCo_2$–$HfAl_2$ section of the Al–Co–Hf system resembles the corresponding segment of the Al–Zr–Co isotherm, rather than the Al–Hf–Fe system (cf Fig. 10*b* with Figs. 8*b* and 10*a*). The binary *C*15 $HfCo_2$, like its counterpart $ZrCo_2$, exhibits about 10 at.-% solubility for Al at 1073 K (Ref. 73) and is in equilibrium with a λ_1 type phase (*C*14), whose compositional range of homogeneity lies along 33 at.-% Hf and extends from ~20 to 50 at.-% Al (Fig. 10*b*). A λ_2 type phase (*C*15), also present in equilibrium with λ_1 and $ZrAl_2$, has a much smaller compositional range of existence than λ_1, extending from ~57 to 60 at.-% Al and lying along the 33 at.-% Hf concentration line. Also present are $HfCo_2Al$ with the $L2_1$ (a = 0·6009 nm) structure, $Hf_6Co_7Al_{16}$ with the $ThMn_{23}$ (a = 1·206 nm) structure, and $HfCoAl_4$ and Hf_6CoAl_2 with hexagonal structures. Similar ternary phases were also identified in the Al–Zr–Co system. Three other ternary phases, L′, H′, and X, were identified and reported to have the compositions 20Hf–70Co–10Al (at.-%), 30Hf–52Co–18Al (at.-%), and 4Hf–22Co–74Al (at.-%), respectively. The crystal structures of the L′, H′, and X phases were not determined.

Unlike the Al–Hf–Co and Al–Hf–Fe systems, a complete isotherm at 1073 K is available for the Al–Hf–Ni system (Fig. 10*c*). It is well known that small additions of Hf to Ni_3Al significantly increase the high temperature strength of this material.[2,75] Markiv and Burnashova showed[74] that the solubility of Hf in Ni_3Al was about 7 at.-% at 1073 K. The Al–Hf–Ni isotherm at 1073 K (Fig. 10*c*) shows a remarkable resemblance to the Al–Zr–Ni system (Fig. 8*c*) in terms of the types and structures of ternary phases occurring in the two systems. As in the Al–Zr–Ni system, $NiAl_3$ is in equilibrium with $D0_{23}$ $HfAl_3$. Ternary phases of the type Hf_6NiAl_2, Hf_5Ni_4Al, HfNiAl, λ_2, $Hf_3Ni_6Al_{16}$, $HfNi_2Al$, and $Hf_6Ni_8Al_{15}$ are present and have crystal structures identical to their Zr-based counterparts in the Al–Zr–Ni system. In addition to these ternary phases, three other ternary compounds are present: λ_2^* (~$HfNi_{1·9}Al_{0·1}$) with a cubic structure (a = 0·6905 nm); *C*14-type λ_1 ($HfNi_{0·6}Al_{1·4}$) with a = 0·518 nm and c/a = 1·62; and L ($Hf_4Ni_{16}Al_5$), whose crystal structure was not determined. The λ_2^* phase was reported to be stable above 1273 K and had the $MgCo_2$-type structure (cubic). Except for Ni_3Al, none of the binary compounds exhibited

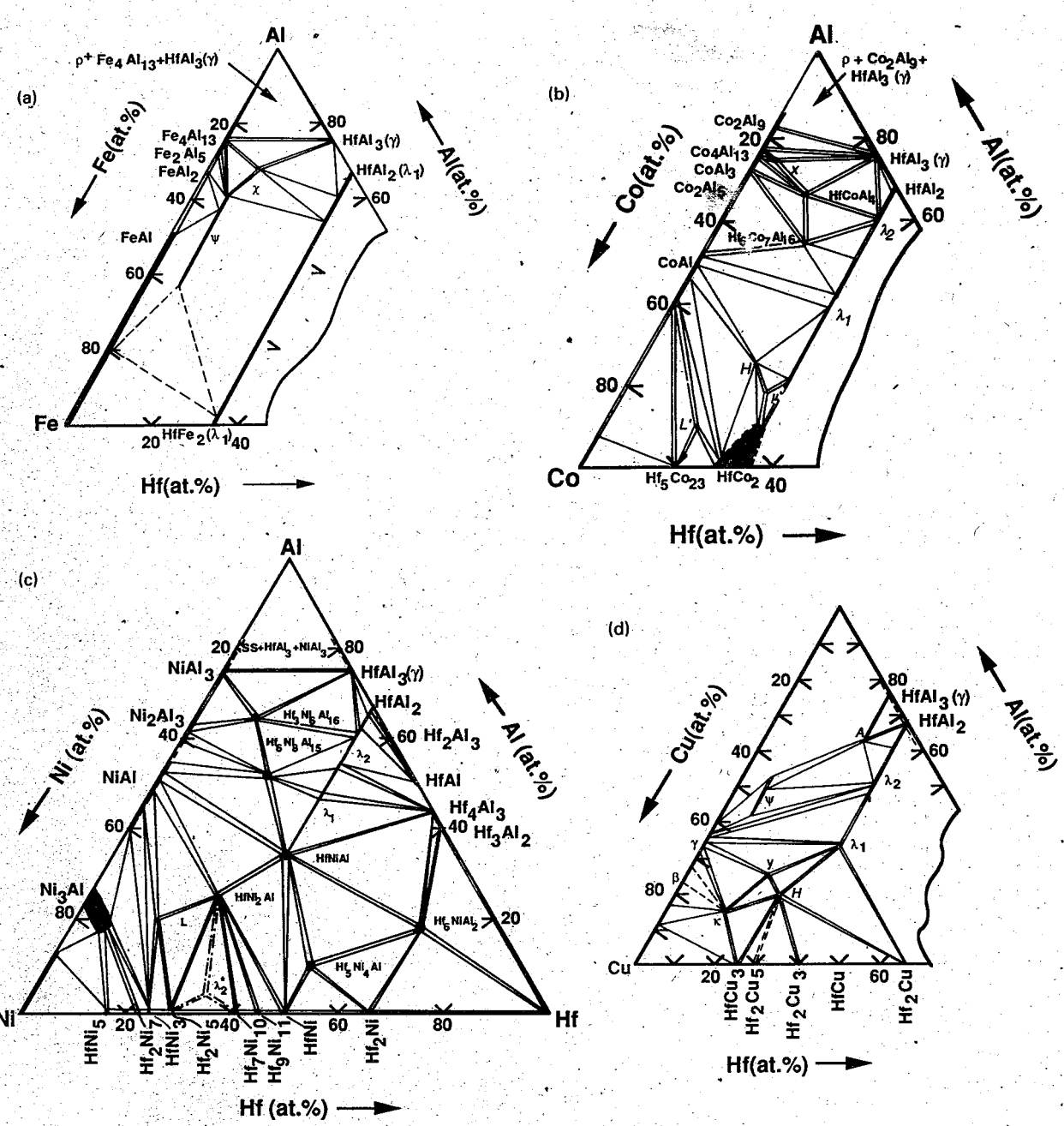

10 Isothermal sections at 1073 K corresponding to *a* Al–Fe–$HfFe_2$–$HfAl_2$ portion of Al–Hf–Fe system (Ref. 72); *b* Al–Co–$HfCo_2$–$HfAl_2$ portion of Al–Hf–Co system (Ref. 73); *c* Al–Hf–Ni system (Ref. 74); *d* Al–Cu–Hf_2Cu–$HfAl_2$ portion of Al–Hf–Cu system (Ref. 76)

any significant solubility for the third component, even at 1073 K. According to Markiv and Burnashova,[74] as in the Al–Zr–Ni system,[61] no ternary Al-rich $L1_2$ compound was present at 1073 K.

In the Al–Hf–Cu system[76] at 1073 K, at least eight ternary phases were identified in the section contained by Al–Cu–Hf_2Cu and $HfAl_2$ (Fig. 10*d*). An $L1_2$ compound, Hf_2CuAl_5, with a lattice parameter of 0·4013 nm was shown to exist, analogous to Zr_2CuAl_5 in the Al–Zr–Cu system (Fig. 8*d*). Other phases identified included a $HfCu_2Al$ (H) with the $L2_1$ structure, HfCuAl (λ_1) with the $MgZn_2$ structure, $HfCu_{0·35}Al_{1·65}$ (λ_2) with the $MgCu_2$ structure, ψ with the $ThMn_{12}$ structure, and the E phase (stable at 773 K) with a chemistry of 12Hf–24Cu–64Al (at.-%), which is similar to the E phase in the Zr–Cu–Al system. In addition, two other ternary phases, K and Y, were identified at 1073 K, with compositions of 14Hf–71Cu–15Al (at.-%) and 20Hf–55Cu–25Al (at.-%), respectively, although their crystal structures were not determined.

As shown in Fig. 10*d*, the $L1_2$ compound Hf_2CuAl_5 exists over a very small compositional range and is in equilibrium with $HfAl_3$, $HfAl_2$, λ, and ψ. None of the binary compounds shows any significant solubility for the third element, and the

only ternary phases with any significant compositional range of existence are λ_2, occurring at 33 at.-% Hf and 48–60 at.-% Al, and ψ, at 7·7 at.-% Hf and 42–52 at.-% Al.

Raman and Schubert[38] examined the $HfZn_3$–$HfAl_3$ pseudobinary section, and showed the presence of an $L1_2$ compound $HfZnAl_2$ with a lattice parameter of 0·403 nm at 973 K. As with the Zr–Zn–Al system, Drasner and Blazina[65] examined the $HfZn_2$–$HfAl_2$ section of the ternary Al–Hf–Zn system after homogenising the alloys at 1273 K, and found a single phase region with the $C15$ structure between $HfZn_{1·25}Al_{0·75}$ and $HfZn_{0·5}Al_{1·5}$. Homogenisation at lower temperatures (1173 K, 1073 K) produced two phase alloys of $C15$ and $L1_2$ type structures, although a single phase $L1_2$ compound was not produced. The observation of an $L1_2$ compound in the $HfZn_2$–$HfAl_2$ structure was attributed to the widely extended homogeneity range of the $L1_2$ phase field in the $HfZn_3$–$HfAl_3$ pseudobinary section.

This review of ternary isotherms of the Group IVA–Al–X systems, where X corresponds to the first row transition elements from V to Zn, does not clearly show a systematic tendency for the formation of Al-rich ternary $L1_2$ compounds upon traversal of the periodic table from Ti to Zr to Hf. While there is good agreement that $L1_2$ compounds are formed with the addition of Mn, Fe, Ni, Cu, and Zn to the Al–Ti system, the situation is not entirely clear for the Al–Zr system. Vanadium addition to Al–Zr produces an $L1_2$ compound, but conflicting evidence exists with respect to Cr, Fe, and Ni additions. Agreement does exist on the ability of Cu and Zn additions to produce a ternary $L1_2$ compound. The behaviour of the Al–Hf–X systems appears to be remarkably similar to that of the Al–Zr–X systems for a particular ternary addition. Cobalt, being sandwiched between Fe and Ni in the periodic table, appears to behave very differently – for example, an Al-rich $L1_2$ phase is present in both the Al–Ti–Fe and Al–Ti–Ni systems, but is absent in the Al–Ti–Co system.

While Fe, Ni, and Cu additions to the Al–Ti system produce only three or four ternary phases, similar additions to the Al–Zr and Al–Hf systems precipitate as many as eight or nine ternary phases, resulting in extremely complex systems. Quite often, only a single investigation was performed on some of these systems, making verification impossible. Clearly, more work is needed in these areas if these systems are to be used.

Al–Group VA–X systems

Al–V–X systems

Although the binary Al–V system contains several compounds, most of them are products of low temperature peritectic reactions at the Al-rich end. Therefore, high temperature ternary isotherms involving the binary Al–V system are relatively less crowded compared with the systems considered in the previous section. In fact, only two binary compounds are stable above 1100 K, Al_3V with a $D0_{22}$ structure and Al_8V_5 with a cubic $D8_2$ structure.

Kopp and Wachtel[77] investigated the phase equilibria of the Al–V–Mn system, primarily in the range 25–60 at.-% Al, and developed portions of the Al–V–Mn isotherms at 1273, 1173, and 873 K, the liquidus projection, and a reaction summary for the three binary systems and their influence on the solidification sequence of ternary alloys. In addition, they also provided an isopleth from 873 to 2073 K for the 60 at.-% Al level from 40 at.-% V at one end to 40 at.-% Mn at the other. The γ-Al–Mn phase and the γ-Al–V phase (V_5Al_8) were reported to exhibit complete mutual solubility to at least 873 K, while the high temperature ε-Al–Mn phase dissolved up to ~5 at.-% V at 1273 K. No ternary phases were identified in the portion of the system investigated.

Raman and Schubert[30] evaluated the Al–V–Cu and Al–V–Ni systems and produced isotherms at 1173 and 1073 K, respectively (Fig. 11*a* and *b*). At 1073 K, no ternary phases are present in the Al–V–Ni system. The binary $B2$ NiAl phase exhibits a significant solubility for vanadium, extending

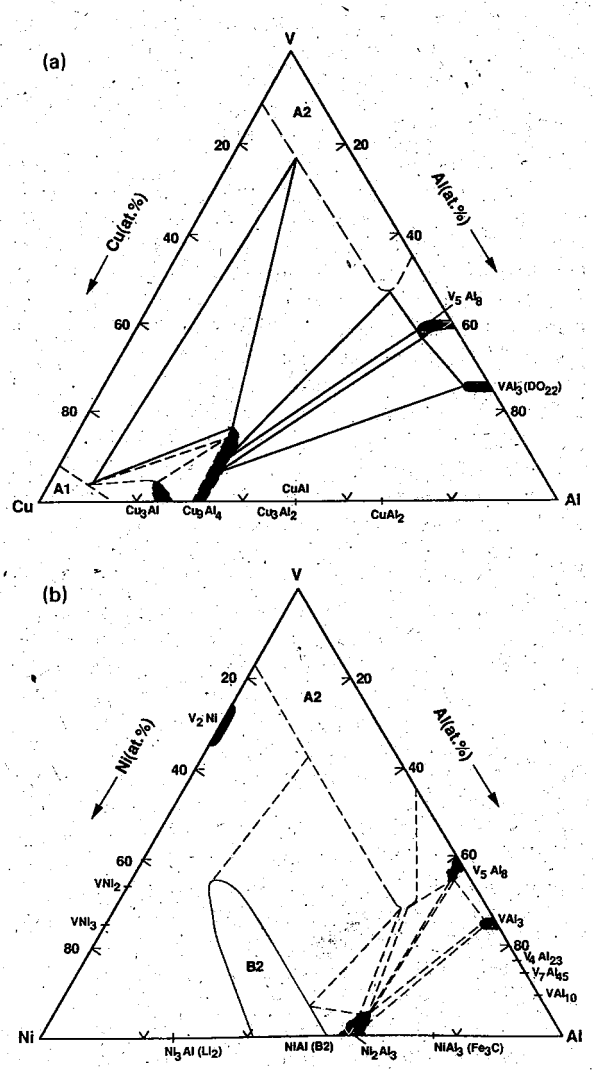

11 Isothermal sections in *a* Al–V–Cu system at 1173 K and *b* Al–V–Ni system at 1073 K (Ref. 30)

up to ~35 at.-% V into the ternary isotherm. Maximum solubility was observed for NiAl containing 50 at.-% Ni. At this temperature, Ni_2Al_3 is in equilibrium with VAl_3, V_5Al_8, and the solid solution *A*2 phase. The vanadium solid solution phase field extends up to ~17 at.-% Ni into the ternary isotherm and the solubility range of the ternary solid solution *A*2 phase extends from about 43 at.-% Al in the binary system up to ~57 at.-% Al at this nickel level. The three binary compounds, Ni_2Al_3, VAl_3, and V_5Al_8, do not show any significant solubility (<5 at.-%) for the third element. Myasnikova *et al.*[78] studied the phase equilibria of the alloys contained in the $NiAl_3$–VAl_3 and Ni_2Al_3–V_5Al_8 sections. In both cases in the solid state, a two phase structure consisting of the starting compounds was present across the entire pseudobinary section. At temperatures above 1073 K, the $NiAl_3$–VAl_3 isopleth showed the presence of a liquid phase, which was associated with three primary crystallisation fields, L + Ni_2Al_3, L + VAl_3, and L + V_5Al_8. $NiAl_3$ melted incongruently over the entire concentration range. In the Ni_2Al_3–V_5Al_8 section, a eutectic reaction was observed with the simultaneous crystallisation of the two phases, Ni_2Al_3 and V_5Al_8.

The Al–V–Cu isotherm of Raman and Schubert[30] at 1173 K is similar to the Al–V–Ni section at 1073 K (Fig. 11*a* and *b*), in that no ternary phases are present and the *A*2 vanadium solid solution phase field exhibits significant solubility for copper, although to a lesser extent than for nickel. At 1173 K, the compound $CuAl_2$ is unstable and the $D0_{22}$ compound VAl_3 is in equilibrium with Cu_9Al_4, V_5Al_8, and liquid. Cu_9Al_4 shows about 15 at.-% solubility for vanadium and is in equilibrium with the Cu-based *A*1 phase and V-based *A*2 phase. VAl_3 and V_5Al_8 exhibit ~5 at.-% solubility for Cu.

In addition to the Al–V–Ti and Al–V–Zr systems (discussed in the previous section), Raman[18] studied the Al–V–Nb, Al–V–Ta, and the Al–V–Mo systems and generated an isotherm for each at 1273 K. These are reproduced in Fig. 12 and discussed below. A detailed discussion of the binary Al–Mo, Al–Nb, and Al–Ta systems is provided in the relevant sections that follow. For now, it will suffice to recognise that in the Al–Nb system, the three intermetallics, Al_3Nb, $AlNb_2$, and $AlNb_3$, are all stable at 1273 K and all exhibit significant solubility for vanadium. At 1273 K, the binary Nb–V system shows unlimited solid solubility, with the *A*2 phase field extending into the ternary isotherm, bounded by ~5 at.-% Al on the Al–Nb binary and ~45 at.-% Al on the Al–V binary (Fig. 12*a*). At the Al-rich end of the ternary system, $NbAl_3$ and VAl_3 are in equilibrium with each other, exhibiting ternary solid solubilities of 12 at.-% V and 8 at.-% Nb, respectively. It is interesting that these two phases do not show complete mutual solid solubility since they have the same $D0_{22}$ crystal structure; rather, they bound a two phase region of a mixture of the two $D0_{22}$ phases. In the heat treated condition (7 days at 1273 K), the $D0_{22}$ Nb(V)Al_3 phase is in equilibrium

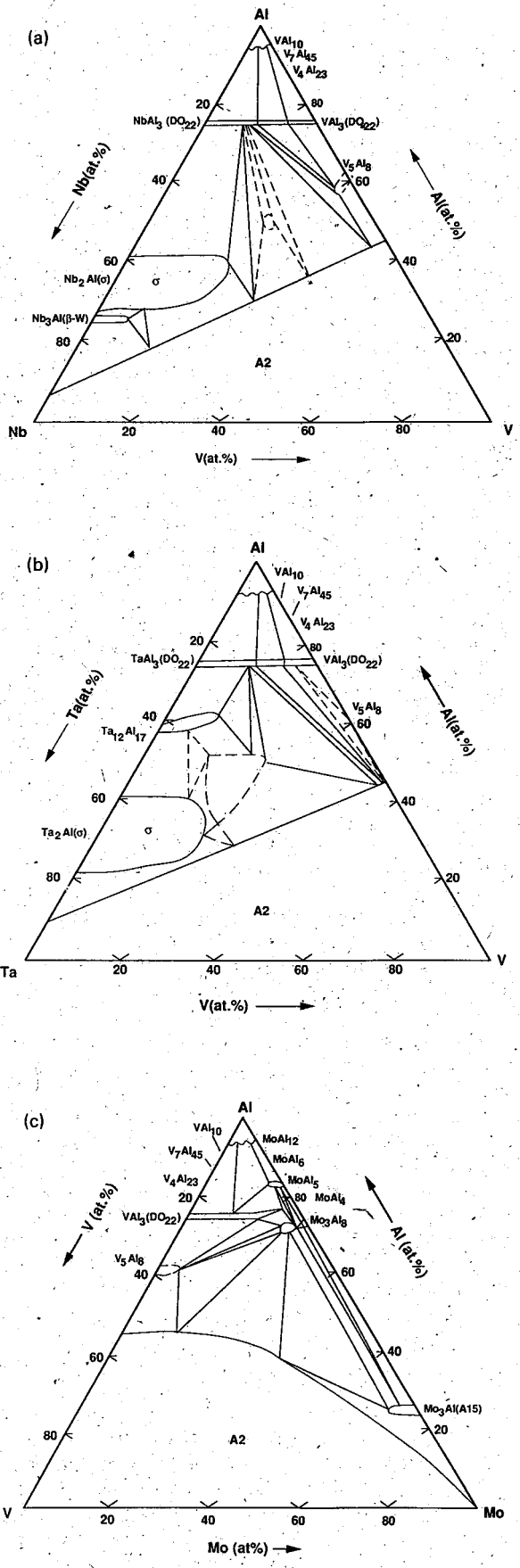

12 Isotherms at 1273 K in *a* Al–V–Nb system; *b* Al–V–Ta system; *c* Al–V–Mo system (Ref. 18)

with a new ternary phase (broken lines represent heat treated isotherm) whose crystal structure was not identified, although a similar ternary phase was also identified in the Al–V–Ta system (Fig. 12*b*) after a similar heat treatment.

The Al–Ta binary system differs from the binary Al–Nb system in that an equivalent of the Nb_3Al compound is absent and instead, a compound $Ta_{12}Al_{17}$ is claimed present in equilibrium with Al_3Ta and Ta_2Al. The ternary Al–V–Ta system (Fig. 12*b*) is very similar to the ternary Al–V–Nb system, in that Al_3Ta, $Ta_{12}Al_{17}$, and Ta_2Al all exhibit significant solubility for vanadium. Likewise, Al_3V shows appreciable solubility for tantalum. The *A*2 phase field is bound by Ta, 90 at.-% Ta–10 at.-% Al, 55 at.-% V–45 at.-% Al, and V. There is a two phase region composed of $D0_{22}$ Al_3Ta and $D0_{22}$ Al_3V, which is in equilibrium with aluminium; however, this equilibrium is unlikely at lower temperatures since a large number of Al-rich binary intermetallics precipitate in the Al–V system which are likely to be in equilibrium with the $D0_{22}$ region. As in the Al–V–Nb system, heat treatment (1273 K for 7 days) produces a ternary phase (whose crystal structure was not determined) that is in equilibrium with $Ta_{12}Al_{17}$, Ta_2Al, *A*2, and Al_3Ta (the heat treatment effect on the isotherm is shown by broken lines). A recent study[79] has verified the existence of two additional compounds, AlTa and Al_2Ta, which would significantly influence ternary phase equilibria, but were, however, not considered in the ternary studies discussed above as their presence was unknown at the time the ternary isotherms were established. Both these phases, Al_2Ta and AlTa, are claimed to be products of peritectic transformations occurring at 1867 and 2043 K. The crystal structure of AlTa was reported to be related to the *Fm3m* space group. The phase referred to as $Ta_{12}Al_{17}$ in earlier studies was shown not to exist. Thus, based on the latest study of the Al–Ta binary system, four compounds are shown to exist. These are Al_3Ta, Al_2Ta, AlTa, and $AlTa_2$. Based on this new information, phase equilibria in ternary Al–Ta–X systems need to be suitably modified.

The Al–Mo binary system is similar to the Al–V binary system in that it too forms a large number of intermetallics, several of which are Al-rich and form as a consequence of a peritectic decomposition below 1273 K. In fact, Al–Mo compounds stable above 1273 K include Mo_3Al (*A*15), Mo_3Al_8 (monoclinic), and $MoAl_4$ (monoclinic). $MoAl_5$ was reported to form at 1050 K,[80] although Raman[18] included it in his 1273 K Al–V–Mo isotherm (Fig. 12*c*), implying stability at this temperature. The V-rich solid solution with the *A*2 crystal structure in the binary Al–V system, showed a decreasing solubility for aluminium as increasing amounts of molybdenum were substituted in it. The $D0_{22}$ Al_3V intermetallic showed a significant solubility for molybdenum, extending to ~20 at.-% Mo. A new ternary phase with the approximate formula $Mo(V,Al)_3$ was identified, but its crystal structure was not determined. A subsequent investigation,[81] however, concluded that this was not a ternary phase, but simply an extension of the solid-solution range of Mo_3Al_8. Umakoshi *et al.*[19] showed that the substitution of Ti in VAl_3 improved ambient ductility in compression by allowing an extra deformation mode, namely, ordered twinning, to occur. Similarly, it is conceivable that the large amount of molybdenum solubility in VAl_3 could influence its deformation behaviour. Such alloying approaches must be explored in greater detail to enhance the properties of these intermetallics.

Al–Nb–X systems

In the field of high temperature materials and, specifically, ordered intermetallics, the Al–Nb system is beginning to draw considerable attention from the research community. In fact, the possible beneficial role of Nb additions to γ-TiAl and, more generally, the ternary phase equilibria in the Al–Ti–Nb system, are currently under investigation.[82,83]

Three intermetallic compounds were reported present in the Al–Nb system: Al_3Nb, a congruently melting (~1880 K) $D0_{22}$ line compound with a density <5·0 g cm^{-3}; the sigma phase (σ), Nb_2Al, a $D8_b$ structure that melted incongruently with a solidus extending from 1823 K at 58·7 at.-% Nb to 2143 K at ~67 at.-% Nb; and Nb_3Al, a Cr_3Si *A*15 structure, which also melted incongruently with a solidus extending from 2143 K at 68 at.-% Nb to 2233 K at 75 at.-% Nb. The *A*15 compound, Nb_3Al, was reported to have a high solidus and a large stoichiometric range of existence. These features have drawn recent interest to this compound, leading to a study of the variation of elastic modulus and elongation with temperature.[84] The brittle to ductile transition occurred around 1200 K for this compound.

Hansen and Raman[85] studied the effect of ternary alloying additions on the σ phase, Nb_2Al, and the extent of solubility of these additions on the Nb_2Al phase field. Nb_2Al formed continuous series of solid solutions with Ta_2Al and Nb_3Rh_2 and dissolved about 14 at.-% Zr. It exhibited a significant solubility for Mo, Ti, Cr, or V. While the σ phase extended towards T_2Al for T = Mo, Ti, Zr, or V, it was towards Nb_3X_2 or Nb_2X when X = Rh, Cr, Co, Cu, or Ni. In the case of Fe, the extension appeared to be towards both 'Fe_2Al' and 'Nb_2Fe'.

The current popular notion that the Al-rich $L1_2$ compounds in the Al–Ti–X systems (where X = Fe, Ni, Cu, or Zn) are actually derivatives of the $D0_{22}$ Al_3Ti intermetallic has created much interest in attempting to 'transform' the low density, higher melting $D0_{22}$ Al_3Nb to a ternary $L1_2$ compound. To data, this attempt has been futile. In a recent investigation, Subramanian *et al.*[86] evaluated the effect of various ternary elements on the stability of the $D0_{22}$ structure of Al_3Nb. Their study did not identify any potential alloying addition for deriving the $L1_2$ structure based ternary compound. Their results on the effect of Fe, Co, Ni, Cu, Cr, Mn, Ag, Mo, and Zr additions to Al_3Nb suggest that Cr and Mn substitute preferentially for Al at constant Nb content, while W, Fe, Cu, Mo, and Zr

substitute for Nb at constant Al content. Zr and Mo showed significant solubility in Al_3Nb, while Co, Ni, and Ag dissolved only to a small extent.

Perkins and co-workers[87] studied the oxidation behaviour of Al_3Nb in air at 1573–1623 K and concluded that a protective continuous Al_2O_3 scale was not formed in Al_3Nb, but rather a scale with alternating layers of alumina and niobium aluminate. This behaviour was attributed to the line compound nature of Al_3Nb, which promotes the formation of Nb_2Al just below the initial alumina layer.

Hunt and Raman[88] examined the effect of Fe, Co, Ni, Cu, Cr, and Mo additions on the phase equilibria of the Al–Nb system and, in the process, generated isotherms for the various systems. In the Al–Nb–Cr system, the isotherm at 1273 K (Fig. 13*a*) reveals significant Cr solubility in Nb_3Al (~15 at.-% Cr) as well as Nb_2Al (~23 at.-% Cr), with Cr claimed to substitute for Al in both cases. However, Al_3Nb dissolves only up to 5 at.-% Cr, with the Cr once again taking up the aluminium sites. The Al-rich portion of the ternary system was not investigated. A ternary $MgZn_2$-type *C*14 phase, in equilibrium with $NbCr_2$, $NbAl_3$, Cr(Al,Nb) solid solution, and the sigma phase, is present over a large compositional range – from 25–37 at.-% Nb and 3–47 at.-% Al. The chromium solid solution, which has a large solubility for Al (>40 at.-% Al) in the binary system, shows about 3–4 at.-% solubility for Nb at this temperature.

Two isotherms for the Al–Nb–Fe system, the first at 1273 K based on Raman's investigation[18] and the second at 1073 K from Burnashova *et al.*,[89] are presented in Fig. 13*b* and *c*, respectively. In both cases, it is apparent that the two binary Fe–Nb compounds, $NbFe_2$ and 'μ' ($Nb_{19}Fe_{20}$ according to Raman[18]) dissolve considerable amounts of aluminium. The *C*14 $NbFe_2$ phase is in equilibrium with the *A*2 phase (Al–Fe), the $D0_{22}$ $NbAl_3$ (with ~5 at.-% solubility for iron at 1273 K (Ref. 18), but significantly lower at 1073 K (Ref. 86), the σ phase (Nb_2Al), and the μ phase. None of the Al–Fe binary compounds shows any appreciable solubility for niobium. Although the isotherms from the two independent investigations differ by only 200 K, the

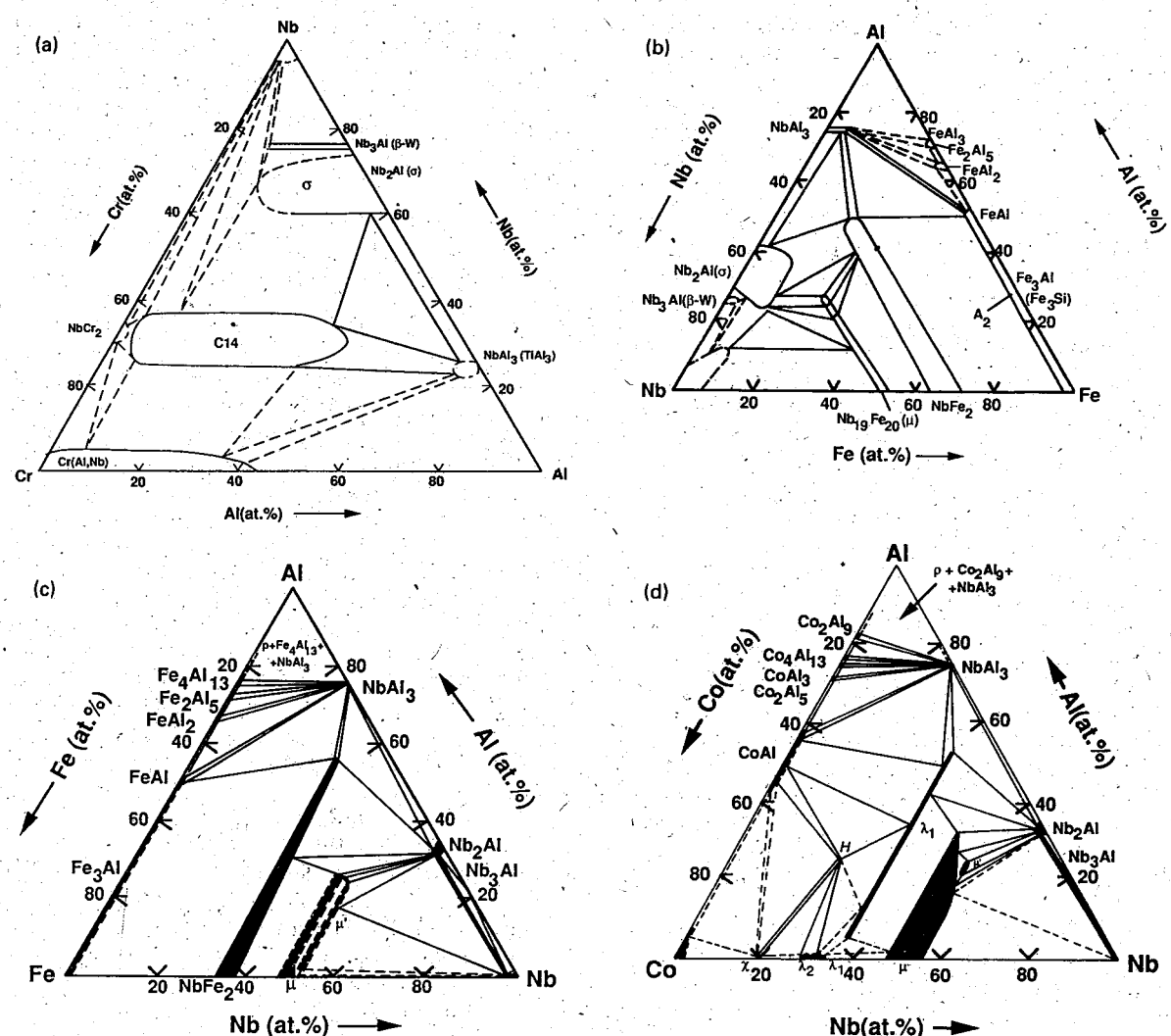

13 Isothermal sections in *a* Al–Nb–Cr system at 1273 K (Ref. 88); *b* Al–Nb–Fe system at 1273 K (Ref. 18); *c* Al–Nb–Fe system at 1073 K (Ref. 89); *d* Al–Nb–Co system at 1073 K (Ref. 89)

reported solubility of iron in the binary niobium aluminides differs significantly in the two studies. For example, according to Raman,[18] the σ phase exhibits ~10 at.-% solubility for Fe, whereas Burnashova *et al.*,[89] showed ~2–3 at.-% solubility of Fe in this phase at 1073 K. Also significant, is the presence of a ternary μ' phase in the 1073 K isotherm along lines of 50–52 at.-% Nb content and from ~3 to 26 at.-% Al. This ternary μ' phase is shown in equilibrium with μ, Nb, and Nb_2Al. Its crystal structure was not determined. At the higher temperature (1273 K), a μ' phase is claimed with a narrow composition range centred around Nb_2FeAl. Why the μ' phase should have such a large compositional range of existence in one investigation and not in the other is not clear. Further, the location of the μ' phase in the two isotherms is very different, which raises the question of whether they are the same or two different phases. In any event, fairly rigorous experiments are required to explain these observed differences.

As a part of a larger study to understand the solubility of transition elements in the binary μ and ternary μ' phases of the Nb–Al–X (X = Cu, Ni, Co, Fe, Cr, Mo) systems, Hunt and Raman[88] examined selected portions of the Al–Nb–Co system at 1273 K and showed the presence of a ternary μ' phase in equilibrium with Nb_2Al (σ) and μ, occurring in a narrow region between the two. The μ phase showed a large solubility for Al. Based on their experiments, they inferred a similar behaviour for the $C14$ $Nb_{36}Co_{64}$ phase. The Nb_2Al σ phase dissolved about 10 at.-% Co. A complete isotherm at 1073 K of the Al–Nb–Co system due to Burnashova *et al.*[89] is provided in Fig. 13*d*. Unlike the work on the Al–Nb–Fe system, these two investigations agree well on the size and location of the μ' phase field, as well as on the solubility limits of Al in the μ phase. While Nb_2Al had about 10 at.-% solubility for Co at 1273 K according to Hunt and Raman,[88] Burnashova *et al.*,[89] showed negligible solubility at 1073 K. $NbAl_3$ did not dissolve any appreciable amount of Co at 1073 K and was in equilibrium with several of the binary cobalt aluminides, as well as a ternary $MgZn_2$ type (λ_1) phase. This ternary λ_1 phase existed along a constant Nb composition of 36·5 at.-%, extending from 55 at.-% Al to almost 5 at.-% Al. (The phase equilibria in the Al-poor region of the Al–Co–Nb system are not well defined in Fig. 13*d*.) In addition, a ternary compound H (Co_2AlNb) with a very small compositional range was present and was identified[36] as having the $L2_1$ structure (Heusler alloy). The presence of a ternary λ_1 phase in equilibrium with a binary λ_2 (Co–Nb) phase and the μ phase contradicts the work of Hunt and Raman,[88] although these researchers specified that their results in that portion of the phase diagram were based on inference rather than experimental observations. Thus, there is not enough experimental evidence in the literature to verify the validity of the ternary Al–Nb–Co isotherm due to Burnashova *et al.*[89]

Of the various Al–Nb–X systems investigated to date (X = Cr, Mn, Fe, Co, Ni, Cu, Zn), the Al–Nb–Ni system has perhaps received the most attention, primarily because Nb has been a popular alloying addition to Ni-based superalloys, as well as to the $L1_2$ intermetallic Ni_3Al. The Ni-rich region of the Al–Nb–Ni system has been the focus of several investigations,[90–93] although isotherms at different temperatures have been determined for the entire ternary system. The ternary Al–Nb–Ni system is extremely complex and involves several ternary intermetallics. The contradictions present in this system serve to illustrate and emphasise the current need for standardised, focused, accurate experiments to resolve the differences that are often observed in such complex systems. A chronological approach for reviewing the Al–Nb–Ni phase equilibria has been adopted in order to provide an appreciation of the evolution of present knowledge of this system.

In 1964, Schubert *et al.*[94] included four Al–Nb–Ni compounds in a long list of ternary compounds of the Group IVA and VA transition metals. These four compounds were $NbNi_2Al$ with a = 0·591 nm and an $L2_1$ structure; a $C14$-type NbNiAl with a = 0·487 nm, c = 0·792 nm if the Nb substituted in the Ni sites and a = 0·496 nm, c = 0·815 nm if it substituted in the Al sites; $NbNiAl_2$ with a cubic structure and a = 1·143–1·150 nm; and an Al-rich $L1_2$ compound, Nb_2NiAl_5 with a = 0·403 nm. Markiv *et al.*[36] independently confirmed the existence of the Heusler compound ($L2_1$), $NbNi_2Al$, with a lattice parameter of 0·5974 nm, which is higher than that reported by Schubert *et al.*[94] In addition, the equiatomic NbNiAl compound with the $C14$ structure was identified, with a = 0·500 nm and c = 0·909 nm.[36]

About the same time, Raman and Schubert[30] investigated Group IVA–, VA–, and VIA–Al–X (X = Cu, Ni) systems with the intent of identifying crystal structures and compositions of ternary phases present, and extensions of the solubilities of binary phases into the respective ternary systems. One of the systems they evaluated was the Al–Nb–Ni system. Their study essentially confirmed the existence of the $L2_1$ compound, $NbNi_2Al$, and the $C14$ phase, NbNiAl. They indicated a wide homogeneity range for the $C14$ phase field; further, their study could not confirm the existence of the Al-rich $L1_2$ compound, Nb_2NiAl_5, claimed earlier by Schubert *et al.*[94] An alloy of composition $Nb_{25}Ni_{13}Al_{62}$ (which is very close to Nb_2NiAl_5) decomposed after heat treatment into a three phase structure of $D0_{22}$, $C14$, and β-NiAl ($B2$). However, Raman and Schubert[30] reported the existence of the ternary Ti_2Ni-type phase with a = 1·15 nm.

In 1966, results of two independent studies[95,96] on the Al–Nb–Ni system were reported in the form of complete isotherms at 1413 K,[95] 1173 K,[96] and the Al-rich portion at 1073 K.[96] These isotherms are presented in Fig. 14*a–c* and the salient features of the two studies are compared with each other and with previous studies. Benjamin *et al.*[95] showed that there was no compound in the binary Nb–Ni system analogous to Ta_2Ni, in good agreement with Duerden and Hume-Rothery,[97] who generated the entire binary Ni–Nb phase diagram about the same

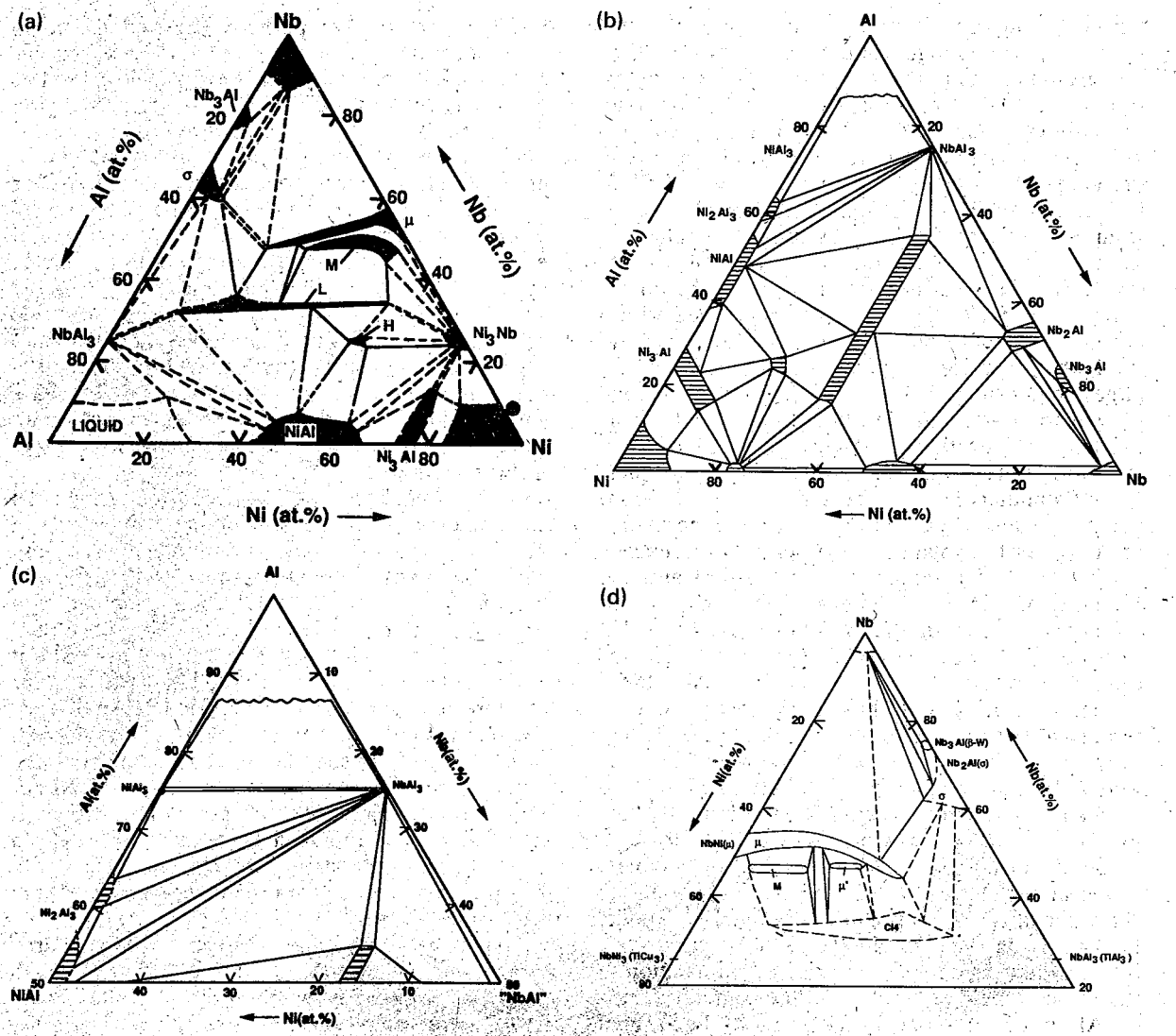

14 Isothermal sections in Al–Nb–Ni system *a* at 1413 K (Ref. 95); *b* at 1173 K (Ref. 96); *c* at 1073 K (Ref. 96); *d* at 1273 K (Ref. 88)

time. The work of Benjamin *et al.*[95] and Markiv *et al.*[96] agrees well in the compositional range of existence for the binary μ (NbNi) phase, although the results on the solubility of Al in the μ phase are a major contradiction (cf Fig. 14*a* with *b*). While Markiv *et al.*[96] show negligible solubility of Al in NbNi at 1173 K, Benjamin *et al.*[95] show the μ phase to be stable up to and in excess of 30 at.-% Al in the ternary system. Subsequently, Hunt and Raman[88] examined a portion of the Al–Ni–Nb isotherm at 1273 K and showed the μ phase to be stable with as much as 35 at.-% Al (Fig. 14*d*), in good agreement with Benjamin *et al.*[95] (in fact, the 35 at.-% Al was a little higher than that indicated by Benjamin and co-workers at the higher temperature of 1413 K). However, Hunt and Raman[88] did point out that they used as few samples as possible to define the phase equilibria. Nevertheless, it is puzzling that Markiv *et al.*[96] did not see the μ phase dissolving a large amount of aluminium because their studies showed that they examined a large number of alloy compositions in that section of the isotherm.

If the results of all of these investigations are correct,[88,95,96] the only explanation for the large difference reported in the solubility of Al in the μ phase is a temperature effect, suggesting that the terminal solid solubility for Al in this phase decreases sharply between 1413 and 1173 K. While this is possible, it appears unlikely particularly because of the extended solubility reported by Hunt and Raman[88] at 1273 K, thus implying that the large change in solubility must occur between 1273 and 1173 K. In this context, the experimental procedures adopted in these three investigations become relevant. Markiv *et al.*[96] annealed their cast alloys at 1173 K for 700 h and then quenched them. Hunt and Raman[88] annealed their castings (2 g in weight) in evacuated capsules for 168 h at 1273 K and then air cooled them, while Benjamin *et al.*[95] vacuum annealed their castings in capsules at 1413 K for 20 h and then water quenched them.

Thus, the data due to Hunt and Raman[88] may not be representative of 1273 K, as air cooling may have allowed some phase transformation to occur during cooling to ambient. Further, extended heat treatments of Al-containing compounds at elevated temperatures in vacuum can result in aluminium loss, and when these castings are only 2 g in weight, such losses are significant. Chemical composition was not measured after casting of these buttons nor after they were heat treated. Hunt and Raman[88] claim there was negligible material loss during melting. Such losses were assumed to result from aluminium loss and accordingly excess aluminium was added to compensate for these losses, particularly in those compositions rich in niobium. Where the loss was more than the compensated weight, compositions were recalculated assuming only aluminium loss. Such approximations will significantly influence the results. Markiv *et al.*[96] specify that they used appropriate amounts of pure Nb, Ni, and Al as starting material and that melting was accomplished under helium. They examined 150 alloy compositions, making an allowance for aluminium loss by oxidation. They, however, assumed final alloy compositions to be those of the starting mixture. In all these studies it is possible that aluminium loss occurred during the casting process and/or during the subsequent heat treatment, particularly at high temperatures for extended periods in vacuum. If this had happened and the final composition was not measured, then the end product would contain less aluminium than assumed. Subsequently, if X-ray diffraction indicated a single phase (NiNb) for a particular composition, then it is possible that a large aluminium solubility was attributed to it based on assumed composition of the alloy, whereas the real composition would indicate a more restricted solubility. Based on this argument, it appears that the results reported by Markiv *et al.*[96] would be the more accurate.

Benjamin *et al.*[95] found three ternary phases, H, L, and M, at 1413 K, whereas Markiv *et al.*[96] identified the H phase ($NbNi_2Al$) and the L phase ($C14$, $Nb(Ni,Al)_2$), but not the M phase (Fig. 14*a* and *b*). The lattice parameters of the H phases from the various studies[36,94,95] agreed. Also, good agreement was observed in the compositional range of existence of the L phase reported by Benjamin *et al.*[95] and Markiv *et al.*[96] The L phase was assigned a formula of the type $Nb(Ni_{1-x}Al_x)_2$, where x varied from 0·19 to 0·83, and the M phase was assigned the composition $Nb_{0·9}Ni_{1-z}Al_z$ with $z = 0·05$–$0·43$.[95] Subsequently, the M phase of composition $Nb_{48}Ni_{39}Al_{13}$ was examined and assigned an orthorhombic structure, with the space group *Pnma* (D_{2h}^{16}) and lattice parameters of $a = 0·9303$ nm, $b = 1·6266$ nm and $c = 0·4933$ nm.[98] Hunt and Raman[88] confirmed the presence of the M phase at 1273 K, in agreement with Benjamin *et al.*,[95] although they show a very much reduced phase field size (cf Fig. 13*a* and *d*). Thus, it is conceivable that this M phase was a high temperature phase stable above 1173 K. This would explain why it was not observed by Markiv *et al.*[96] and had a relatively small phase field size at 1273 K (Ref. 88) which became larger at 1413 K.[95] An alternative possibility is that Markiv *et al.*[96] did not see the M phase or observe Al solubility in the μ phase for similar reasons.

Ni_3Al shows significant solubility for Nb, with Nb substituting for as much as 5% of the Al, whereas Nb_3Al and σ show low solubility for Ni. The ternary $NbNiAl_2$ compound tested by Schubert *et al.*[94] and reported to have a cubic structure with $a = 1·143$ nm was not seen by Markiv *et al.*[96] or Benjamin *et al.*[95] In fact, Markiv *et al.*[96] examined an alloy composition corresponding to the composition $NbNiAl_2$ and found that this alloy existed as a two phase material of β-NiAl and the $C14$ $Nb(Ni,Al)_2$ at 1173 K. Similarly, the Al-rich $L1_2$ compound Nb_2NiAl_5,[94] which also was not seen,[95,96] corresponded to a three phase structure of NiAl, $NbAl_3$, and $Nb(Ni,Al)_2$.[96] Benjamin *et al.*[95] did not encounter the Ti_2Ni-type phase that Raman and Schubert[30] reported in the Al–Nb–Ni system, and attributed its presence in the latter study to impurities that stabilised this structure. In addition to the ternary phases discussed for this system, Hunt and Raman[88] also identified a μ' phase similar to the one found in the Al–Nb–Fe system. This μ' phase was evidenced neither by Benjamin *et al.*[95] nor Markiv *et al.*[96] Hunt and Raman[88] showed that this phase was not in equilibrium with the M phase (Fig. 13*d*), but that each of these two phases was in equilibrium with the μ and $C14$ phases.

Several investigators have examined the Ni–Ni_3–Al–Ni_3Nb portion of this ternary system. Pertinent studies include that of Cisse and Davies,[92] who determined the 1473, 1273, and 1073 K isotherms and concluded that the addition of Nb widens the Ni_3Al phase field; Duvall and Donachie,[91] who examined the solubility of Nb and Al in the Ni terminal solid solution at 1023 and 1423 K and were in fair agreement with the results of Markiv *et al.*[96] but not those of Duerden and Hume-Rothery;[97] and Nash *et al.*,[90] who suggested a peritectoid reaction of the type $NiAl + Ni_3Nb \rightleftharpoons Ni_3Al + AlNi_2Nb$ based on a comparison of their own effort at 1473 K and that of Markiv *et al.*[96] at 1073 K. Finally, Giessen and Ray[99] examined a splat quenched Ni-rich Al–Nb–Ni alloy of the composition $Al_{0·125}Nb_{0·125}Ni_{0·75}$ and identified a metastable phase of the type $AlNbNi_6$ that was isostructural with its stable counterpart $AlTaNi_6$ in the Al–Ta–Ni system.[100]

In 1964, Nowotny and Oesterreicher[101] reported the occurrence of $MgZn_2$-type $C14$ Laves phases in the Al–Nb–Cu and Al–Ta–Cu systems with stoichiometries of the type $Nb(Cu,Al)_2$ and $Ta(Cu,Al)_2$ and a large compositional range of existence. In addition, in the Al–Ta–Cu system, a μ phase of the type $Ta_6(Cu,Al)_7$ was also reported. In the following year, Oesterreicher *et al.*,[102] presented the results of a more extensive study on the phase equilibria of Group VA–Al–Cu systems and claimed the existence of an additional ternary compound in Al–Nb–Cu and Al–Ta–Cu samples sintered at 1573 K. Also, a μ phase with a hexagonal structure and similar to $Ta_6(Cu,Al)_7$ was identified in the Al–Nb–Cu system, and lattice parameters for the particular composition 53 Nb–27Cu–20Al (at.-%) were reported. For the

Laves phase, $Nb(Cu_xAl_{1-x})_2$, an alternating cubic and hexagonal structure was assumed, and lattice parameters were measured for x varying from 0·18 to 0·66, implying that this phase was stable at least over the specified composition range, if not a larger one. This contradicts the results of Raman and Schubert,[30] who analysed an alloy composition $Nb_{25}Cu_{50}Al_{25}$ held for six days at 1173 K and identified a $C14$ compound to which they assigned the formula NbCuAl. This formula implies that the boundary of the $C14$ phase lay at the equiatomic composition, whereas, in the previous study, it was shown to extend up to 44 at.-% Cu and 23 at.-% Al. Thus, a minor discrepancy exists in the size of the $C14$ phase fields reported. The lattice parameters of $a = 0{\cdot}497$ nm and $c/a = 1{\cdot}62$ were in good agreement with the corresponding values of $a = 0{\cdot}503$ nm and $c/a = 1{\cdot}621$ reported by Oesterreicher *et al.*[102] for $Nb(Cu_xAl_{1-x})_2$ with $x = 0{\cdot}48$.

A more elaborate study of the Al–Nb–Cu system by Hunt and Raman[88] resulted in a 1273 K isotherm, shown in Fig. 15. They confirmed the presence of the μ phase reported earlier,[102] though they did not find it in the as cast condition in the Nb-rich alloys but after annealing. The μ phase was assigned a composition $Nb_{46}Cu_{27}Al_{27}$ and was claimed to have a very narrow and small single phase field. The σ phase, Nb_2Al, was found to dissolve as much as 10 at.-% Cu at 1273 K, whereas Nb_3Al and $NbAl_3$ dissolved only up to 5 at.-% Cu. Based on extensions of the Nb_3Al, Nb_2Al, and Al_3Nb phase fields, Hunt and Raman[88] suggested that Cu substituted preferentially for Nb rather than Al in the structure. This would be significant since, in the Al–Ti–Cu or Al–Zr–Cu systems, the $L1_2$ compounds Al_5CuTi_2 and Al_5CuZr_2 are considered to derive from $D0_{22}$ Al_3Ti and Al_3Zr through a Cu for Al substitution. It is also clear that in the Al–Nb–Cu system, no such $L1_2$ derivative of $D0_{22}$ Al_3Nb exists, possibly because the Cu atoms substitute preferentially for Nb rather than Al.

Drasner and Blazina[103] examined the effect of aluminium substitution for zinc in the Nb–Zn and Ta–Zn systems, thereby enabling them to study portions of the ternary Nb–Zn–Al and Ta–Zn–Al systems. Specifically, they examined the $NbZn_2$–'$NbAl_2$', the $NbZn_3$–$NbAl_3$, and the $TaZn_2$–'$TaAl_2$' tie lines. In the Nb–Zn system, $NbZn_3$ was cubic ($L1_2$), while in the Nb–Al and Ta–Al systems, $NbAl_3$ and $TaAl_3$ had the $D0_{22}$-type structures. Compounds corresponding to $TaAl_2$, $NbAl_2$, and $TaZn_3$ did not exist.

On the $NbZn_2$–$NbAl_2$ tie line, two ternary phases were identified, with compositions of NbZnAl and $NbZn_{1{\cdot}25}Al_{0{\cdot}75}$. NbZnAl was hexagonal $C14$, while $NbZn_{1{\cdot}25}Al_{0{\cdot}75}$ was cubic $L1_2$ with a lattice parameter of 0·3944 nm and a compositional range of existence varying from $NbZn_{1{\cdot}25}Al_{0{\cdot}75}$ to $NbZn_{1{\cdot}5}Al_{0{\cdot}05}$. Along the $NbZn_3$–$NbAl_3$ tie line, $NbZn_3$ dissolved aluminium up to 25 at.-%, with aluminium substituting for zinc (corresponding to the formula $NbZn_2Al$) and, thus, defining the limit of the $L1_2$ phase field along this tie line. The presence of the $L1_2$ compound along the AB_2 stoichiometry tie line (i.e. $NbZn_2$–$NbAl_2$) was attributed to the widely extended homogeneity range of the $L1_2$ phase field in the $NbZn_3$–$NbAl_3$ section. Drasner and Blazina[103] compared the $MgCu_2$-type ($C15$) and $MgZn_2$-type ($C14$) phases in $Al_xZ_{2-x}Y$ systems (where Z = Cu, Ni, Zn and Y = Zr, Hf, Nb, Ta) in terms of valence electron concentration and relative atomic sizes. Based on the observed trends, it appeared that in all the systems, electron transfer took place from Ni, Cu, or Zn, and/or Al to Zr, Hf, Nb, or Ta, increasing from Ni to Zn and from Group IV to Group V. In such a proposed scheme, Zn would lose its d electrons and behave like a transition element.

Two other ternary systems of interest especially for elevated temperature systems are the Al–Nb–Mo and the Al–Nb–Zr systems. As a part of a larger investigation of alloy chemistry of σ-related phases, Hunt and Raman[88] examined the Al–Nb–Mo system. An isotherm at 1273 K from their work is shown in Fig. 16*a*. The binary compounds Nb_3Al and Mo_3Al both exhibit the β-W structure and complete mutual solid solubility across the ternary isotherm, as do the pure elements Nb and Mo. At ~50 at.-% Nb, the Nb–Mo solid solution dissolves up to 12 at.-% Al and is in equilibrium with the Nb_3Al–Mo_3Al solid solution section. $AlNb_2$ and Al_3Nb both dissolve significant amounts of molybdenum, which was claimed to substitute for niobium. Al_3Nb dissolves up to 15 at.-% Mo and is in equilibrium with a ternary phase Y claimed to be similar to the $Mo(V,Al)_3$-type phase (specifically $Mo_{25}V_5Al_{70}$) identified by Raman[18] and discussed above. However, as before, a subsequent investigation[81] showed that this compound was only an extension of Mg_3Al_8. Also, recent efforts[86] have shown a much smaller molybdenum solubility in Al_3Nb (~6 at.-%) at an even higher temperature, 1673 K. Two interesting possibilities should be explored in relation to the large solubility of molybdenum in Al_3Nb: the ability to modify the properties of $D0_{22}$ Al_3Nb via Mo additions, and the possibility of transforming the alloyed ternary Al_3Nb (i.e. $Al_3(Mo,Nb)$) from $D0_{22}$ to a quaternary $L1_2$.

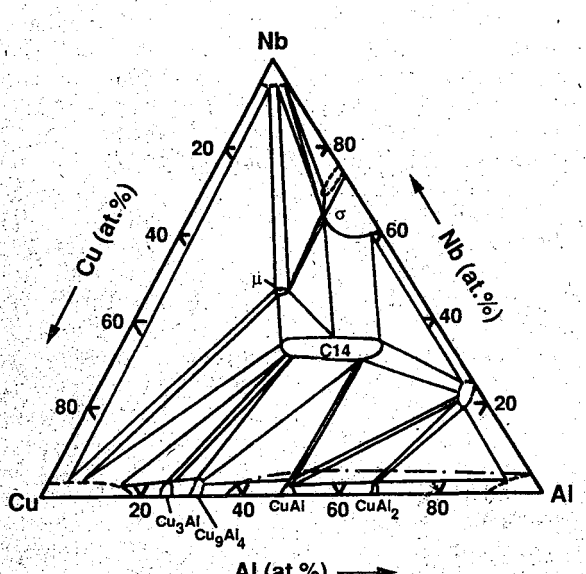

15 Isothermal section of Al–Nb–Cu system at 1273 K (Ref. 88)

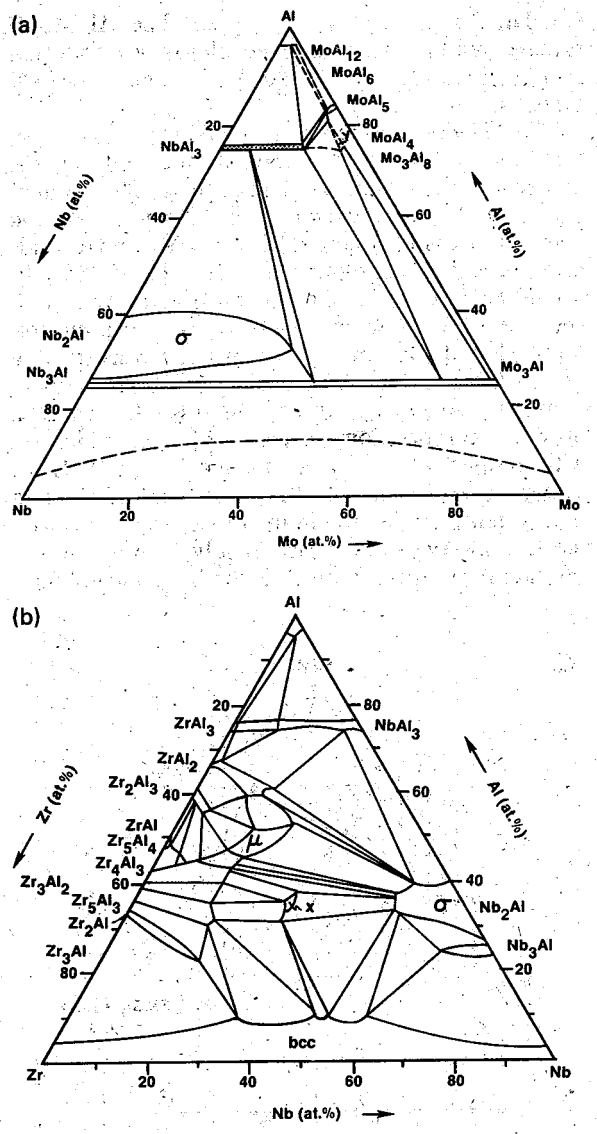

16 Isothermal sections in *a* Al–Nb–Mo system at 1273 K (Ref. 88) and *b* Al–Nb–Zr system at 1200 K (Ref. 85)

The Al–Nb–Zr system is probably more complex than the other Al–Nb–X systems simply because the Al–Zr binary system by itself contains several high temperature intermetallic compounds; in addition, there are at least two ternary compounds that are in equilibrium with the various binary intermetallics. A representative isotherm for the Al–Nb–Zr system at ~1200 K is reproduced from the work of Hansen and Raman[85] in Fig. 16*b*. The two ternary compounds denoted by X and μ occur at $Zr_{35}Nb_{30}Al_{35}$ and around $Zr_{30}Nb_{20}Al_{50}$. The μ phase has an elliptical shaped, single phase field bounded by the formula $Zr_5Nb_2Al_6$–$Zr_3Nb_3Al_7$. The crystal structure of the X phase was not determined; although its powder pattern resembled that of Mn_5Si_3, it could not be indexed with a hexagonal unit cell. The $D0_{22}$ compound Al_3Zr exhibits about 2 at.-% solubility for Nb, whereas Al_3Nb, also $D0_{22}$, dissolves about 17 at.-% Zr. It would be interesting to find out if this ternary $D0_{22}$ compound containing a large amount of dissolved Zr can be transformed to a quaternary $L1_2$ via Cu additions, since binary $D0_{22}$ Al_3Zr (but not binary $D0_{22}$ Al_3Nb) can be transformed $L1_2$ using ternary Cu additions. Unlike Al_3Zr, Al_2Zr dissolves a significant amount of Nb (~15 at.-%), as do Al_3Zr_4, Al_3Zr_5, and $AlZr_2$. However, it was speculated that ZrAl, Al_2Zr_3, and $AlZr_3$ dissolve only small quantities of niobium.

Al–Ta–X systems

The ternary Al–Ta–X systems are very similar in many respects to the ternary Al–Nb–X systems. Thus, rather than a discussion of the various aspects of each of the Al–Ta–X ternary systems sequentially here, their similarities and differences with respect to the Al–Nb–X systems are emphasised. Besides, considerably less work has been done on the Al–Ta–X systems than on the Al–Nb–X systems.

Hunt and Raman[88] studied portions of the Al–Ta–X (X = Fe, Co, Ni) ternary systems and proposed partial isotherms at 1273 K. Their results showed the μ' phase, observed in the Al–Nb–X systems, in all three Al–Ta–X systems, although the μ' phase field in the Al–Ta–Fe system was unusually large. In all three systems, the σ and μ phases had similar compositional ranges of stability. In the Al–Ta–Ni system, the *C*14 phase was a uniquely ternary phase, whereas, in the Al–Ta–Co system, it extended from the Ta–Co binary deep into the ternary, very similar to the case in the Al–Nb–Co system. An equivalent *C*14 phase was not shown in the Al–Ta–Fe system. An additional ternary compound was claimed to exist in the ternary Al–Ta–Ni system, although its crystal structure was not determined.

Markiv *et al.*[36] showed the existence of two ternary compounds, TaNiAl (*C*14) and $TaNi_2Al$ ($L2_1$), analogous to NbNiAl and $NbNi_2Al$ in the Al–Nb–Ni system. Similarly, a composition, $TaCo_2Al$, was claimed to exist with a Heusler alloy structure. The equiatomic composition TaNiAl, identified by Kusma and Nowotny[104] as having the *C*14 structure and subsequently confirmed by Markiv *et al.*,[36] was actually a part of the *C*14 phase field described by Hunt and Raman.[88]

Giessen and Grant[100] identified a ternary Ni-rich intermetallic, Ni_6TaAl, with the $D0_{24}$ structure (hexagonal Ni_3Ti) in the Al–Ta–Ni system. This was subsequently confirmed by Mints *et al.*,[105] who investigated the pseudobinary Ni_3Al–Ni_3Ta section and found the compound Ni_6TaAl to be a stable phase that melted congruently at ~1800 K and was very brittle. The addition of Ta to Ni_3Al reduced the aluminide's thermal expansion coefficient. In contradiction to these results, an earlier study[106] claimed the presence of a pseudobinary eutectic between Ni_3Al and Ni_3Ta, similar to that seen in the Ni_3Al–Ni_3Nb section. Subsequent work by Nash and West[98] clarified the situation in favour of the results of Mints *et al.*,[105] i.e. there was indeed no pseudobinary eutectic reaction analogous to the Al–Ni–Nb system. In addition, as mentioned in an earlier section of this review, Ni_6AlNb was observed in the Al–Nb–Ni system, but only as a metastable phase.[99] The compound Ni_6TaAl had a substantial range of solubility in the direction of a constant Ta/Al ratio, but a

more limited solubility range for constant Ni composition. Evidence was also obtained for the occurrence of a peritectoid reaction of the type $NiAl + NiTa \rightarrow Ni_2TaAl + NiTaAl$ between 1273 and 1573 K.[98] No information was available on the Al-rich corner of the Al–Ta–X systems (X = Fe, Co, Ni).

Limited studies on the Al–Ta–Cu system[30,102] showed that the types of ternary phases present were very similar to those in the Al–Nb–Cu system.

A phase analysis along the $TaZn_2$–'$TaAl_2$' tie line[103] in the Al–Ta–Zn system revealed no $L1_2$ phase analogous to that found along the $NbZn_2$–'$NbAl_2$' tie line. The only single phase composition identified was the equiatomic TaZnAl, with the $MgZn_2$ structure and lattice parameters of $a = 0{\cdot}5038$ nm and $c/a = 1{\cdot}643$.

Two other ternary systems of interest are the Al–Ta–Ti (Ref. 18) and the Al–Ta–Nb (Ref. 85) systems, where Al_3Ta and Al_3Ti, as well as Al_3Ta and Al_3Nb, were shown to exhibit unlimited mutual solid solubility. Since Fe, Ni, and Cu additions are known to produce the $L1_2$ structure in Al_3Ti, but not in Al_3Ta, it remains to be seen what would happen if these alloying additions were incorporated into, for example, $Al_3(Ti_{0.5}Ta_{0.5})$. Further, because of the unlimited solubility, the effect of large amounts of ternary additions on the deformation behaviour of these $D0_{22}$ structures (e.g. Nb or Ti in Al_3Ta; Ta in Al_3Ti and Al_3Nb) can be studied. In the Al–Ta–Ti system, Ta_2Al (σ) was shown to exhibit a large solubility for Ti, as did TiAl for Ta, while in the Al–Ta–Nb system, Nb_2Al and Ta_2Al formed an uninterrupted series of solid solutions. Thus, across the Al–Ta–Nb isotherm, there exists a large two phase region comprising the Al_3Nb–Al_3Ta solid solution and the $AlNb_2$–$AlTa_2$ solid solution regions. The possibility of varying the composition of the two phases and their relative volume fractions over a wide range seems an intriguing prospect for producing 'tailored' multiphase materials.

In summary, this review of the ternary isotherms of the Group VA–Al–X systems, where X = first row transition elements from V to Zn and selected refractory elements, revealed no $L1_2$ compound at the Al-rich corner of any of these systems. In several instances, the $D0_{22}$ Al_3X (X = V, Nb, Ta) compounds dissolved a large amount of the third element. In some cases (e.g. Al_3Ta and Al_3Nb; Al_3Ta and Al_3Ti), two $D0_{22}$ compounds were completely mutually soluble, forming a series of solid solutions. A ternary Al-rich phase was initially identified in the systems Al–V–Mo and Al–Nb–Mo, but, based on the similarity of its crystal structure to that of Mo_3Al_8, was concluded to be simply a solid solution extension of binary Mo_3Al_8. In addition, a ternary M phase with an orthorhombic structure was identified in the Al–Nb–Ni system, in contradiction to the Soviet work. In most of the ternary systems, the three most commonly observed ternary phases were the $C14$, μ, and μ'.

Al–Group VIA–X systems

In this section, only the Al–Mo–X systems (X = Fe, Co, Ni, Cu, Ti, Zr) are reviewed. The Al–Mo–X ternary systems have received almost no attention relative to the Al–Ti–X, Al–Zr–X, and Al–Nb–X systems.

The Al–Mo–Ti system is unusual in that it is one of the very few systems, if not the only one, that contains an expanded Al_3Ti phase field in the ternary system (Fig. 17*a*). Al_3Ti, which is a binary $D0_{22}$ line compound, dissolves about 20 at.-% Mo and extends to compositions containing as little as 62 at.-% Al at ~1200 K.[85] Also, Ti and Mo form a solid solution (bcc) at ~1200 K with ~35–40 at.-% maximum solubility for aluminium. Thus, an alloy consisting of 25 at.-% Mo, 35 at.-% Al, and 40 at.-% Ti is a single phase bcc solid solution at ~1200 K. A ternary σ phase of composition $Ti_{1.5}Mo_{1.5}Al_2$ in equilibrium with the bcc solid solution is stable at ~1200 K, as shown by the ternary isotherm and can serve as a second phase dispersion in the bcc matrix. Similarly, the $L1_0$ binary γ-TiAl phase dissolves up to 8 at.-% Mo and is in equilibrium with the bcc solid solution

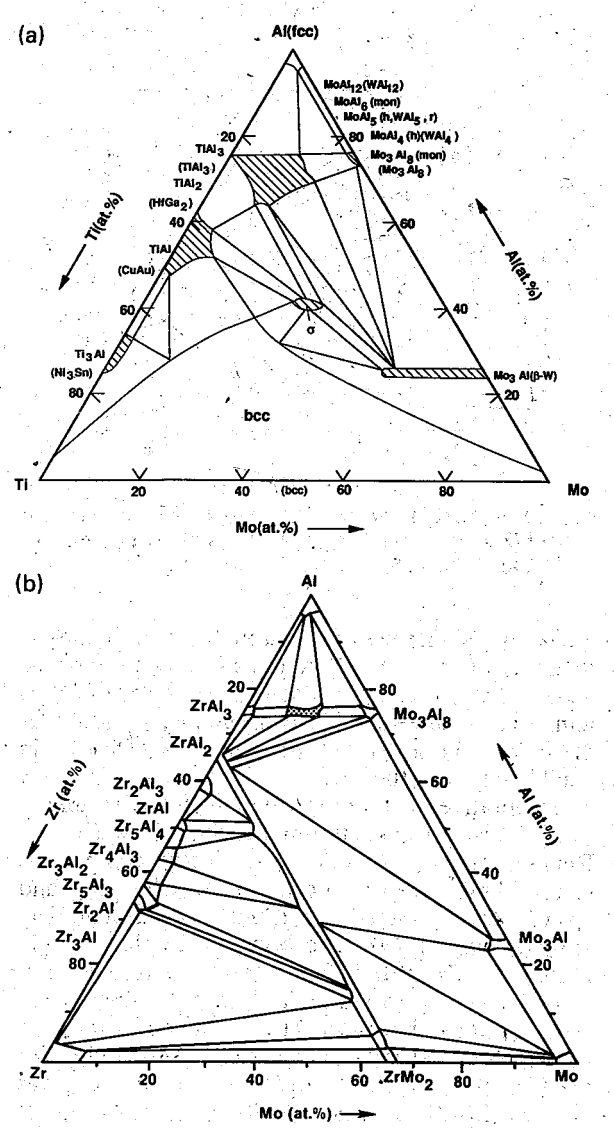

17 Ternary isotherms at ~1200 K in *a* Al–Mo–Ti system and *b* Al–Mo–Zr system (Ref. 85)

over a wide compositional range. Such phase relationships may be useful in designing multiphase alloys for high temperature applications with acceptable levels of density and ambient plasticity. Also in this ternary system, Mo_3Al dissolves up to 20 at.-% Ti and Mo_3Al_8 dissolves about 2 at.-% Ti. It was speculated that Mo substitutes in both the Ti and Al sites in TiAl. Similar behaviour was confirmed in the case of Al_3Ti, where Mo was found to substitute for Ti and Al.

An ~1200 K isotherm for the Al–Mo–Zr system, due to Hansen and Raman,[85] is shown in Fig. 17*b*. It reveals the presence of a unique ternary $D0_{22}$ phase with the formula $Zr_{0.5}Mo_{0.5}Al_3$, in equilibrium with the $D0_{23}$ $ZrAl_3$ and Mo_3Al_8. The $D0_{23}$ $ZrAl_3$ has very low solubility for Mo, unlike its $D0_{22}$ Al_3Ti counterpart in the Al–Ti–Mo system. The ternary $D0_{22}$ phase $ZrMoAl_6$ is in equilibrium with Al and exists over a finite composition range. Lattice parameters for the composition $ZrMoAl_6$ were reported as $a = 0{\cdot}3866$ nm and $c = 0{\cdot}8673$ nm. The lattice constants were slightly higher than those of $NbAl_3$ on the Zr-rich side, and lower on the Mo-rich side, which was attributed to the smaller size of the Mo atoms. For the same reason, when Mo substitutes for Al in Al_3Ti, the c parameter drops rapidly, reducing the axial ratio to 2·15 and also decreasing the unit cell volume. Similar behaviour was observed for solid solutions of $NbAl_3$ and $TiAl_3$ containing Mo, where Mo substituted for Nb and Ti. The $ZrAl_2$ phase field in the Al–Mo–Zr system extends towards $ZrMo_2$ and dissolves about 61 at.-% Mo. None of the other binary phases shows any significant solubility for the third element.

Markiv *et al.*[107] investigated the Al-rich portion of the Al–Mo–Fe system in detail. Figure 18*a* and *b* reproduce two of their isotherms, at 1323 and 1073 K, respectively. The isotherms show an $MoAl_3$ phase in the binary Al–Mo system, in contradiction to Hunt and Raman,[88] who contended that there was no binary $MoAl_3$ compound. A more recent Al–Mo binary phase diagram[80] also did not include $MoAl_3$. Thus, the phase relationships shown in Fig. 18*a* and *b* are questionable to the extent that, for example, Fe_4Al_{13}, $MoAl_4$, and Mo_3Al_8 are in equilibrium with $MoAl_3$. However, the presence or absence of $MoAl_3$ does not raise questions about the existence of ternary compounds N and S in the 1323 K isotherm or the phase relationships involving them since they are not in equilibrium with '$MoAl_3$'. The N phase was assigned a formula $MoFe_{0.28}Al_{2.72}$ and has a tetragonal structure ($D0_{22}$) with $a = 0{\cdot}376$ nm and $c = 0{\cdot}843$ nm. The compound, however, is not present at 1073 K and is, thus, a high temperature Al-rich $D0_{22}$ ternary phase. The S phase, whose composition corresponds to 5 at.-% Mo, 35 at.-% Fe, 60 at.-% Al, was not studied in detail nor was its crystal structure identified. It was determined to be stable only above 1273 K.

Using data derived from X-ray diffraction, electron microprobe analysis, and microstructural analysis, Burnashova *et al.*[108] constructed a 1273 K isotherm for the Al–Mo–Co system (Fig. 18*c*). This system includes a ternary $D0_{22}$ phase (N in Fig. 18*c*) described by $MoCo_{0.28}Al_{2.72}$, with lattice parameters

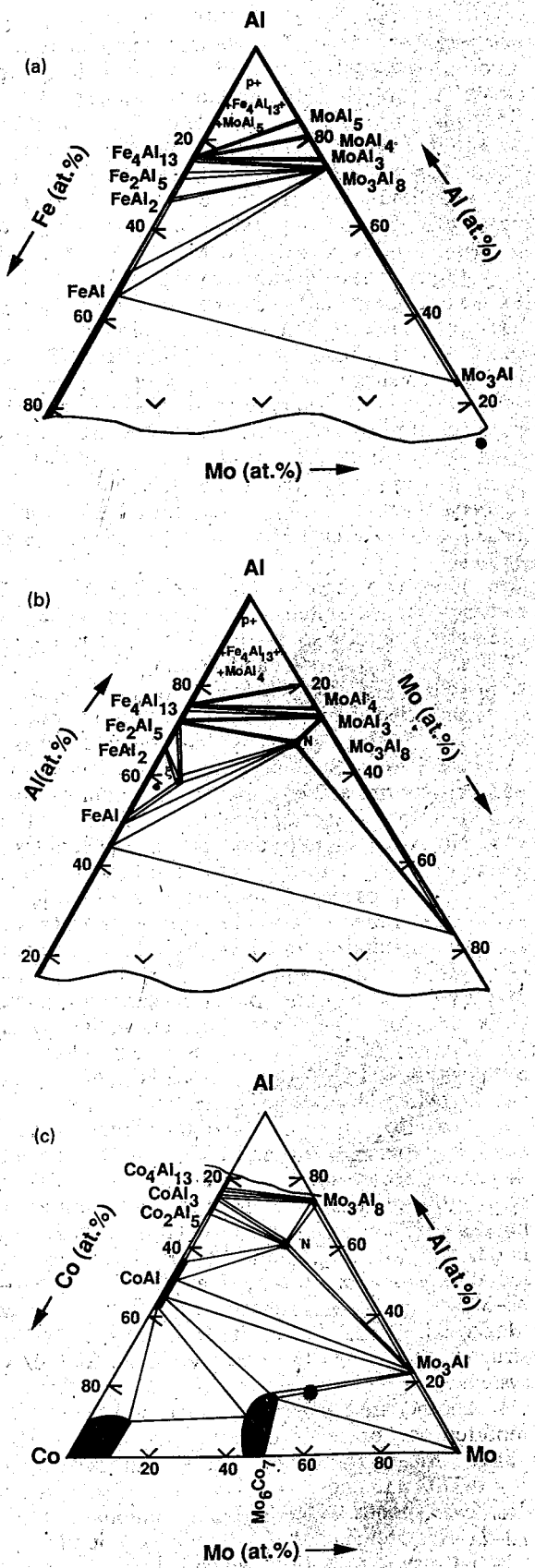

18 Ternary isothermal sections in *a* Al–Mo–Fe system at 1323 K (Ref. 107); *b* Al–Mo–Fe system at 1073 K (Ref. 107); *c* Al–Mo–Co system at 1273 K (Ref. 108)

$a = 0{\cdot}3743$ nm and $c = 0{\cdot}8401$ nm and a narrow compositional range of existence. This compound, reported to crystallise directly from the melt, is very similar to the N phase in the Al–Mo–Fe system (Fig. 18*a*), although no equivalent of the 'S phase seen in that system is present. While the N phase is not present in the Al–Mo–Fe system at 1073 K, it is not clear if the same is true in the Al–Mo–Co system. From Fig. 18*c*, the N phase is in equilibrium with Mo_3Al_8, Co_2Al_5, CoAl, and Mo_3Al, but none of these ternary phases exhibits any significant solubility for the third element. In fact, the only compound with any appreciable solubility for the third element is Mo_6Co_7, which dissolves ~20 at.-% Al at 1273 K. It is also interesting to note that the Al–Mo binary axis of the Al–Mo–Co ternary isotherm does not show the presence of $MoAl_3$ while the Al–Mo–Fe system does, even though both these isotherms appear to have been generated by the same group.[107,108] It is conceivable that the group recognised an error in their result between the times of these two investigations.

In 1966, two separate efforts on the Al–Mo–Ni ternary system resulted in two complete isotherms, one at 1073 K due to Markiv *et al.*,[109] and one at 1223 K due to Virkar and Raman.[81] These are compared in Fig. 19*a* and *b*. In addition, Markiv *et al.*[109] provided the Ni–NiAl–Mo section of the isotherms at 1473 and 1273 K. The types of phases present and the nature of the phase fields in these two partial isotherms are very similar. For example, they both show the absence of the ψ phase of composition $Mo_{7{\cdot}5}Ni_{58}Al_{34{\cdot}5}$, in contradiction to an earlier investigation of this system by Guard and Smith,[110] who reported the presence of this compound at 1448 K but did not determine its crystal structure. Neither was such a compound observed in the 1223 K isotherm (Fig. 18*b*) by Virkar and Raman.[81] However, when they used relatively low purity nickel, they found weak lines of a new phase corresponding to an $MgZn_2$-type ($C14$) Laves phase in alloys of composition $Mo_{50}Ni_{25}Al_{25}$, $Mo_{43}Ni_{31}Al_{26}$, and $Mo_9Ni_{53}Al_{38}$. The last of these compositions was fairly close to the composition of the earlier reported ψ phase,[110] leading Virkar and Raman to conclude that the ψ phase did not occur in the Mo–Ni–Al system, but was easily stabilised by small amounts of impurities. They further supported this conclusion by noting that Guard and Smith[110] observed a ψ phase (50 at.-% Ni, 32 at.-% Mo, 18 at.-% Si) in the Mo–Ni–Si system that was subsequently shown to be an $MgZn_2$-type phase,[111] a result consistent with the $C14$ structure they themselves observed in the Al–Mo–Ni system.

In another investigation, Raman and Schubert[30] reported the presence of a ternary $D0_{22}$ Al-rich phase, Mo_2NiAl_5, with lattice parameters of $a = 0{\cdot}3702$ nm and $c = 0{\cdot}8361$ nm. This composition corresponds to the Zr_2NiAl_5 compound in the Al–Zr–Ni system and the Ti_2CuAl_5 compound in the Al–Ti–Cu system, both of which have an $L1_2$ structure. This phase was also observed in a later investigation by Virkar and Raman,[81] who showed that it had a small homogeneity range along a constant 25 at.-% Mo line, extending from about 4 to 12 at.-% Ni (Fig. 19*b*). Markiv *et al.*[109] agreed with Virkar and Raman[81] regarding the existence of such an Al-rich $D0_{22}$ phase, but claimed that it had a very narrow compositional range of existence centred around 25 at.-% Mo, 3 at.-% Ni, 72 at.-% Al, or entirely outside the range specified by Virkar and Raman. In addition, Markiv *et al.*[109] reported the existence of an X phase in equilibrium with $NiAl_3$ which had a composition corresponding to 5 at.-% Mo, 18 at.-% Ni, 77 at.-% Al_3, and a small homogeneity range. Such a compound was not seen by Virkar and Raman.[81] The ternary $D0_{22}$ phase was found[109] to be similar to the N phase observed in the Al–Mo–Fe and Al–Mo–Co systems, and in the Al–Mo–Ni system, to be in equilibrium with the ternary X phase, whose crystal structure was not determined. Both the isotherms (Fig. 19*a* and *b*) show that the third element is not significantly soluble in any of the binary compounds.

Analogous to the ternary $D0_{22}$ Mo_2NiAl_5 in the Al–Mo–Ni system is a ternary $D0_{22}$ compound, Mo_2CuAl_5, reported by Raman and Schubert[30] in the Al–Mo–Cu system, with lattice parameters of $a = 0{\cdot}368$ nm and $c = 0{\cdot}837$ nm. Subsequently, Prevarskii *et al.*[112] examined various ternary alloys in the Al–Mo–Cu system that were annealed at 873 K for 400 h and water quenched. Using metallography and X-ray diffraction analysis, they identified the phases present in the various alloys and generated a complete isotherm at 873 K (Fig. 19*c*). This isotherm shows that none of the binary compounds exhibit any appreciable solubility for the third component at 873 K. Two Al-rich ternary phases are present: Mo_2CuAl_5, with $a = 0{\cdot}3716$ nm and $c = 0{\cdot}8445$ nm and the Al_3Ti structure (in agreement with the earlier report of Raman and Schubert[30]), and $MoCu_2Al_7$, with an orthorhombic structure ($a = 0{\cdot}505$ nm, $b = 0{\cdot}841$ nm, and $c = 1{\cdot}968$ nm). The latter is in equilibrium with aluminium, while the former exhibits a two phase region with '$MoAl_3$', Mo_3Al_8, $MoCu_2Al_7$, and several of the binary Al–Cu intermetallics. The $D0_{22}$ ternary phase is very similar to the ternary Mo_2NiAl_5 observed in the Al–Mo–Ni system.

Thus, in the Al–Mo–X systems (X = Fe, Co, Ni, Cu), various researchers have found a ternary $D0_{22}$ phase with a composition close to that of Mo_2XAl_5. This phase is stable only at high temperatures in the Al–Mo–Fe system (it is not present in the 1073 K isotherm), may or may not be stable at lower temperatures in the Al–Mo–Co system (only a 1273 K isotherm is available), and is present at 1073 K in the Al–Mo–Ni system and at 873 K in the Al–Mo–Cu system. Based on the limited information available, it appears that in the progression from Fe- to Cu-based Al–Mo ternary systems, the $D0_{22}$ ternary compound starts off as a high temperature phase and increases its temperature range of existence. Another interesting feature, mentioned above, is the similarity of the composition of this $D0_{22}$ phase to the $L1_2$ phase in the Al–Ti–X, Al–Zr–X, and Al–Hf–X systems (X = Cu, Ni). In addition, in the Al–Mo–Zr system, a ternary $D0_{22}$ phase of the composition $MoZrAl_6$ is present in equilibrium with Al_3Zr and Mo_3Al_8.

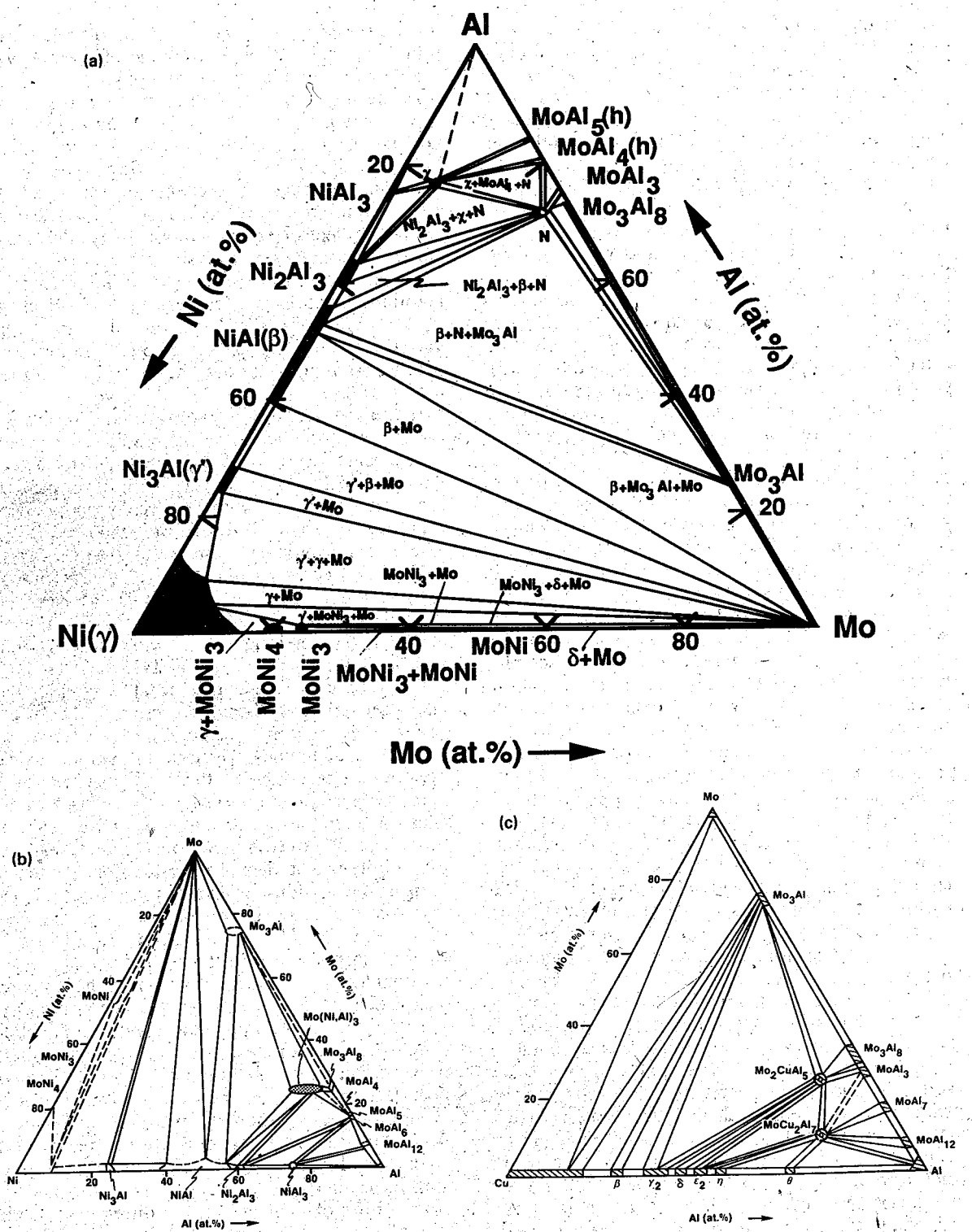

19 Isotherms in *a* Al–Mo–Ni system at 1073 K (Ref. 109); *b* Al–Mo–Ni system at 1223 K (Ref. 81); and *c* Al–Mo–Cu system at 873 K (Ref. 112)

Assessment of experimental procedures

Experimental inaccuracy can stem from inadequate care in processing, high impurity levels in starting constituents, or limitations in characterisation methods.

In all the investigations examined in this review, impurities, particularly interstitials such as C, O, N, and H, were never monitored for their influence on phase stability. The composition of the cast material was almost always assumed to be the same as the intended composition. Frequently, samples were less than 10 g in size and occasionally as small as 2 g. These samples were arc melted and weighed after casting to ensure compositional integrity. Such an

indirect procedure does not guarantee accuracy in composition; for instance, volatilisation of aluminium is possible, causing a weight loss which can be compensated partially by oxidation of the refractory element, thereby producing only small changes in weight, but a significant deviation from the intended composition. Loss in weight was frequently anticipated due to aluminium and was compensated for by the addition of excess aluminium to the melt. Rarely has any mention been made regarding the homogeneity of the cast samples and it is well known that arc melted buttons need to be turned over and remelted several times to ensure compositional homogeneity throughout the casting.

Heat treatment practices have typically involved extended exposure of the sample to a particular temperature, usually in vacuum after encapsulation of the sample in a quartz ampoule or alternately in an inert atmosphere, followed by cold water quenching and on occasion, air cooling. Such differences in heat treatment practices can result in a variety of microstructures, some of which are not necessarily representative of the temperature of interest. The resulting microstructures were often characterised using X-ray diffraction and optical microscopy. It is not exactly clear how the various phase boundaries can be accurately determined in a ternary system using only these two techniques. While it is possible to determine the nature of the phases present and their respective volume fractions using these characterisation methods, in a ternary system, where the tie lines determine the equilibrium between two phases, it would be indeed difficult if not altogether impossible to locate phase boundaries accurately. Further, none of these studies has used thermal analysis techniques such as DSC/DTA to identify phase transformation temperatures, nor did any of them use quantitative energy/wavelength dispersive X-ray analysis to determine matrix or precipitate compositions, leading to the conclusion that many of the isotherms in this review may be considered only approximate.

Several of the studies cited in this review date back to the mid 1960s and early 1970s when analytical abilities were restricted. Today, however, sophisticated analytical electron microscopy techniques coupled with thermal analysis have made it possible to determine phase diagrams, particularly ternary isotherms, with a high degree of precision. It must be pointed out that while such analytical tools are available, it is still extremely tedious to determine a complete ternary isotherm accurately. However, such ternary and higher order phase equilibria are critical to successful alloy design for demanding applications; one needs only to look at the history of steels to appreciate the significance of this statement.

To emphasise the relevance of experimental accuracy and the importance of detailed microstructural characterisation to complex ternary phase diagram determinations, the Al-Ti-Nb system will be used as an example. This system was selected, partly because of the current interest in titanium aluminides, and also because two recent studies[83,113] have independently generated a complete isotherm at the same temperature of 1473 K. In one study,[83] a variety of techniques was used in characterising the microstructure, whereas in the other,[113] X-ray diffraction was primarily used, although a couple of samples were examined using microprobe analysis.

In the first study,[83] samples were prepared from high purity elements (Al, Ti, Nb) by repeated arc melting in an argon atmosphere and annealed at 1473 K for up to two weeks. Subsequently, the annealed samples were chemically analysed and phase equilibria were determined by optical and scanning electron microscopy, X-ray diffraction, electron microprobe analysis, differential thermal analysis, and transmission electron microscopy. In addition, diffusion couples were made of select samples, carefully heat treated, and examined using various techniques. The complete experimental details essential for developing the 1473 K isotherm are provided.

In the second study,[113] the starting materials were in high purity elemental form and were arc melted in an arc beam furnace with a non-consumable W electrode in a high purity argon atmosphere. Some of the arc melted samples were chemically analysed and found to be very close to the intended composition. The as cast samples were homogenised in argon at 1473 K and cooled rapidly in a cold high pressure argon stream. Most of the cast alloys were heat treated at 1473 K for 24 h. Those samples that had relatively high melting points were first heat treated at 1673 K for 24 h and then at 1473 K for a further 168 h. The as cast and heat treated samples were characterised using X-ray diffraction, optical microscopy, and occasionally, microprobe analysis.

In spite of being fairly rigorous studies using a variety of techniques, there is significant disagreement between the results of these two studies. This is a reflection of the complexity of the system and possibly, differences arising from the heat treatments used in the two studies. The first major difference is seen in the liquidus projections presented in these two studies. A maximum in liquidus is shown by Perepezko *et al.*[83] in the Al_3Ti–Al_3Nb region, whereas this is absent in the second study.[113] While the liquidus projection looks similar in the two cases, a close examination reveals the liquid flow pattern to be different, suggesting an entirely different solidification sequence for the alloys. Further, there is significant disagreement between the two studies with respect to the presence or absence of ternary phases. Perepezko *et al.*,[83] show the presence of *T*2 and *B*2 ternary phases, whereas these are not shown in the isotherms due to Kaltenbach *et al.*[113] Since the authors of both these studies claim to know the composition of their alloys, the differences in their results must arise from differences in their heat treatment practices, or inadequate sampling. From their paper, it appears that Perepezko *et al.*[83] examined in detail at least 170 samples, if not more, compared with Kaltenbach *et al.*,[113] who claim to have examined only 22 binary and 35 ternary compositions. More specifically, in the latter study,[113] very few compositions were examined in the region adjacent to the *T*2 and *B*2 phases claimed by Perepezko *et al.*[83] Thus, one must attach more credibility to the 1473 K isotherm due to Perepezko *et al.*[83] Similarly, it is possible that Kaltenbach *et al.*[113] missed the

maximum in the liquidus of the Al_3Nb–Al_3Ti section because of an insufficient number of samples. It must be pointed out, however, that Kaltenbach *et al.*[113] specify that the Ti-rich part of their Al–Ti–Nb isotherm is still preliminary in nature. Finally, and probably of some relevance, is the fact that Kaltenbach *et al.*[113] have also evaluated the Al–Ti binary system and claim the presence of a high temperature phase lying between Al_2Ti and Al_3Ti, with a sizeable compositional range at 1473 K. This phase is absent in the isotherm due to Perepezko *et al.*[83] and accordingly influences the phase equilibria of the ternary system. In this context, the recent work of Ducastelle[114] on the binary Al–Ti system shows the presence of a high temperature phase between Al_3Ti and Al_2Ti analogous to that observed by Kaltenbach *et al.*[113] If this phase does indeed exist, then the 1473 K isotherm due to Perepezko *et al.*,[83] also needs corrections.

Thus, in spite of rigorous experiments as well as sophisticated characterisation of microstructure, it is still not clear whether the isotherm at 1473 K for the Al–Ti–Nb system is correct; what is important, however, is that it is a stride in the right direction.

Summary

Available experimental data on the phase equilibria of ternary Al-based systems have been reviewed, and inconsistencies between various investigations highlighted. Particular emphasis was placed on the compositional range of existence of ternary compounds, their crystal structure, and their stability as a function of temperature. It is evident from this survey that there are inconsistencies regarding the existence of some intermetallic phases even in certain binary phase diagrams. In several ternary systems, there is very little agreement regarding the presence or absence of ternary phases, their structure, and the compositional range over which they exist as a single phase. In several cases, no comparisons are possible because there is only one source of information, and seldom is there more than one isotherm available at any particular temperature per ternary system.

Based on this review of experimental data on the phase equilibria of ternary Al-based systems, a systematic pattern appears to emerge for the structure and stability of Al-rich compounds, specifically the Al_3X-type compounds. In the Group IIIA–Al binary systems – for example, Al–Sc – a binary $L1_2$ Al_3Sc is known to exist as a stable phase. Moving to the right in the periodic table to the Group IVA–Al systems, binary Al_3Ti, Al_3Zr, and Al_3Hf with the $D0_{22}$ structure (or $D0_{23}$) occur, as well as ternary $L1_2$ compounds with stoichiometries of the type Al_5CuTi_2 or Al_5CuHf_2, which appear to be produced by the addition of Cu, Ni, Fe, or Zn to Al_3Ti, Al_3Zr, and Al_3Hf. While all four of the specified alloying additions transform $D0_{22}$ Al_3Ti to $L1_2$, only Cu appears capable of effecting such a transformation for Al_3Zr and Al_3Hf. Binary Group VA–Al systems contain stable $D0_{22}$ Al_3V, Al_3Nb, and Al_3Ta, but no alloying addition is known to transform these to ternary $L1_2$ structures. No binary '$MoAl_3$' compound exists in the Group VIA–Al binary systems (e.g. Mo–Al); however, addition of Fe, Co, Ni, or Cu stabilises ternary $D0_{22}$ compounds of the type Al_5Mo_2Cu, which are similar in composition to $L1_2$ Al_5Ti_2Cu. Thus, it appears that the ease of forming an Al-based $L1_2$ compound decreases in the progression from Group IIIA to Group VIA systems.

A point of interest in the Group IVA–Al binary systems is the presence of $D0_{22}$ Al_3Ti, $D0_{23}$ Al_3Zr, and a $D0_{22}/D0_{23}$ Al_3Hf (depending on temperature), which suggests that the sequence of the alloying elements in the group should be Ti, Hf, and Zr rather than Ti, Zr, and Hf. Interestingly enough, Pettifor[115] arranged the periodic table in a one dimensional sequence of the type Zr, Hf, Ti, Ta, Nb, V, W, Mo, Cr, which is consistent with the observed gradation in crystal structures of the Al_3X compounds from $D0_{23}$ to $D0_{23}/D0_{22}$ to $D0_{22}$.

Theoretical studies for predicting crystal structure stability and alloy phase diagrams

It is not the intention in this section to provide an exhaustive review and a critical assessment of the progress to date in computational capabilities for predicting entire phase diagrams and the stability of various crystal structures. Rather, a brief update on the various techniques is presented to complement the previous sections and to provide the reader with an appreciation of the kinds of efforts in progress and their success. Progress to date in the design of alloys has been made largely by ordering and collating an enormous amount of empirical data. To avoid this time consuming work, researchers would clearly find it desirable to be able to predict phase diagrams and crystal structure stability. Dramatic new advances in theory and computational capabilities have now opened up such prospects in the design of new complex alloys.

Attempts to relate crystal structure stability to intrinsic atomic properties can be traced back to the early 20th century, when Hume-Rothery pointed out the existence of definite correlations between the electron/atom ratio (e/a) and specific crystal structures. Many factors play a role in stabilising a given structure and these have been extensively studied. Massalski[116] reviewed the influence of the ratio of valence electrons to atoms, while Pauling[117] elucidated the role of the electronegativity difference between the constituent atoms in affecting structural stability. The difference in size of the constituent atoms also determines the stability of a particular phase, as shown by Laves.[118]

Attempts to understand the relative phase stability of various types of A_3B compounds led to consideration of the electron concentration criterion[119] and the atomic size difference criterion.[63,120,121] Sinha[119] noted an increase in the hexagonality of the A_3B structure with an increase in the e/a ratio, while van Vucht[121] found an increase in hexagonality with an increase in the atomic radius ratio (R_B/R_A) for an A_3B compound. These criteria predict that an increase in either factor will shift the crystal structure not only from cubic to hexagonal stacking, but also

from rectangular ordering ($D0_{22}$)[122] to triangular ordering on the close packed planes ($L1_2$).

A phenomenological approach based on existing experimental data has led to the generation of structural stability maps. This approach groups crystal structures on the basis of (a) Pauling's electronegativity difference and average principal quantum numbers of the constituent elements,[123] (b) *s*- and *p*-orbital radii of the constituent elements,[124] and (c) the difference between Zunger's pseudopotential radii sums, the Martynov–Batsanov electronegativity difference, and the sum of the number of valence electrons.[125–127] These three investigations are limited in that the coordinates are classical and not quantum in nature. Therefore, Villar's maps,[125–127] for example, cannot account for the NiAs structure, even though it is the fifth most important of the 20 AB-type structures. In addition, Villar's maps are three dimensional and cumbersome to use.

Pettifor[115] emphasised that only quantum mechanics could predict the structure and properties of a material, because the way in which constituent atoms of any material bind together is determined by the valence electrons, and these follow quantum mechanics in the form of Schrödinger's equation rather than the classical laws of Newtonian mechanics. Wigner and Seitz[128,129] applied a cellular method to calculate the energy bands of metallic sodium using Schrödinger's equation and obtained theoretical values for the cohesive energy and atomic volume of metallic sodium that were within 10% of experimental values. Soon after, Slater[130] extended their method to include more than just the one *s* wavefunction and, thereby, actually calculated the excited energy levels previously estimated by Wigner and Seitz. The Wigner–Seitz and Slater approximations were subsequently improved significantly by von der Lage and Bethe[131] and Howarth and Jones.[132]

Slater and Johnson[133] described a self-consistent field (SCF) method (often referred to as the Xα cluster method) of calculating electronic energy levels for polyatomic solids, whereby the one electron potential is approximated using the 'muffin tin' approximation and the resulting equation is solved using a multiple scattering method. Morinaga *et al.*[134] applied this technique to study the effect of alloying additions on the electronic structure of the $L1_2$ compound Ni_3Al. Using a cluster of the type [M $Ni_{12}Al_6$], they substituted M for an Al atom and were able to obtain the energy level of *d*-orbitals, ionicity, and bond order for various transition elements.

Pettifor[135] proposed a chemical scale χ, which ordered all the elements along a single axis χ, so that the Mendeleev type features of the periodic table were preserved. He was thus able to retain the quantum characteristics of the alloying elements, while reducing the two dimensional structure of the periodic table to a single coordinate. He then used χ_A and χ_B as the coordinates for constructing two dimensional structure maps for binary, ternary, and quaternary compounds of various stoichiometries. Subsequently, Pettifor and Podloucky[136] used a microscopic approach, via a tight binding model, to explain the origin of the different structural domains of *pd*-bonded (transition metal–non-transition metal) AB compounds within a fundamental quantum mechanical framework. The AB_3 structure map[137] can be used to explain the $D0_{22}$ to $L1_2$ transformation of Al_3Ti resulting from the addition of Fe, Ni, Cu, or Zn. The Pettifor maps are limited in their predictive capabilities, but if a particular structural transformation is known to occur, they can provide an estimate of the amount of a particular element that must be incorporated to change the weighted Mendeleev number and thus move from one structural domain to another.

Using the Ising model, and assuming first and second neighbour interaction, Richards and Cahn[138] showed that for the A_3B composition, the $L1_2$ structure is the ground state (i.e. the lowest configurational energy) if V_2/V_1 is negative, where V_i is the *i*th neighbour interaction parameter and V_1 is always positive. If V_2/V_1 is positive, then the $D0_{22}$ structure was shown to be the lowest energy structure for the A_3B stoichiometry. Allen and Cahn[139] used the cluster method to provide a rigorous mathematical proof for these proposed ground state structures.

In the past decade, the prediction of structural stabilities of phases at 0 K has become possible through precise electronic band structure computations[140–142] based on local density functional theory.[143,144] Recently, first principle approaches have even been used[145–147] with reasonable success to compute phase stability away from 0 K. Using an extremely accurate first principles approach, based on the full potential, linearised augmented, plane wave method (FLAPW),[140] Guo *et al.*[148] were able to study the energetics and bonding properties of the binary compound LiAl, and concluded that the *B*32 phase contained a mixture of covalent and metallic bonding and that the *B*32 to *B*2 transition occurred at a pressure of 140 kbar.

Recently, results from two independent studies[149,150] have been published to explain the $D0_{22}$ to $L1_2$ transition in the Group IV trialuminides. Eberhart *et al.*[150] have presented an electronic model for this transition, based on cluster calculations, and attribute the phase transition to the *d*-character provided in the Al *sp*-bonding region by the transition metal substitution, which preferentially orders the Al second neighbour atoms. Carlsson and Meschter[150] performed total energy calculations, using the augmented spherical wave (ASW) method, for the Group III, IV, and V transition metal trialuminides in the $L1_2$, $D0_{22}$, and $D0_{23}$ structures with ideal and non-ideal *c*/*a* ratios. Their results showed that the stability of the $D0_{22}$ structure relative to the $L1_2$ increased rapidly as the transition metal *d*-electron count increased. The calculated electronic densities of states (DOS) showed each structure to have a minimum in the DOS distribution at a characteristic *d*-electron count and the preferred crystal structure was one where the Fermi level lay in the minimum.

It must be mentioned that the presence of free surfaces in cluster calculations[149] prevents total energy calculations meaningful to bulk solids. However, these cluster calculations provide an adequate description of the bonding and changes resulting from impurities since the electronic perturbations are spatially localised. Thus, when these cluster

calculations[149] are coupled with total energy calculations,[150] the changes in bonding which cause the changes in total energy can be often understood and explained.

While all these studies describe various approaches to predict crystal structure stability, parallel research efforts are ongoing with a fair degree of success to calculate entire alloy phase diagrams from first principles. Alternately, Kaufman and co-workers[31,151,152] have, over the past two decades, developed an extremely useful set of computer programs for calculating the equilibrium and metastable phases of alloys. These programs do not start from first principles, but rely on information extracted from known binary systems to predict metastable structures, as well as ternary phase diagrams for which very little experimental data are often available. Some of the data that are essential to run the computer programs can be inferred only from the behaviour of the phase diagrams and cannot be experimentally verified. Thus, the reliability of the predictions depends on the accuracy and validity of these parameters.

During the course of investigating various superalloy phase diagrams, Kaufman and Nesor[31] found good agreement between calculated and observed ternary isotherms in the Al–Ti–Ni and Al–Mo–Ni systems. Similarly, Kaufman and Dew-Hughes[151] computed the Al–Ti–Fe isotherm and initially found poor agreement with experimental data when they assumed that Al substituted for Ti in FeTi and Fe_2Ti. A subsequent iteration with appropriate modifications revealed a good fit between experimental and calculated isotherms. The work of Chart[53] on the Al–Cr–Zn system was discussed above. The validity of the parameters used in these programs will directly influence the accuracy of the calculated isotherms; therefore, it is important to confirm the consistency of these input parameters using first principle calculations based on quantum mechanics.

The task of calculating alloy phase diagrams from first principles is challenging because the necessary calculations must combine both quantum mechanical and statistical thermodynamical elements with a high level of accuracy. This usually involves combining the tight binding (TB) electronic band structure calculations with a free energy expression from a statistical mechanical method called the cluster variation method (CVM). The TB method solves the Schrödinger equation for the motion of an electron in a periodic potential by starting with the wavefunctions of electrons in individual atoms and combining them in a suitable way to form approximations in the crystal. The CVM[153] requires, as input, interaction parameters which determine ordering or clustering reactions occurring in the alloy systems. These interaction parameters must be defined carefully and then obtained by means of electronic structure calculations using, for example, the Gautier–DuCastelle[154] generalised perturbation method. Prototype phase diagrams have been calculated by Sanchez and de Fontaine[155] and by Turchi *et al.*[145] for fcc based systems, by Sigli and Sanchez[156,157] for bcc systems, and by Sluiter *et al.*[146] for the combined fcc–bcc Ti–Rh system. Recently, total energies of Al, Li, and various Al–Li compounds computed by the FLAPW method were used to calculate the Al–Li phase diagram according to the CVM.[158] Remarkable agreement with experimental data was observed. These authors[158] hope that in the near future they can use basic information for pure A and B (and C), such as electronic structure, bulk modulus, melting points, and allotropic transition temperatures, to construct the corresponding A–B (or A–B–C) phase diagram, with no additional 'alloy' data – in other words, an interpolating scheme for predicting stable and metastable alloy phase equilibria using as input only pure element parameters.

Summary comments

Early attempts to correlate the crystal structure of AB_3-type compounds with radius ratio or electron concentration have not been altogether successful as neither of these two correlations could be applied to all AB_3 phases. For example, the sequence hcp → fcc with increasing electron/atom (e/a) ratio is in a direction opposite to that for ordered close packed AB_3 structures where the hexagonality increases with increasing e/a. However, seven binary alloy structures, isotypical with Ni_3Ti, which is 50% hexagonal, occur at a higher electron concentration ($e/a = 8{\cdot}5$) than that for the 100% hexagonal $MgCd_3$-type structure ($e/a = 8{\cdot}25$) known to be present in at least six binary AB_3-type alloys. Similarly, the hexagonality of the rare earth metals and that of their trialuminides change in opposite directions along the rare earth series and finally, the sequence of ordered close packed AB_3 structures formed by transition elements is not easily explained. The presence of small amounts of impurities such as oxygen and/or carbon contamination significantly influences the stability of a crystal structure and if overlooked, causes disagreement and confusion between theory and observations. These impurities can result either from the source materials or processing condition. For example, pure $ErAl_3$ has an $L1_2$ structure (three layers per repeat period). Van Vucht and Buschow[120] claim that if $ErAl_3$ is melted in a ZrO_2 crucible instead of an Al_2O_3 crucible, the resulting structure of $ErAl_3$ has a 15 layer repeat period; thus, the $L1_2$ structure is destabilised. Similarly, Philipsborn and Laves[64] have shown that for the Cr_3Si-type $A15$ compounds, Ti_3Au, V_3Au, and V_3Pt, contamination caused by oxygen, nitrogen, or carbon, but not hydrogen, stabilises the $L1_2$ structure in favour of the $A15$ structure and, further, that such a transformation is irreversible. Remelting the $L1_2$ compound under a high vacuum condition did not restore the $A15$ structure. The amount of interstitial needed to effect the $A15$ to $L1_2$ transformation completely was dependent on the interstitial type and the intermetallic compound. Finally – as a closing comment on the effect of radius ratio and electron concentration criteria on structural stability – these two parameters are not independent; rather they are interactive and the exact interactions are not well defined, thereby reducing their utility for predictive purposes.

Structural stability maps, as pointed out above, are based on a phenomenological approach. With the exception of Pettifor's maps, the remaining earlier

efforts rely on Newtonian mechanics and the shortcomings of not using quantum mechanical coordinates have been discussed. While Pettifor's maps have been more successful in interpreting observed crystal structures than previous efforts, they too have severe limitations in their predictive capabilities. Attempts to use the Pettifor map to explain the $D0_{22}$ to $L1_2$ transformation of Al_3Ti with Cu, Ni, and Fe additions have been successful, although attempts to transform $D0_{22}$ Al_3Nb to an $L1_2$ compound using Pettifor's maps have not met with success to date.

The Xα cluster method, while adequate to describe bonding and the changes in bond energy caused by impurities and therefore crystal structure stability, is limited by the size of the cluster. When a cluster larger than 19 atoms is used, the computational abilities of the most advanced computers are quickly exhausted. This 19 atom cluster, therefore, excludes studies on the effect of dilute additions on structural stability. Fortunately a $D0_{22}$ to $L1_2$ transformation of Al_3Ti, for example, requires major alloying (Al_5CuTi_2) and thus, can be examined using the Xα technique. Another limitation is the presence of free surfaces in such cluster calculations which preclude total energy calculations meaningful to bulk solids. Total energy calculations, while being more accurate, are much more rigorous and extremely time consuming in terms of supercomputer time.

In a recent article, Freeman *et al.*[48] discussed advances in such total energy computational approaches using a number of illustrative examples, including the phase stability of Ni_3Al, $ZrAl_3$, and titanium aluminides, the effect of alloying on the phase stability, phase diagram determination, interfacial properties (APB energy) of intermetallics such as Ni_3Al and NiAl, and the role of alloying elements in influencing these interfacial properties. They have shown theoretically that vanadium addition to Ni_3Al would cause a slight hardening effect which is in agreement with experimental work; for their prediction that Li addition to Al_3Zr would stabilise the $L1_2$ structure in favour of the $D0_{22}$ structure, experimental verification is absent. In another area, they have tried to predict alloying additions to lower APB energies in NiAl in an attempt to improve its ambient ductility. Their studies recommended vanadium addition to NiAl to decrease the APB energy and therefore to improve ductility. Experimental results showed vanadium additions to increase flow stress and further decrease ductility compared with binary NiAl. Whether this is due to a failure in predictive capabilities, or insufficient understanding of what metallurgical factors contribute to the ductility of intermetallics is not clear. In addition, a particular alloying element will influence more than one property when added to a system. In the above example, vanadium addition may lower the APB energy, but could simultaneously influence another parameter and therefore a simple consideration of only the APB energy may be inadequate to address the ductility issue. Nevertheless, it appears that theoretical approaches attempting to predict mechanical behaviour have met with little or no success to date. At present it appears that it would be more fruitful for such theories and computations to focus their emphasis on crystal structure stability and phase diagram predictions rather than the mechanical behaviour of materials. While the fundamental elements that play a role in materials deformation include defects such as grain boundaries, dislocations, and vacancies, these are not currently incorporated in theoretical calculations and will influence the predicted results negatively.

Perhaps the greatest promise of theoretical computations to date has been in the area of phase diagram prediction. However, it must be pointed out that these studies have been typically restricted to fairly simple binary systems such as the Al–Li system. In this system, good agreement is observed between theory and experiment. Limitations on the size of the supercell has limited such studies to experimentally known phase diagrams where complicated structures are absent. Thus, complex ternary systems of the type discussed in this review are at present out of the scope of such calculations.

In this respect, it must be mentioned that had it not been for the sustained and focused efforts of the German group at the Max Planck Institute and the Soviet group from the Ukraine, the vast majority of the ternary phase equilibria information reviewed here would not have been available. Thus, while theoretical techniques to predict phase stability and structure must be encouraged, there is no substitute for experimental phase diagram determination in the forseeable future and efforts in this fundamental area of metallurgy must be intensified.

Although physicists today have at their disposal a spectrum of precise theories and computational capabilities, metallurgists have yet to familiarise themselves with these physical theories, muct less exploit them to the fullest extent. Similarly, the physicists and chemists need to gain a better appreciation of metallurgical experiments, applications, and relevance to fit their theories better to industrial needs. Very close interaction among the various disciplines is essential to ensure progress. Physicists and metallurgists have both advanced significantly in their own arenas, although it was not until very recently that these two disciplines started recognising their mutual need to progress in the theory and design of alloy phases.

Conclusions

The purpose of this review was to bring together a large body of knowledge on phase equilibria of ternary alloys containing aluminium, with emphasis on the intermetallic compounds. This body of information has been extracted largely from the Soviet and German literature. Where available, the observations and inconsistencies between various researchers have been compared and contrasted. Potential ternary intermetallics of interest to the aerospace industry, based on their crystal structure, density, melting point, and compositional range of existence, have been emphasised. The changes in the crystal structure of Al-rich compounds with the location of the constituent elements in the periodic table has been noted.

The last section of the review provides an outline of various theoretical approaches available to date for predicting crystal structure stability, as well as entire binary and higher order phase diagrams. The merits of a quantum mechanical approach versus the classical approach are discussed, and illustrative examples are provided to highlight the progress in predictive capabilities.

References

1. 'Structural uses for ductile ordered alloys', Final Report from NMAB to DARPA by the Committee on Application Potential for Ductile Ordered Alloys, Report No. NMAB–419, Procurement Instrument Identification No. MDA–83–C–020, Washington, DC, Aug. 1984.
2. C. T. LIU: in 'High temperature alloys: Theory and design', (ed. J. O. Stiegler), 289–308; 1984, Warrendale, PA, Metallurgical Society of AIME.
3. T. TAKASUGI, N. MASAHASHI, and O. IZUMI: *Scr. Metall.*, 1986, **20**, 1317–1321.
4. S. M. L. SASTRY and H. A. LIPSITT: *Metall. Trans.*, 1977, **8A**, 1543–1552.
5. Y. CALVAYRAC and M. FAYARD: *Phys. Status Solidi (a)*, 1973, **17**, 407–421.
6. C. T. LIU and H. INOUYE: *Metall. Trans.*, 1979, **10A**, 1515–1525.
7. E. R. SCHULSON and D. R. BARKER: *Scr. Metall.*, 1983, **17**, 519–522.
8. N. S. STOLOFF: in 'High temperature ordered intermetallic alloys', (ed. C. C. Koch *et al.*), Mater. Res. Soc. Symp. Proc., 1985, **39**, 3–27.
9. A. INOUE, H. TOMIOKA, and T. MASUMOTO: *J. Mater. Sci. Lett.*, 1982 **1**, 377–380.
10. A. INOUE, H. TOMIOKA, and T. MASUMOTO: *Metall. Trans.*, 1983, **14A**, 1367–1377.
11. O. NOGUCHI, Y. OYA, and T. SUZUKI: *Metall. Trans.*, 1981, **12A**, 1647–1653.
12. T. SUZUKI, Y. OYA, and S. OCHIAI: *Metall. Trans.*, 1984, **15A**, 173–181.
13. T. TAKASUGI, N. MASAHASHI, and O. IZUMI: *Acta Metall.*, 1987, **35**, 381–391.
14. D. P. POPE and S. S. EZZ: *Int. Metall. Rev.*, 1984, **29**, 13–167.
15. R. W. CAHN, P. A. SIEMERS, J. E. GEIGER, and P. BARDHAN: *Acta Metall.*, 1987, **35**, 2737–2751.
16. M. YAMAGUCHI, Y. UMAKOSHI, and T. YAMANE: *Philos. Mag. A*, 1987, **55**, 301–315.
17. M. YAMAGUCHI, Y. SHIRAI, and Y. UMAKOSHI: in 'Dispersion strengthened aluminum alloys', (ed. Y.-W. Kim and W. M. Griffith), 721–740; 1988, Warrendale, PA, The Minerals, Metals, and Materials Society.
18. A. RAMAN: *Z. Metallkd.*, 1966, **57**, 535–540.
19. Y. UMAKOSHI, M. YAMAGUCHI, T. YAMANE, and T. HIRANO: *Philos. Mag. A.*, 1988, **58**, 651–665.
20. K. S. KUMAR and J. R. PICKENS: *Scr. Metall.*, 1988, **22**, 1015–1018.
21. J. TARNACKI and Y.-W. KIM: *Scr. Metall.*, 1988, **22**, 329–334.
22. W. O. POWERS, J. A. WERT, and C. D. TURNER: *Philos. Mag. A.*, 1989, **60**, 227–244.
23. C. D. TURNER, W. O. POWERS, and J. A. WERT: *Acta Metall.*, 1989, **37**, 2635–2643.
24. K. S. KUMAR and J. R. PICKENS: in 'Dispersion strengthened aluminum alloys', (ed. Y.-W. Kim and W. M. Griffith), 763–786; 1988, Warrendale, PA, The Mineral, Metals, and Materials Society.
25. S. ZHANG, J. P. NIC, and D. E. MIKKOLA: *Scr. Metall.*, 1990, **24**, 57–62.
26. S. MAZDIYASNI, D. B. MIRACLE, D. M. DIMIDUK, M. G. MENDIRATTA, and P. R. SUBRAMANIAN: *Scr. Metall.*, 1989, **23**, 327–331.
27. E. P. GEORGE, W. D. PORTER, H. M. HENSON, W. C. OLIVER, and B. F. OLIVER: *J. Mater. Res.*, 1989, **4**, 78–83.
28. V. Ya. MARKIV, V. V. BURNASHOVA, and V. P. RYABOV: *Akad. Nauk Ukr. SSR, Metallofiz.*, 1973, **46**, 103–110.
29. A. SEIBOLD: *Z. Metallkd.*, 1981, **72**, 712–719.
30. A. RAMAN and K. SCHUBERT: *Z. Metallkd.*, 1965, **56**, 99–104.
31. L. KAUFMAN and H. NESOR: *Metall. Trans.*, 1974, **5**, 1623–1629.
32. P. G. NASH, V. VEJINS, and W. W. LIANG: *Bull. Alloy Phase Diagrams*, 1982, **3**, 367–374.
33. S. C. HUANG, E. L. HALL, and M. F. X. GIGLIOTTI: *J. Mater. Res.*, 1988, **3**, 1–7.
34. P. VIRDIS and U. ZWICKER: *Z. Metallkd.*, 1971, **62**, 46–51.
35. W. HEINE and U. ZWICKER: *Naturwissenschaften*, 1962, **49**, 391.
36. V. Ya. MARKIV, Yu.V. VOROSHILOV, P. I. KRIPYAKEVICH, and E. E. CHERKASHIN: *Sov. Phys. Crystallogr.*, 1965, **9**, 619–620.
37. V. Ya. MARKIV: *Izv. Akad. Nauk SSSR, Met.*, 1966, (1), 156–158.
38. A. RAMAN and K. SCHUBERT: *Z. Metallkd.*, 1965, **56**, 40–43.
39. A. E. DWIGHT: *J. Less-Common Met.*, 1974, **34**, 279–284.
40. H. MABUCHI, K. HIRUKAWA, and Y. NAKAYAMA: *Scr. Metall.*, 1989, **23**, 1761–1766.
41. E. M. SCHULSON and J. A. ROY: *Acta Metall.*, 1978, **26**, 15–38.
42. P. HOLDWAY and A. E. STATON-BEVAN: *J. Mater. Sci.*, 1986, **21**, 2843–2849.
43. M. S. ZEDALIS, M. V. GHATE, and M. E. FINE: *Scr. Metall.*, 1985, **19**, 647–650.
44. E. NES: *Acta Metall.*, 1972, **20**, 499–506.
45. N. RYUM: *Acta Metall.*, 1969, **17**, 269–278.
46. F. W. GAYLE and B. VANDERSANDE: *Acta Metall.*, 1989, **37**, 1033–1046.
47. J. H. SCHNEIBEL and W. D. PORTER: in 'High temperature ordered intermetallic alloys III', (ed. N. S. Stoloff *et al.*), Mater. Res. Soc. Symp. Proc., 1989, **133**, 335–340.
48. A. J. FREEMAN, T. HONG, and J.-H. XU: in 'Atomistic simulation of materials: Beyond pair-potentials', (ed. V. Vitek and D. Svolovitz), 41–54; 1989, New York, Plenum Press.
49. A. J. FREEMAN: Personal communications.
50. M. E. DRITS, E. S. KADANER, and V. I. KUZ'MINA: *Izv. Akad. Nauk SSSR, Met.*, 1969, (5), 170–173.
51. O. S. ZARECHNYUK, A. N. MALINKOVICH, E. A. LALAYAN, and V. Ya. MARKIV: *Russ. Metall.*, 1967, (6), 105–107.
52. V. Ya. MARKIV and V. V. BURNASHOVA: *Sov. Powder Metall. Met. Ceram.*, 1970, **12**, 998–1002.
53. T. G. CHART: NBS Spec. Publ. 496, Vol. 2, 1186–1199; 1978, Washington, DC, National Bureau of Standards.
54. V. Ya. MARKIV and V. V. BURNASHOVA: *Dop. Akad. Nauk Ukr. RSR A, Fiz.-Mat. Tekh.*, 1969, **31**, (5), 463–464.
55. V. V. BURNASHOVA and V. Ya. MARKIV: *Dop. Akad. Nauk Ukr. RSR A, Fiz.-Mat. Tekh.*, 1969, **31**, (4), 351–353.
56. V. V. BURNASHOVA and V. Ya. MARKIV: *Dop. Akad. Nauk Ukr. RSR A, Fiz.-Mat. Tekh.*, 1969, **31**, (1), 59–61.
57. V. V. BURNASHOVA and V. Ya. MARKIV: *Visn. L'viv. Derzh. Univ., Ser. Khim.*, 1969, (11), 34–37.
58. V. Ya. MARKIV and P. I. KRIPYAKEVICH: *Sov. Phys. Crystallogr.*, 1967, **11**, 733–738.
59. P. I. KRIPYAKEVICH, V. V. BURNASHOVA, and V. Ya. MARKIV: *Dop. Akad. Nauk Ukr. RSR A, Fiz.-Mat. Tekh.*, 1970, **32**, 828–831.
60. V. Ya. MARKIV, P. I. KRIPYAKEVICH, and N. N. BELYAVINA: *Dop. Akad. Nauk Ukr. RSR A, Fiz.-Mat. Tekh.*, 1982, (3), 76–79.
61. V. Ya. MARKIV, N. F. MATUSHEVSKAYA, S. N. ROZUM, and Yu. B. KUZ'MA; *Izv. Akad. Nauk SSSR, Neorg. Mater.*, 1966, **2**, (9), 1581–1585.
62. A. RAMAN and K. SCHUBERT: *Z. Metallkd.*, 1965, **56**, 44–52.
63. J. H. N. van VUCHT and K. H. J. BUSCHOW: *J. Less Common Met.*, 1965, **10**, 98–107.
64. H. PHILIPSBORN and F. LAVES: *Acta Crystallogr.*, 1964, **17**, 213–214.
65. A. DRASNER and Z. BLAZINA: *Z. Naturforsch. B*, 1981, **36B**, 1547–1550.
66. P. VILLARS and L. D. CALVERT: in 'Pearson's handbook of crystallographic data for intermetallic phases', Vol. 2; 1985, Metals Park, OH, American Society for Metals.
67. T. B. MASSALSKI *et al.* (eds): 'Binary alloy phase diagrams', Vol. 1, 118–119; 1986, Metals Park, OH, American Society for Metals.
68. S. HORI, N. FURUSHIRO, and W. FUJITANI: *Aluminium*, 1981, **57**, 556–557.
69. S. HORI, Y. UNIGAME, N. FURUSHIRO, and H. TAI: *J. Jpn Inst. Light Met.*, 1982, **32**, 408–412.
70. S. HORI, N. FURUSHIRO, and W. FUJITANI: *J. Jpn Inst. Light Met.*, 1981, **31**, 649–654.
71. N. FURUSHIRO and S. HORI: *Acta Metall.*, 1985, **33**, 867–872.

72. V. V. BURNASHOVA, V. R. RYABOV, and V. Ya. MARKIV: *Dop. Akad. Nauk Ukr. RSR A, Fiz.-Mat. Tekh.*, 1969, **31**, (8), 741–743.
73. V. V. BURNASHOVA, V. Ya. MARKIV, and G. B. STROGANOV: *Dop. Akad. Nauk Ukr. RSR A, Fiz.-Mat. Tekh.*, 1971, **33**, (12), 1122–1124.
74. V. Ya. MARKIV and V. V. BURNASHOVA: *Russ. Metall.*, 1969, (6), 113–115.
75. F. HEREDIA and D. P. POPE: in 'High temperature ordered intermetallic alloys II', (ed. N. S. Stoloff *et al.*), Mater. Res. Soc. Symp. Proc., 1987, **81**, 213–220.
76. V. Ya. MARKIV, A. I. STOROZHENKO, and I. N. PANYUTA: *Dop. Akad. Nauk Ukr. RSR A, Fiz.-Mat. Tekh*, 1974, **36**, (5), 463–466.
77. W. U. KOPP and E. WACHTEL: *Z. Metallkd.*, 1969, **60**, 713–719.
78. K. P. MYASNIKOVA, L. F. PONOMAREVA, L. I. PRYAKHINA, and I. K. MARSHAKOV: *Izv. Akad. Nauk SSSR, Met.*, 1971, (1), 186–189.
79. P. R. SUBRAMANIAN, D. B. MIRACLE, and S. MAZDIYASNI: *Metall. Trans.*, 1990, **21**, 539–545.
80. T. B. MASSALSKI *et al.* (eds): 'Binary alloy phase diagrams', Vol. 1, 133–134; 1986, Metals Park, OH, American Society for Metals.
81. A. V. VIRKAR and A. RAMAN: *Z. Metallkd.*, 1969, **60**, 594–600.
82. L. A. BENDERSKY and W. J. BOETTINGER: in 'High temperature ordered intermetallic alloys III', (ed. N. S. Stoloff *et al.*), Mater. Res. Soc. Symp. Proc., 1989, **133**, 45–50.
83. J. H. PEREPEZKO, Y. A. CHANG, L. E. SEITZMAN, J. C. LIN, N. R. BONDA, T. J. JEWETT, and J. C. MISHURDA: in 'High temperature aluminides and intermetallics', (ed. S. H. Whang *et al.*), 19–47; 1990, Warrendale, PA, Metallurgical Society of AIME.
84. D. L. ANTON, D. N. DUHL, and D. M. SHAH: 'Development potential of advanced intermetallic materials', Interim Technical Report 6 to AFWAL Materials Laboratory, Contract F33615–87–C–5214, Project 2420, United Technologies, Pratt & Whitney, West Palm Beach, FL, 1988.
85. R. C. HANSEN and A. RAMAN: *Z. Metallkd.*, 1970, **61**, 115–120.
86. P. R. SUBRAMANIAN, J. P. SIMMONS, M. G. MENDIRATTA, and D. M. DIMIDUK: in 'High temperature ordered intermetallic alloys III', (ed. N. S. Stoloff *et al.*), Mater. Res. Soc. Symp. Proc., 1989, **133**, 51–56.
87. R. A. PERKINS, K. T. CHIANG, and G. H. MEIER: *Scr. Metall.*, 1988, **22**, 419–424.
88. C. R. HUNT, Jr and A. RAMAN: *Z. Metallkd.*, 1968, **59**, 701–707.
89. V. V. BURNASHOVA, V. R. RYABOV, and V. Ya. MARKIV: *Dop. Akad. Nauk Ukr. RSR A, Fiz.-Mat. Tekh.*, 1970, **32**, (8), 747–750.
90. P. NASH, F. P. L. KAVISHE, and D. R. F. WEST: *Met. Sci.*, 1980, **14**, 147–149.
91. D. S. DUVALL and M. J. DONACHIE, Jr *J. Inst. Met.*, 1970, **98**, 182–187.
92. J. CISSE and R. G. DAVIES: *Metall. Trans.*, 1970, **1**, 2003–2006.
93. L. N. GUSEVA, R. S. MINTS, and Yu. S. MALKOV: *Russ. Metall.*, 1969, (5), 120–122.
94. K. SCHUBERT, H. G. MEISSNER, A. RAMAN, and W. ROSSTEUTSCHER: *Naturwissenschaften*, 1964, **51**, 287.
95. J. S. BENJAMIN, B. C. GIESSEN, and N. J. GRANT: *Trans. AIME*, 1966, **236**, 224–226.
96. V. Ya. MARKIV, N. F. MATUSHEVSKAYA, and Yu. B. KUZ'MA: *Izv. Akad. Nauk SSSR, Met.*, 1966, (6), 127–133.
97. I. J. DUERDEN and W. HUME-ROTHERY: *J. Less-Common Met.*, 1966, **11**, 381–387.
98. P. NASH and D. R. F. WEST: *Met. Sci.*, 1979, **13**, 670–676.
99. B. C. GIESSEN and R. RAY: *J. Less-Common Met.*, 1971, **23**, 95–97.
100. B. C. GIESSEN and N. J. GRANT: *Acta Crystallogr.*, 1965, **18**, 1080–1081.
101. H. NOWOTNY and H. OESTERREICHER: *Monatsh. Chem.*, 1964, **95**, 982–989.
102. H. OESTERREICHER, H. NOWOTNY, and R. KIEFFER: *Monatsh. Chem.*, 1965, **96**, 351–359.
103. A. DRASNER and Z. BLAZINA: *Z. Naturforsch.*, 1982, **37B**, 1225–1229.
104. J. B. KUSMA and H. NOWOTNY: *Monatsh. Chem.*, 1964, **95**, (1), 428–430.
105. R. S. MINTS, N. P. D'YAKONOVA, Ya. S. UMANSKII, Yu. A. BONDARENKO, and T. A. BONDARENKO: *Sov. Phys. – Dokl.*, 1973, **17**, 904–906.
106. F. MOLLARD, B. LUX, and J. C. HUBERT: *Z. Metallkd.*, 1974, **65**, 461–468.
107. V. Ya. MARKIV, V. V. BURNASHOVA, and V. R. RYABOV: *Dop. Akad. Nauk Ukr. RSR A, Fiz.-Mat. Tekh.*, 1970, **32**, (1), 69–72.
108. V. V. BURNASHOVA, P. K. STARODUB, and G. B. STROGANOV: *Izv. Akad. Nauk SSSR, Met.*, 1977, (5), 235–236.
109. V. Ya MARKIV, V. V. BURNASHOVA, L. I. PRYAKHINA, and K. P. MYASNIKOVA: *Izv. Akad. Nauk SSSR, Met.*, 1969, (5), 180–185.
110. R. W. GUARD and E. A. SMITH: *J. Inst. Met.*, 1959–60, **88**, 283–285.
111. E. I. GLADYSHEVSKII and Yu. B. KUZMA: *Zh. Strukt. Khim*, 1960, **1**, 66.
112. A. P. PREVARSKII, Yu. B. KUZ'MA, and M. M. ONYSHKEVICH: *Izv. Akad. Nauk SSSR, Met.*, 1977, (4), 201–203.
113. K. KALTENBACH, S. GAMA, D. G. PINATTI, K. SCHULZE, and E. T. HENIG: *Z. Metallkd.*, 1989, **80**. 535–539.
114. F. DUCASTELLE: *Rech. Aérosp.*, 1986, **4**, 11–38.
115. D. G. PETTIFOR: *New Scientist*, 1986, **110**, (1510), 48–53.
116. T. B. MASSALSKI: in 'Theory of alloy phases', 63–123; 1956, Cleveland, OH, American Society for Metals.
117. L. PAULING: in 'Theory of alloy phases', 220–242; 1956, Cleveland, OH, American Society for Metals.
118. F. LAVES: in 'Theory of alloy phases', 124–198; 1956, Cleveland, OH, American Society for Metals.
119. A. K. SINHA: *Trans. AIME*, 1969, **245**, 237–240; 911–917.
120. A. E. DWIGHT and P. A. BECK: *Trans. AIME*, 1959, **215**, 976–979.
121. J. H. N. van VUCHT: *J. Less-Common Met.*, 1966, **11**, 308–322.
122. Y. MISHIMA, Y. OYA, and T. SUZUKI: in 'High temperature ordered intermetallic alloys', (ed. C. C. Koch *et al.*), Mater. Res. Soc. Symp. Proc., 1985, **39**, 263–277.
123. E. MOOSER and W. B. PEARSON: *Acta Crystallogr.*, 1959, **12**, 1015–1022.
124. A. ZUNGER: *Phys. Rev. Lett.*, 1980, **44**, 582–586.
125. P. VILLARS: *J. Less-Common Met.*, 1983, **92**, 215–238.
126. P. VILLARS: *J. Less-Common Met.*, 1984, **99**, 33–43.
127. P. VILLARS: *J. Less-Common Met.*, 1984, **102**, 199–211.
128. E. WIGNER and F. SEITZ: *Phys. Rev.*, 1933, **43**, 804–810.
129. E. WIGNER and F. SEITZ: *Phys. Rev.*, 1934, **46**, 509–524.
130. J. C. SLATER: *Phys. Rev.*, 1934, **45**, 794–801.
131. F. C. von der LAGE and H. A. BETHE: *Phys. Rev.*, 1947, **71**, (9), 612–622.
132. D. J. HOWARTH and H. JONES: *Proc. Phys. Soc.*, 1952, **65A**, 355–368.
133. J. C. SLATER and K. H. JOHNSON: *Phys. Rev. B*, 1972, **5**, 844–853,
134. M. MORINAGA, N. YUKAWA, and H. ADACHI: *J. Phys. Soc. Jpn*, 1984, **53**, 653–663.
135. D. G. PETTIFOR: *Solid State Comm.*, 1984, **51**, 31–34.
136. D. G. PETTIFOR and R. PODLOUCKY: *Phys. Rev. Lett.*, 1984, **53**, (11), 1080–1083.
137. D. G. PETTIFOR: *J. Phys. C, Solid State Phys.*, 1986, **19**, 285–313.
138. M. J. RICHARDS and J. W. CAHN: *Acta Metall.*, 1971, **19**, 1263–1277.
139. S. M. ALLEN and J. W. CAHN: *Acta Metall.*, 1972, **20**, 423–433.
140. H. J. F. JANSEN and A. J. FREEMAN: *Phys. Rev. B*, 1984, **30**, (2), 561–569.
141. H. L. SKRIVER: *Phys. Rev. B*, 1985, **31**, (4), 1909–1923.
142. R. PODLOUCKY, H. J. F. JANSEN, X.-Q. GUO, and A. J. FREEMAN: *Phys. Rev. B*, 1988, **37**, (10), 5478–5482.
143. P. HOHENBERG and W. KOHN: *Phys. Rev.*, 1964, **136**, (3B), 864–871.
144. W. KOHN and L. J. SHAM: *Phys. Rev.*, 1965, **140**, (4A), 1133–1138.
145. P. TURCHI, M. SLUITER, and D. de FONTAINE: *Phys. Rev. B*, 1987, **36**, (6), 3161–3174.
146. M. SLUITER, P. TURCHI, FU ZEZHONG, and D. de FONTAINE: *Phys. Rev. Lett.*, 1988, **60**, (8), 716–719.
147. K. TERAKURA, T. OGUCHI, T. MOHRI, and K. WATANABE: *Phys. Rev. B*, 1987, **35**, (5), 2169–2173.
148. X.-Q. GUO, R. PODLOUCKY, and A. J. FREEMAN: *Phys. Rev. B*, 1989, **40**, (5), 2793–2800.
149. M. E. EBERHART, K. S. KUMAR, and J. M. MACLAREN: *Philos. Mag. B*, 1990, **61**, 943–956.
150. A. E. CARLSSON and P. J. MESCHTER: *J. Mater. Res.*, 1989, **4**, 1060–1063.

151. L. KAUFMAN and D. DEW-HUGHES: in Proc. Conf. 'Calculation of phase diagrams and thermochemistry of alloy phases', 46–71; 1979, Warrendale, PA, Metallurgical Society of AIME.
152. L. KAUFMAN and H. NESOR: 'Computer calculated phase diagrams for the Ni–W–Al, Ni–Al–Hf, Ni–Cr–Hf and Co(Cr, Ni)–Ta–C systems', Report to NASA Lewis Research Center, Contract NAS3–17304, Manlabs, Inc., Jan. 1974.
153. R. KIKUCHI: *Phys. Rev.*, 1951, **81**, (6), 988–1003.
154. F. DuCASTELLE and F. GAUTIER: *J. Phys. F, Met. Phys.*, 1976, **6**, (11), 2039–2062.
155. J. M. SANCHEZ and D. de FONTAINE: *Phys. Rev. B*, 1982, **25**, (3), 1759–1765.
156. C. SIGLI and J. M. SANCHEZ: *Acta Metall.*, 1986, **34**, 1021–1028.
157. C. SIGLI and J. M. SANCHEZ: *Acta Metall.*, 1988, **36**, 367–375.
158. M. SLUITER, D. de FONTAINE, X.-Q. GUO, R. PODLOUCKY, and A. J. FREEMAN: in 'High temperature ordered intermetallic alloys III', (ed. N. S. Stoloff *et al.*), Mater. Res. Soc. Symp. Proc., 1989, **133**, 3–16.